Personal Identification Based on Live Iris Image Analysis

Zhang, Dexin

Award date:
2006

Awarding institution:
University of Bath

Personal Identification Based on Live Iris Image Analysis

Dexin Zhang

Thesis Submitted For the Degree of Doctor of Philosophy

University of Bath
Department of Electronic and Electrical Engineering

Dec 2006

ProQuest LLC
789 East Eisenhower Parkway
P.O. Box 1346
Ann Arbor, MI 48106-1346

To

My Parents

Shixun Zhang, Lanyun Shi

&

My Wife

Yan Xu

Acknowledgments

Upon finishing this dissertation, my sincere gratitude firstly goes to my supervisors, Prof. Don Monro. Without his patience and generous support, this dissertation could never have been completed. His encouragement and guidance have made every day of the past three years worthwhile and enjoyable.

I would also like to thank Mr. Martin George, CEO of Smart Sensors Ltd, who not only generously sponsored my PhD project, but also gave me a lot of invaluable assistance and suggestions during my research.

Thanks for my colleague and also my good friend Soumyadip Rakshit, for his constant help to my work. Our cooperation in this project has always been pleasant. My gratitude should also go to all the group members in the Signal & Image Processing Group: Sean, Rachel, Leo, Fei, Yuanyuan for all the inspiration I have got from discussion with them.

With all my love, I am in debt to my parents, who raised me up and shaped me with their heart and love. They are always my source of confidence and energy.

Luckily, I met my wife in Bath University and decided we would hold our hands in the rest of our lives. Thanks for her accompany and assistance through the years behind and into the years to come. Thanks to my father-in-law and mother-in-law, for their trust, encouragement and support.

Abstract

Live iris image analysis based personal identification has received more and more attention in today's highly mobile and inter-connected society, with deteriorating situation in public security. Huge amount of work has been done and great progress achieved in this area. However, some critical problems still persist and significant work needs to be done before mass-scale deployment on national and international levels can be achieved. Recognition performance and the system speed are the two hot topics in iris recognition research. The research aim in this thesis is trying to answer the following two questions: (1) what kind of information within the iris textures could be utilized for authentication? (2) how the algorithms could be speeded up for real time system requirement?

The state of the art in iris recognition technologies is reviewed at first and the research difficulties are pointed out. In order to carry out the research in Bath, the Bath Iris Recognition Research Environment is built based on extensive literature review and comparison. Then four algorithms are proposed with the aim of answering the two questions above.

A fast and robust iris localization algorithm based on Random Sample Consensus (RANSAC) is proposed in Chapter four, which could not only maintain a high localization rate, but also perform the procedure much faster than the leading algorithms proposed by Daugman or Wildes. This work contributes to question 2.

Chapter four also reported a fast and robust eyelid removal algorithm, which could be carried out at a very high speed while still keeping a satisfying correct removal rate. This work also contributes to question 2.

Chapter five proposed a local frequency amplitude variation based iris coding algorithm, which could greatly reduce the processing time while still maintain a

very high distinguishing capability. This work contributes to both question 1 and 2.

An effective eyelash removal algorithm based on local area analysis has been proposed in chapter six. Unlike other previous eyelash removal methods, which generally tried to detect and mask the eyelashes or the eyelash areas, the proposed method recreates iris pixels occluded by eyelashes using information from their non-occluded neighbors.

Extensive experiments and comparisons have been done to prove the effectiveness and low computation complexity of these four proposed algorithms.

Through the research in this thesis, two possible answers to the questions proposed at the beginning of this thesis could be given: (1) Local image variation is the essential unique information for one iris class to be differentiated from another. Apart from utilizing the local phase or intensity variations, this thesis used the local frequency variation, which is also proved to be very effective. Statistically, the local iris image pixels are related to each other, which could be used to reconstruct occluded iris pixels. (2) The adoption of Fast Fourier Transform (FFT) makes the feature extraction procedure very time efficient. Thus the fast representation of local feature information is a very effective way to speed up the coding process. Also the adoption of fast iris image pre-processing techniques would contribute to the system speed.

Key Words: Iris Recognition, Iris Localization, Eyelid Detection, Iris Coding, Eyelash Removal

Content

List of Figures

List of Tables

Statement of Originality

The author considers the following elements to be original contributions of this work to the literatures in biometrics, pattern recognition, image processing and signal processing.

Chapter Two

- A comprehensive study of the biological characteristics of the human iris for iris recognition has been made. Also some iris behaviour principles have been summarized, which could be used for live iris recognition, non-linear iris normalization, etc.
- Review of the state of the arts for the automated iris recognition technologies in most aspects, including iris image capture machine, iris liveness detection, image quality assessment, iris image segmentation, iris image normalization, iris image registration, feature extraction, matching and practical applications. In each aspect, the leading theories and methods have been introduced.

Chapter Four

- A new pupil area finding method based on the standard deviation analysis for each projection line is proposed. According to the experiments, this method could greatly enhance the pupil finding accuracy.
- In edge point detection, a threshold adaptive canny edge detector is designed to make the numbers of edge points in a certain amount using a self-adaptive threshold variable.
- The RANSAC method is applied to the iris boundary fitting and encouraging performance is achieved.
- Enormously additional checking criterions were proposed based on the 8 bit gray scale image.
- An effective edge point selection method for eyelid detection.

Chapter Five

- Patch operation and parameter exploration in iris image coding.
- Extracting the local frequency amplitude variation as the feature vector to represent the iris image.
- Proposing that the local frequency amplitude variation is also the key information for one iris class to be differentiated from another.
- Weighing scheme in space domain and frequency domain for iris matching.

Chapter Six

- Proposing the eyelash area verifying method based on the gradient direction variance of edge points in a windowed area. This method works well in detecting eyelash area in our experiments
- Using 1D non-linear filter along a direction perpendicular to the eyelash to reconstruct the eyelash occluded pixel.
- Proposing an adaptive metric $Recover$ to decide if the filtered pixel is eyelash pixel or not. For each pixel, if $Recover$ is positive, the pixel is replaced by the filtered value, otherwise the filter is not applied.

1 Introduction

1.1 Why Iris Recognition

1.1.1 Security Challenges in Information Security

Personal identification has been a long studied problem since the inception of human being societies, in which identity has to be associated with individuals in daily life. In tribal primitive societies, where everyone knows everyone, there was not an urgent need for high confidence personal identification method. With the progress of modern transportation methods and information technology, today's society is becoming extraordinarily complex, geographically mobile, electronically interconnected and globally woven. More and more questions have been raised with regard to identifying a person accurately and reliably: Is the person a citizen in this country? Is this individual the right holder of this bank account? Does this passenger match one item in the criminal database?

In the last few decades, many crimes and frauds have been done due to lack of accurate identification methods. Fraudulent multiple identities have caused $1 billion loss in welfare benefits annually in the United States. $450 million per year was estimated by MasterCard because of credit card fraud. $1 billion worth cellular phone calls have been made by cellular band thieves from stealing SIM cards or PINs. $3 billion ATM cash machine fraud was made each year under current legitimate owner authentication method [1]. Thus more and more research has been done on accurate identification methods in order to deter crime and fraud, streamline business process, etc.

The problem of resolving a person's identity could be categorized into two types: recognition and verification. Verification means confirming or denying a person's claimed identity (Is he what he claims). Recognition refers to the establishment of a subject's identity. In some literatures, identification has the same meaning with recognition, while in this thesis, we define that identification means both recognition and verification to make the narration easier.

The engineering solution of personal identification problems focuses on identifying a concrete entity related to the individual. Traditionally, these entities go into two categories: (1) the subject's belongs (what you have), such as keys, ID cards, ATM Cards, etc. (2) the subject's knowledge of a piece of information (what you know), such as user-id, password, etc. Some systems, e.g., smart card based access control, use the combination of the above two methods, which groups "what you have" (smart card) and "what you know" (password) into one intelligent system for the purpose of individual recognition and verification.

The disadvantages of these traditional identification methods are quite obvious. Possessions could be lost or stolen, forgotten or misplaced. The privileges of the authorized person could be easily abused once the identifying possessions are in control of the impostors. People always find that it is difficult to remember so many passwords while using easily recallable Passwords or PINs also stands for easily guessed or cracked. According to recent research, about 25% ATM card users write their PINs on the back of the cards, thus the combination technique becomes useless in combating malicious unauthorized users.

Personal identification based on biometrics is an alternative approach to the "individual entity crisis". Instead of using "what you have" or "what you know", biometrical techniques utilize a person's biological traits (face, fingerprints, iris, hand geometry, etc.) or behavioral characteristics (gaits, voice, handwriting, etc.) to recognize and verify individuals. Since these biological traits or behavioral characteristics are "what you are", they can not be stolen or forgotten as the traditional methods. In this manner, biometrics based identification methods give a very promising direction for identity related problems.

1.1.2 Biometrics As a Solution

1.1.2.1 History of Biometrics

The term biometrics came from the Greek word bio (life) and metric (to measure). The first known biometrics application dates back to the 14th century in China where people stamped children's palm prints and footprints on paper

with ink to distinguish the young person from each other. In the 1890s, an anthropologist Alphonse Bertillion exploited a set of bodily measurement, such as the size of the skull or the length of their fingers to identify the repeated offenders for the police. Almost at the same time, Sir Edward Richard Henry developed a fingerprints based identification method in Scotland Yard, which has been widely used in forensic applications. [2, 3, 4, 5]

1.1.2.2 Biometrical Traits for Human

A human biological or behavioral characteristic needs to accord with the following properties in order to be a biometrical trait: (1) *universality*, which means generally all the people should have this characteristic, (2) *uniqueness*, which indicates that every individual's trait should be different after representation according to the system matching metric, (3) *Permanence*, which refers to the stability during time of these traits. In engineering practice, some other properties should also be met: (4) *collectability*, which refers to how easily these traits could be measured, (5) *performance*, which indicates how well the recognition rate could be achieved and the resource requirement to achieve it, (6) *acceptability*, which means how far people would be willing to use such technology, (7)*circumvention*, which refers to how easily this system could be spoofed.

1.1.2.3 Research Review on Current Biometric Technologies

Different biometrical technology has different strengths and limitations, thus quite a few biometrics have been proposed and researched, each of which appeals to different particular identification applications. This section will give a brief description of the existing and burgeoning biometrics technologies, including the identification based on faces, fingerprints, irises, voices, ears, gaits, signature, odors, retinas and hands geometry.

Face recognition has been immensely researched owing to its non-intrusiveness, easy acceptability, good recognition rate, etc. Identification

systems based on faces have been use widely in today's society, especially in unattended authentication applications. The research on facial recognition comes from two ways: eigenface based or geometry based. The former uses a set of orthogonal basis vectors to represent the face image, while the latter utilizes the geometric properties of facial attributes like nose, eyes, etc. to characterize different candidates. The challenging problem for face recognition is to tolerate the effect of aging, expression, illumination and the relative distance between the candidate and the camera. [1]

Fingerprint is one of the most mature biometrical technologies with its most application in forensic division. The flow-like fingerprints patterns and ridges are formed during embryonic period. In automated fingerprints recognition, the electronic images could be captured by scanning from inked paper impression or live fingerprints scanner. [7, 8, 9]

People naturally use voice to differentiate each other in their daily life, thus voice could be easily accepted. With the development of telecommunication technologies, voice recognition could be the only choice in some circumstances like remote identification through telephones. Whereas voice identification also has quite a few disadvantages: (1) voice does not provide enough information for highly reliable identification, (2) voice signal would typically be degraded by capture apparatus such as microphone, communication channel or digitizer, (3) behavioral characteristics such as voice could be easily affected by human health status, (4) voice could be simply spoofed, especially by someone who is very good at mimicking another's voice. [1, 6]

Any object with temperature would radiate heat, including human body, thus the patterns of human body heat radiation could be acquired by an infrared sensor. These images are called thermograms. This technology could be very useful for covert identification solutions or identical twins distinguishing. The disadvantages for thermograms based recognition include the following: (1) the

thermogram images depend quite much on the extraneous factors, (2) Infrared sensors are prohibitively expensive. [1]

Gait characteristics have been fully studied in biomechanics to detect lower extremity joint abnormalities. Also, people are quite used to distinguish others by their gate at a distance. There do not exist any commercial gait based recognition systems so far, probably due to the following limitations: (1) gait does not have sufficient information for high accurate identification, (2) human gaits are easily affected by weight fluctuation, health status or even personal wearing, (3) gait authentication involves processing of videos, thus it is computing intensive. [10]

Signature authentication could be based on static impressions or dynamic signatures. In static mode, the signature impressions are normalized to fixed size and decomposed into strokes. Features are extracted based on the shapes and relationships of these strokes. In dynamic mode, not only the statistical features are employed, but also the dynamic information, such as acceleration, velocity, and trajectory profiles are also utilized. [1, 2]

The rich structures of retinal vasculature could be used for personal identification, which has already been boasted in some movies. Since the vasculature is quite complex and it is very difficult to change or replicate it, retinal based recognition system is claimed to be highly reliable. The image acquisition needs the operator's cooperation by peeping into the eye-piece and focusing on a pre-determined spot. [2, 4, 5]

Hand geometry has become very popular recently in access control biometrics area. First, the operator has to put his hand on a capture panel, on which a set of pegs were fit in order to align the fingers. Generally, the feature vector representing hand geometry is quite small, which is quite useful for bandwidth or memory limited systems. The disadvantages of this technology are: (1) the

hand geometry is not fully unique, although it is peculiar, for identification, (2) the candidate's cooperation is necessary for system. [2, 4]

Each biometrical technology has its own advantages and disadvantages, which restricts its application in some specific areas. Table 1-1 gives a clear comparison of the biometrics discussed above in several aspects. Of all the biometric methods, iris based recognition is a newly emerging technique. With quite a few desirable properties such as high reliability, lifelong stability, non-obtrusive capture process, etc., iris based identification has been focused more and more from both academia and industries. [1]

Universality	*Uniqueness*	*Stability*	*Accuracy*	*Anti-spoofing*	*Biometrics*
High	Low	Medium	Low	Low	*Face*
Medium	High	High	High	Medium	*Fingerprint*
Medium	Low	Low	Low	Low	*Voice*
High	High	Low	Medium	High	*Thermogram*
Medium	Low	Low	Low	Medium	*Gait*
Low	Low	Low	Low	Low	*Signature*
High	High	Medium	High	High	*Retinal*
Medium	Medium	Medium	Medium	Medium	*Hand Geometry*
High	High	High	High	High	*Iris*

Table 1-1 Biometrics Technologies Comparison

1.1.3 Iris Recognition

The human iris, as shown in Figure 1-1, is an annular part between the pupil (generally appearing black) and the sclera (white area around the iris). The extraordinary texture structure, which was made from many interlacing minute characteristics such as freckles, coronas, stripes, arises in the development

anatomical structures during embryonic process, thus these characteristics are believed to be unique for identification. In addition, the detailed fine iris structure is not fully determined genetically but develops by random process. It was believed that the iris patterns of eyes from the same individual or identical twins are completely independent and uncorrelated [28]. But recent research in CASIA showed that the textures from the identical twins are correlated, although they could also be recognized quite easily [97]. These highly complex and unique structures make the recognition rate very accurate [11]. Although iris is inner organ covered by cornea, it is visible in a distance from outside, which makes the capture process non-obtrusive. Further more, iris patterns are believed to be stable through out people's life time. To sum up, iris based personal authentication has the following advantages compared with other biometrical technologies: (1) iris texture provides much more unique information for identification than faces, voices, handwritings, gaits, etc, (2) iris capture process is non-obtrusive, which is more acceptable than fingerprints, retinal, (3) iris texture is not affected quite evidently by aging, healthy status, emotion, weight as gait, voice, handwriting, etc. All of the above advantages give iris-based identification a very promising research and application future.[1-5, 25-33]

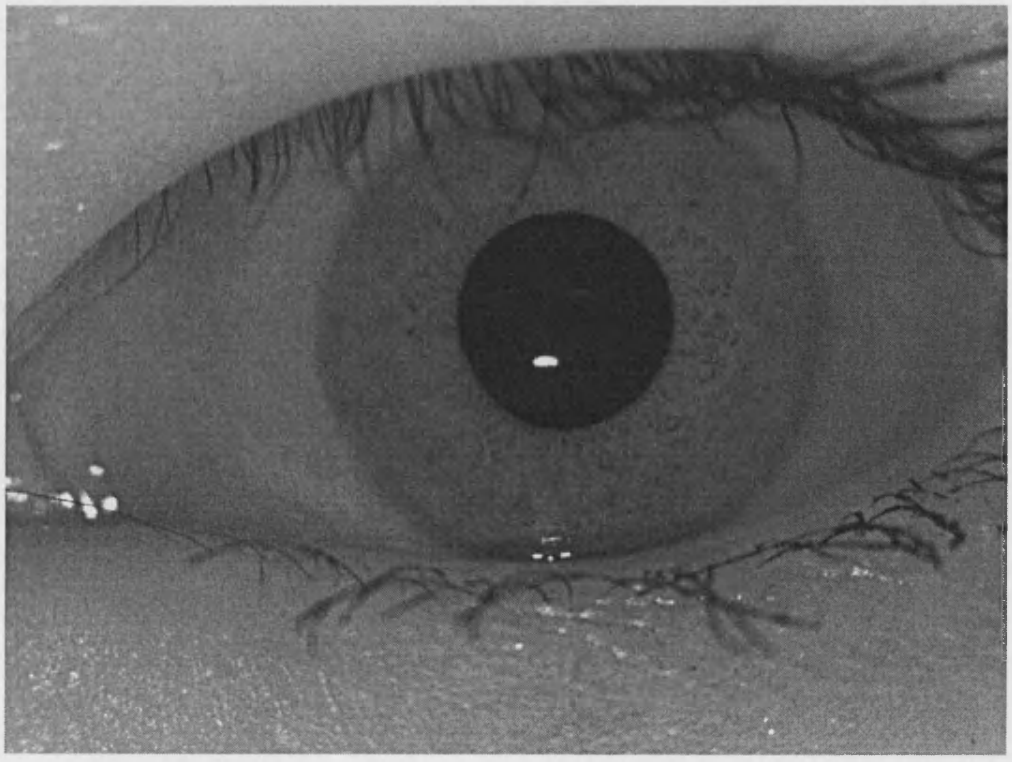

Figure 1-1 Sample Iris Images From Bath Database

Extensive work has been done on iris based human identification both in academic research and in industries [19-41]. Pioneering work on iris recognition was done by Daugman using Gabor wavelets. His system has been widely implemented and tested [28]. Recently other researchers including Wildes et al [32], Boles and Boashash [34] and Tan et al [39] have contributed quite a few new methods. The next chapter will give a review on current iris recognition technologies.

However, some critical problems still persist and significant work needs to be done before mass-scale deployment on national and international levels can be achieved. This thesis will contribute to the following questions: (1) what kind of information within the iris textures could be utilized for authentication? (2) how could the algorithms be speeded up for real time system requirement?

1.2 Research Targets and Methodology

The research target of this thesis is to build a high speed, scalable iris identification algorithm, in which iris image capture, image quality assessment and automatic sorting, image pre-processing, feature extraction and matching should all be researched. The research methods are shown in Figure 1-2.

- **Capture Apparatus Design and Database Construction**

A major hindrance to research in this field of iris recognition has been a shortage of publicly available images. Until recently, CASIA database provided by Professor Tan was the only publicly available image database. We also designed an infrared iris camera and established the Bath iris database, which consists of candidates from many countries and ethnical groups. At the time of writing, over 800 classes of eyes have been collected.

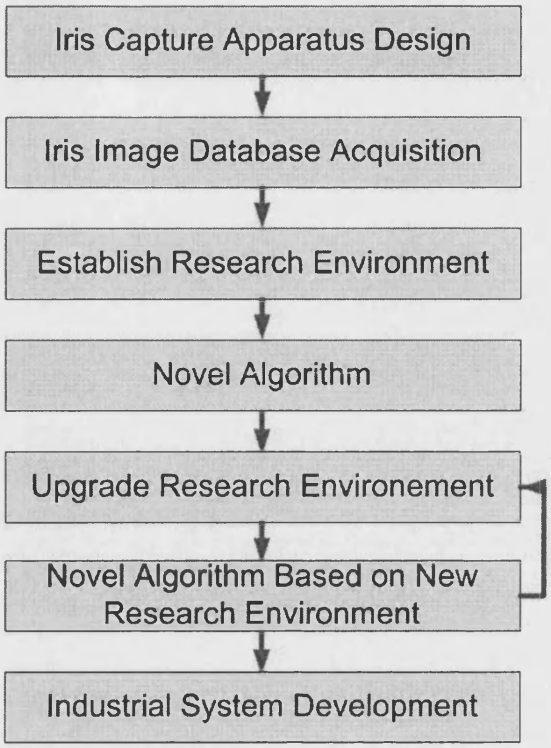

Figure 1-2 Research Methodology

- **Establish Research Environment**

Based on intensive literature review, some basic algorithms have been implemented in image quality assessment and sorting, iris localization, image normalization. These implemented algorithms are called research environments, based on which new algorithms will be tested.

- **Novel Algorithm Research and Research Environment**

A novel iris coding and matching method was proposed first and thoroughly tested. Then these programs were put into the research environment to form a full iris recognition system. Any research to improve the system will be based on the upgraded environment.

- **New Algorithm Based on Upgraded Research Environment**

After proposing the iris image coding and matching method, further research will focus on iris boundary localization, eyelid detection and masking, eyelash removal. All the research will be based on the Bath iris research environment. Every time a new algorithm is proposed and tested, the research environment will be upgraded accordingly.

➢ **Industrial System Development**

The former steps will be repeated and the algorithms tested extensively until the system achieves a desirable performance. Then the corresponding algorithms implemented in Matlab will be transformed into C Language and the SDK produced.

1.3 Thesis Outline

Chapter Two will give a review on state of the art for iris recognition technologies. First, a simple biological study on the human iris will be given to show how physiologically these iris textures are. Then iris recognition history will be introduced briefly. In order to describe the current research situation clearly, the current solutions for this technology will be illustrated in the following aspects: (1) iris image capture machine, (2) iris liveness detection, (3) iris image quality assessment, (4) iris image Segmentation, (5) iris image normalization, (6) iris image registration, (7) feature extraction and match, (8) industrial application. In each aspect, the primary methods will be listed and compared. The research difficulties and direction will also be discussed in this aspect.

Chapter Three will illustrate in detail the Bath iris research environment, which includes iris camera design, Bath iris image database building, image quality assessment and automatic sorting, iris image pre-processing techniques.

A new iris Segmentation method will be proposed in Chapter Four. Iris segmentation includes iris localization and eyelid Removal. For seriously eyelid-occluded images, eyelid removal has to be performed before coding the iris. For normal quality images, only iris localization is performed in order to speed up the system. Iris segmentation could influence the recognition system in two aspects: (1) in practical situations, the correct recognition rate highly depends on the correct segmentation rate, (2) iris segmentation is the most time consuming step apart from image coding. In most real time iris recognition systems, iris segmentation is the bottleneck for the recognition rate and speed of these

systems. In this chapter, the commonly used segmentation methods will first be reviewed. Then our approach is proposed and compared with the leading methods.

Chapter Five will propose the Monro Iris Transform technique. Much work has been done on coding the human iris image: Daugman used a bank of multi-scale Gabor filters to demodulate the phase information of the iris image [28]. Tan used a specially designed wavelet to record the local sharp variations of the image intensity as feature vectors. Both methods have achieved very good result [77]. In this chapter, we will exploit the local frequency variation as another novel method for coding the iris image. Extensive experiments will be carried out and the excellent results will show that frequency amplitude variations are also exploitable information apart from phase and intensity variation. Besides, the proposed Monro Iris Transform has a quite low computational complexity, which is very useful for real time or embedded systems.

Eyelash is a regular contaminator for the area of interest used in iris identification. Chapter Six will give an effective eyelash removal algorithm. Through a specially designed filter, this method would allow partially occluded regions of the iris to be included in iris coding, which would previously have been excluded. This method will be applied with three leading iris coding algorithms (Daugman, Tan, Monro) and encouraging performances will be shown.

The thesis is concluded in chapter eight, in which the main contributions are summarized and future research directions given.

2 Iris Recognition Technologies Review

2.1 Foreword

Before we carry out the research, it would be great helpful to go through the existing main methods in each aspect of iris recognition to facilitate our future research. The biological study of the human iris will be given first, followed by the history introduction of iris recognition. The iris recognition technologies will be categorized into seven aspects and illustrated. In each aspect, the primary methods will be listed and compared. The research difficulties and emphasis will be discussed at the end of this chapter.

2.2 Biological Study on Human Iris

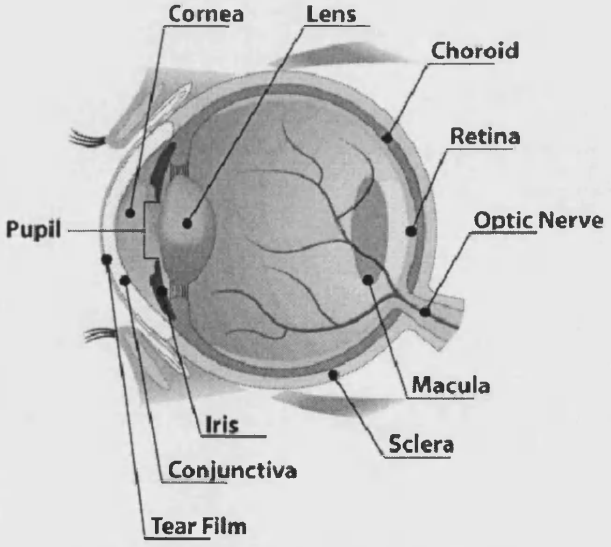

Figure 2-1 The Human Eye [92]

Figure 2-1 is an anatomical picture for the human eye, in which iris is a circular diaphragm lying between the cornea and the lens. The support of the lens gives iris a shape of truncated cone in three dimensions. The iris is attached to the ciliary body at one end and opens to the pupil on the other end. The dilation and constriction of the iris will determine the light ray amount entering the eye, which is very useful in human iris liveness detection. The transparent cornea covers the front part of the iris and protects it from damage. It is reported from clinic observation that typically the iris centre is lower and closer to the nasal

compared with the pupil centre. This non-concentricity will be taken care of in iris image localization. [13-18]

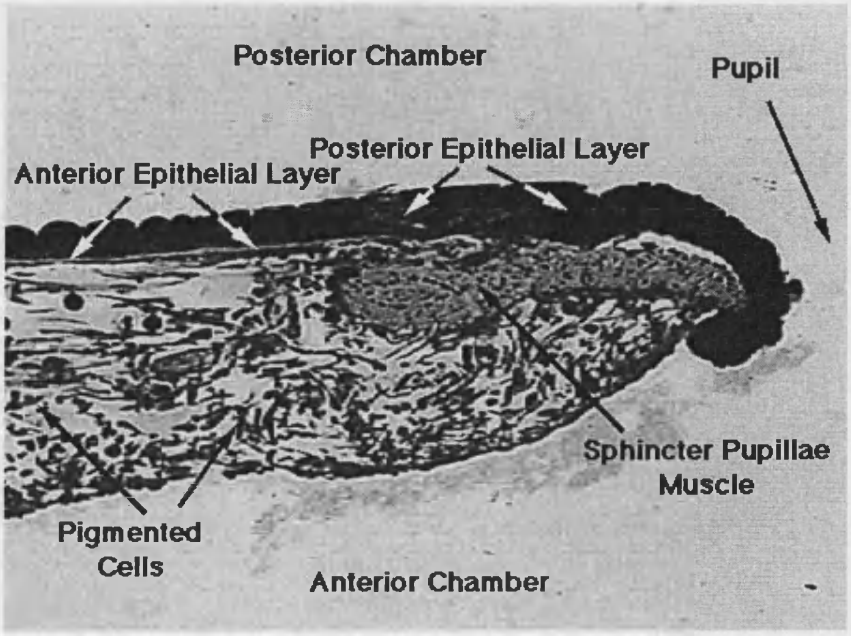

Figure 2-2 Anatomy of the Human Iris [33]

More detailed structures of the human iris are shown in Figure 2-2. The iris is composed of several layers and the visual appearance of the iris is the direct result of its multilayered structure. The evidences from two main sources support the claim that the structure of the iris is unique for each individual and stable with age:

- The first source is from clinical observation. Through extensive examining during daily work, ophthalmologists and anatomists found that the human iris seem to be unique, even between left eye and right eye of the same person, or between identical twins. Through further observations, the structures vary quite little.
- Developmental biology provides the second source. Through the research of developmental biologist, it is found that although the general structure of the iris is genetically determined, the details of the minutiae depend on the random development information in embryo or infant period. Developmental biology evidence also bears on the stability of iris structures. It points out that the healthy iris changes little after childhood, although slight depigmentation and shrinking of the average pupillary opening are standard with advanced age. [33]

Another interesting aspect of the iris physical characteristics is the pupil oscillation (hippus). Due to the complex interplay of the iris' muscles, the diameter of the pupil is in a constant moment-to-moment dynamics. This pupil oscillation characteristic could be monitored in iris recognition systems to make sure the candidate iris to be evaluated is live.

Through the study of the physiological characteristics of the human iris, the following conclusions could be drawn: (1) The iris texture patterns are highly unique due to the greatly distinctive iris textures. (2) After adolescence, the iris typically tends to be stable with age. (3) Some interesting biological characteristics, such as hippus, contraction with illumination, would be very useful in live specimen detection. Thus the physiological base for human iris recognition is built. [73-76]

2.3 Iris Recognition History

The first use of iris patterns as a basis for personal identification goes back to 1890s, when a French anthropologist Alphonse Bertillion exploited a set of bodily measurement, including the iris colors and shapes, to identify the repeated offenders for the police. In 1936, ophthalmologists proposed the concept that using the unique iris patterns to recognize individuals [77]. The concept of automated iris recognition is put forward in 1987 by two ophthalmologists Aran Safir and Leonard Flom, whom were awarded a patent for this iris recognition concept, although they did not develop a working system. In 1991, the first recorded automated iris recognition system was realized in Los Alamos National Laboratories in the United States [33]. Soon after that in 1993, John Daugman invented a highly reliable iris recognition algorithm, on which most commercialized iris recognition systems are based [28]. In 1996, Dr Richard Wildes made another iris recognition system prototype [32]. Professor Tan realized a high performance iris recognition system in CASIA in 2000 and published the first publicly available research iris image database [38]. In recent

years, more and more researchers, institutes and industrial companies have entered this area. And some practical applications have been exploited.

2.4 State of the Art

2.4.1 Iris Recognition System Structure

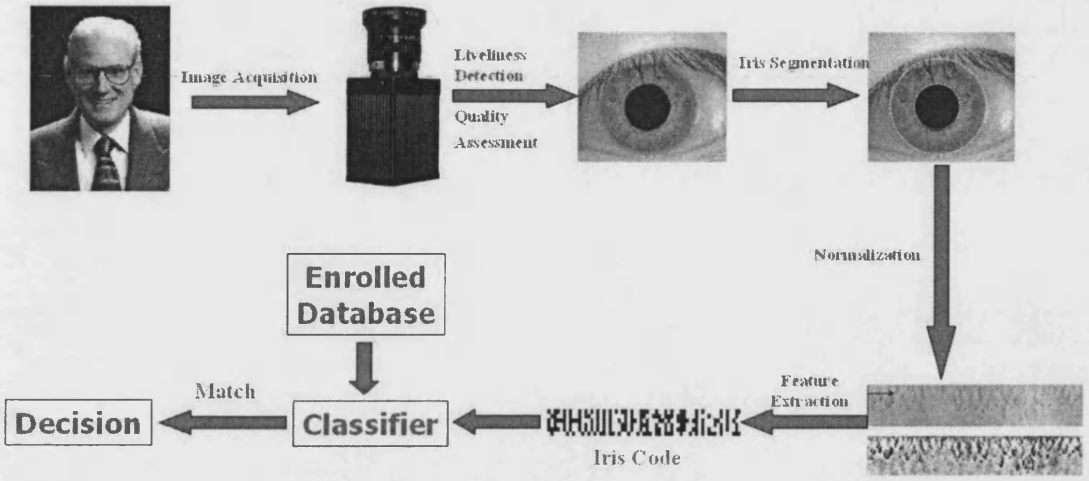

Figure 2-3 Iris Recognition System Structure

Figure 2-3 shows the conceptual structure of an automated iris recognition system. Thus this section will be divided into the following parts: (1) iris image capture machine, (2) iris liveness detection, (3) iris image quality assessment, (4) iris image segmentation, (5) iris image normalization, (6) iris image registration, (7) feature extraction and match, (8) industrial application. In each part, the primary methods will be listed and compared. The research difficulties and direction will also be discussed in this part.

2.4.2 Iris Image Capture Machine

Since iris is quite a small area (generally about 1 cm in diameter) and human is quite sensitive about their eyes, great care must be taken in designing iris image capture machine. Capturing high quality iris images is one of the major challenges in automated iris identification. Low quality images will greatly decrease the recognition system performance by increasing the false match

rate (FMR) and the false non-match rate (FNMR). The following aspects must be considered during the design of iris image capture machines:

- The acquired image should have sufficient resolution for iris recognition. Ideally more than 200 pixels will stretch across the iris diameter.
- The illumination intensity should be strong enough to make enough contrast in the image, especially in the interior of iris textures, without causing any uncomfortable feeling for the subject. Also the local radiation regulations must be accorded with.
- The system should provide self-positioning scheme without using too much constraint against the subject.

Early iris capturing machines were generally designed by researchers in computer vision for academic purposes. Thereafter, with the emerging profitable iris recognition market, more and more industrial companies have got involved in iris capturing machine design. Since 1990s, many technologies have been commercialized by experts in optics and electronics, including self positioning, remote imaging, automatic imaging, etc. Thus more and more commercialized iris cameras products appeared in the market, such as BM-ET series in Panasonic, IrisAccess series in LG, Pier series in SecuriMetrics, IrisCam series in IriTech, IRISPASS series in OKI as shown in Figure 2-4.

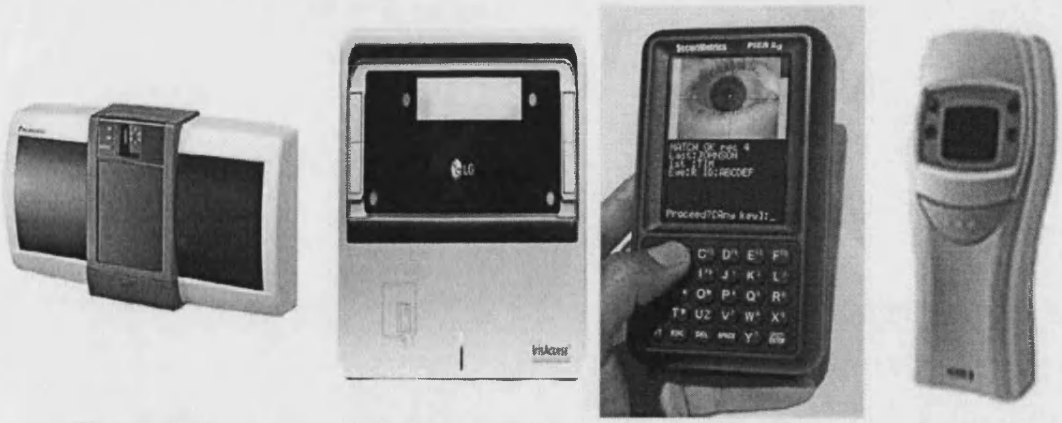

BM-ET 500 Panasonic | IrisAccess 4000 LG | PIER 2.3 SecriMetrics | IrisPass-h OKI

Figure 2-4 Iris Cameras

Most current commercial iris cameras require relatively close proximity from the eye and significant cooperation from the subject, as well as imposing constraints on the subject's position and movement. Recently, Sarnoff has

released an iris capturing framework called: Iris on the Move (IOM). IOM can capture the iris images while the subject walks through the capturing portal at a normal walking pace. It is reported that up to 20 subjects could be captured and identified in a minute. Figure 2-5 shows a sample image captured by IOM. We can see that 8 infrared light sources have been fit in the capturing port and thus leaving 8 specular reflections on the images. One of the drawbacks for this design is that these specular reflections are generally in iris area, thus covering the most useful texture information for identification.

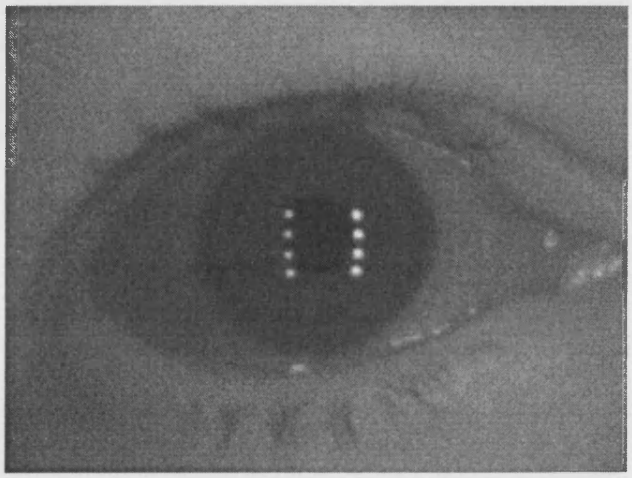

Figure 2-5 Sample Image From IOM

2.4.3 Iris liveness Detection

The reason for using biometrics based personal identification is the urgent need in anti-identity-spoofing. As some samples in Figure 2-6 show, all biometrics could be spoofed, including iris. Thus liveness detection is highly desirable in practical applications. Iris recognition systems could be spoofed by printed photographs, a video playback, a glass eye or other artifacts. This section will list some of the iris recognition properties that could be used for anti-spoofing countermeasures.

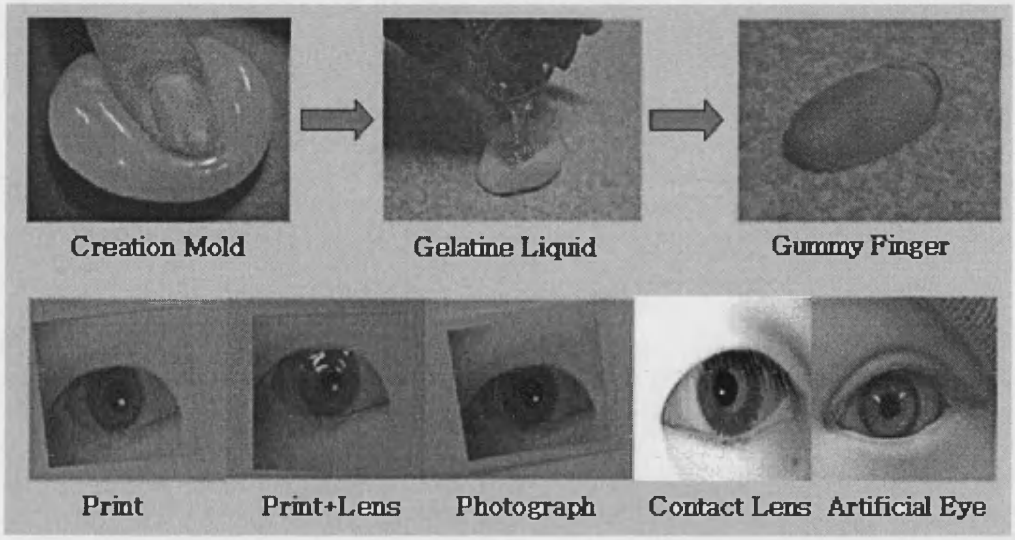

Figure 2-6 Some Biometrics Spoofing Methods [93]

- *Spectrographic properties of living tissue*: Different component of living tissue (such as fat, blood, etc) has different spectrographic signatures. Comparing the light fractions reflected in 600nm ~ 1000nm band can distinguish them. Also the melanin (pigments on both human skin and the anterior layer of the iris) has a distinctive spectrum absorption characteristic.
- *Retinal back* reflection ("red eye" effect): The retina will reflect the light beam from the light source through the pupil. If the camera is coaxial (or nearly coaxial) with the light source, the reflected light beam will be imaged in the camera, which makes the pupil appear bright and red in the photos.
- *Purkinje reflections*: From the optics' point of view, the eye has four optical layers: the inner and outer boundary of the cornea and the lens, which will reflect four times in the imaging process. By analyzing the four reflections, we can tell if the eye has responded and tracked the light source dynamically and correctly.
- *Hippus:* As mentioned earlier in this chapter, hippus (pupil oscillation) is controlled by automatic nervous system and oscillates twice per second.
- *Pupillary light reflex*: Controlled by the brainstem, the pupil will dilate and constrict according to the environmental illumination.
- *Conscious eye control*: The eye could move and the eyelid could blink under the system command.
- *Frequency domain properties*: The most popular method to fake iris is by printing. The dot matrix which creates the printed iris will introduce some extra noise at certain frequencies in the frequency domain while the natural

iris won't. So by analyzing the Fourier domain spectrum energy distribution, the printed iris can be identified. [78]

In conclusion, iris liveness detection techniques are highly desirable for recognition systems. Although it is under-researched, the characteristics of human iris have inspired many researching directions.

2.4.4 Image Quality Assessment

The performance of iris recognition system could be significantly undermined by poor quality iris images. Surprisingly high false reject rates (FRR) and failure to enroll rates (FTE) are reported due to poor quality iris images caused by a variety of reasons such as defocusing, motion, occlusion, non-uniform illumination.

A number of efforts have been tried on iris image quality assessment in the past. Apart from the general image quality assessment method, some proprietory characteristics of iris recognition had been employed in quality evaluating. The rest of this section will give an overview of the solutions by leading researchers.

- Since the blurring process (defocusing blur and motion blur) will decrease the high frequency spectrum power, Daugman set a criterion to measure the high frequency power through 2D Fourier transform. This method is a common approach for focus assessment. [79]
- Some specific characteristics of iris images were employed by Zhang et al. [80] in designing the evaluation method. Zhang set a descriptor w to analyze the sharpness of the boundary between the pupil and iris:

$$\frac{1}{W} = \frac{S}{M_i - M_p} \tag{2-1}$$

In equation (2-1), S denotes the average absolute gradient value of the pixel set along the pupil iris boundary, M_I stands for the average intensity value of the iris pixels which are close to the pupil-iris-boundary, M_p indicates the average intensity value of the pupil pixels near the boundary. This descriptor is based on such an idea: the sharper the boundary is, the better the image quality is. As far as this equation is concerned, the bigger

the descriptor *w* is, the better the image quality is. A rough localization is needed before the evaluation.

- Tan categorized the iris image qualities into four classes (clear, defocused, motion blurred, occluded) and proposed a classification scheme to differentiate each class by analyzing the frequency distribution of two selected iris area in the image [77]. A 2D descriptor *D* is designed as show in equation (2-2):

$$D = [(F_1 + F_2 + F_3);\ \frac{F_2}{F_1 + F_3}]$$
$$F_i = \iint_{\Omega=\{(u,v)|\, f_1^i < \sqrt{u^2+v^2} <= f_2^i\}} |F(u,v)|\, dudv \qquad i = 1, 2, 3 \tag{2-2}$$

Here, $F(u,v)$ is the 2D Fourier transform spectrum of the selected iris area, in which the low, medium and high frequency spectrum are indicated by F_1, F_2 and F_3 separately. f_1^i and f_2^i are the frequency radiuses partitioning the F_i. The first element in descriptor *D* is the total spectrum power in the selected iris area, by which the severely occluded iris images could be discriminated. The second element stands for the ratio of medium frequency power to the others, by which the defocused or motion blurred images could be picked out. Support Vector Machine (SVM) is used to describe the boundary between the four classes in the 2D descriptor space. Figure 2-7 illustrates all the four kinds of images and their corresponding Fourier domain spectrum. The two squares in the iris area indicate the two selected area for frequency spectrum analysis.

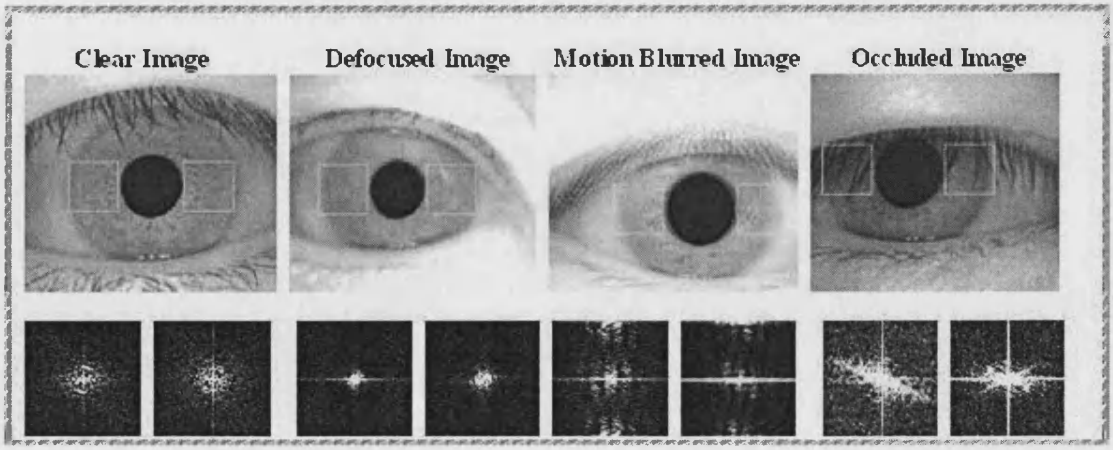

Figure 2-7 Spectrum Analysis for Bad Quality Images [77]

- Kalka et al. emphasize their research on three kinds of bad quality images: Defocus, Motion and Off-Angle. For the first time, the Off-Angle images

were studied in iris image quality assessment. (1) Similar to Daugman's method, defocused images are assessed by measuring high frequency content in the overall image or segmented iris region. Experiments shown that the local assessment is much more sensitive than the global measure. In addition, the focus score was not attenuated much by non –canonical iris images containing too much high frequency content such as eyebrows or eyelashes. (2) The motion blur is detected by analyzing the directional properties of the frequency spectrum of the image. The image is first transformed into Fourier or Wavelet domain. Then 36 equal-spaced directional masks between radian [0, π] are applied to the frequency domain of this image. The total power in each mask is calculated and the perpendicular of the maximum mask is assumed to be the motion direction. (3) The off-angle (out-of-plane rotation) iris images are also researched in Kalka's work. Kalka assumed an initial rough angle estimate is known and found the optimal estimate by exhaustively searching over all possible angles. Although this method looks like time consuming and needing some pre-knowledge (rough estimate), it is quite useful for the following image pre-processing stage. The off-angled image could be projectively transformed into frontal view and thus coded and matched within the system. [81]

- A wavelet-based quality measure is proposed by Jain et al [82]. This method could determine the local iris image quality meticulously and thereby incorporate local quality index in the matching algorithm. This special weighting technique could greatly decrease the equal error rate (EER). The area of interested (pure iris textures) will be firstly segmented from the sclera, eyelid, eyelash and others. Then multiple concentric annulus bands with fixed width are constructed and applied by a Mexican hat wavelet with three scales. The advantages of using wavelet instead of 2D Fourier transform are: (1) The Fourier transform does not localize in space, while the wavelet transform obtains smooth representation in both space and frequency. (2) Mexican wavelet is quite sensitive to features exhibiting sharp variations, which are the main iris texture features.

- Kee measures the image quality from three aspects. (1) The images are firstly divided into M*N small blocks evenly and the severely eyelid occluded images are detected through the intensity analysis between these blocks. The basic idea is that the eyelids are generally illuminated more heavily than irises and pupils. (2) Then the images containing clustered dark blocks are thought to be images with pupil and set as candidate images for the following check. (3) The Sobel edge detector is utilized to analyze the gradient distribution in the image. Obviously this method is very fast, but the accuracy is sacrificed. Thus it is only a preliminary assessment. [83]

The current quality assessment methods could be categorized in two: space domain based and frequency domain based. (1) The concepts often used by space domain based methods are: intensity, gradient, edge point distribution, etc. The methods proposed by Zhang et al. or Kee et al. are space domain based. (2) In frequency based methods, Fourier transform or wavelet transform are applied to the whole iris image or different local areas within this image. As the transformed image is concerned, the low frequency describes the general information of the image while the high frequency depicts the detailed minutiae. Thus, the clear images, which have many detailed iris structures, should contain much middle frequency or high frequency information in the transformed domain, while the defocused images should contain more low frequency information. The methods proposed by Daugman, Tan, Kalka, Jain are generally frequency domain based.

The problem of image quality assessment should be considered in the whole system of iris recognition, in which every stage contributes in different aspect and works together to run the system. For example, if the iris camera could effectively locate and focus the iris area or the iris coding and matching algorithm could tolerate low quality images to a certain extent, the requirement for iris image quality assessment will be much reduced. Otherwise, the quality assessment step will be more difficult.

2.4.5 Iris Image Segmentation

Automated iris recognition should impose as few constraints on the subjects as possible when capturing the iris images. Thus not only the interested iris area, but also some data derived from the immediately surrounding eye region are introduced within the captured images. Therefore, prior to image coding and matching, it is important to find the portion of the acquired image that corresponds to the iris.

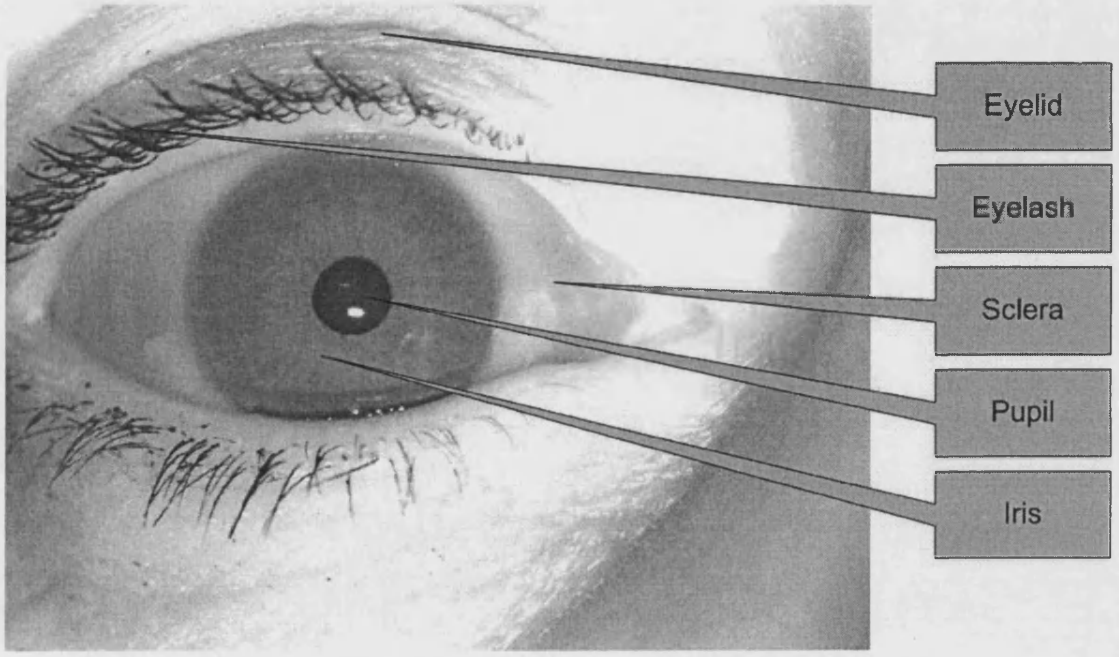

Figure 2-8 Human Eye Structure

As shown in Figure 2-8, the iris is an annular part between the dark pupil and bright sclera. The captured iris images generally contain unrelated parts such as eyelid, eyelash, sclera, pupil, specular reflections and sometimes even eyebrow. In order to fully effectively utilize the iris texture information for identification without the interferences of the unrelated parts, the useful iris area needs to be segmented out and other parts masked, as shown in Figure 2-9.

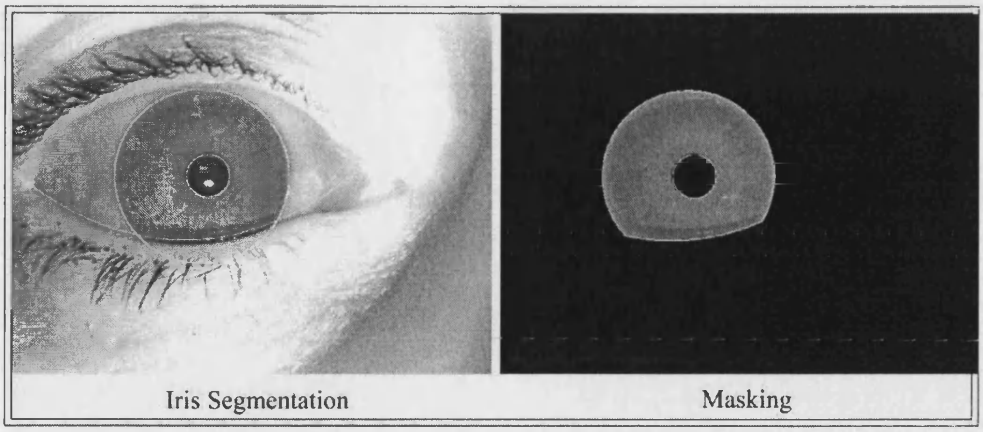

Figure 2-9 Iris Segmentation & Masking

Iris segmentation includes iris localization and eyelid removal. Iris segmentation is one of the research difficulties and considered as the *bottleneck* in real time iris recognition systems due to the following reasons:

- Correct and accurate segmentation is the precondition for image coding and matching, and thus is the premise of the success of the whole iris recognition system.
- Many iris image pre-processing methods, such as image quality assessment, iris normalization, also need the segmentation results to carry on.
- Iris segmentation is generally the most time consuming stage in the whole recognition procedure. Thus it is the bottleneck in building the real time iris identification system.
- Iris segmentation has to cope with pictures taken by enormous numbers of iris cameras under different illumination circumstances.

In conclusion, iris segmentation is the bottleneck for a practical real-time recognition system and thus is a hot research topic recently. The speed and accuracy are the two keywords for iris segmentation. The leading current methods will be introduced, as well as a fast and robust segmentation method proposed in chapter four.

2.4.6 Iris Image Normalization

The iris size in captured iris images always varies due to a number of reasons: (1) different candidates, (2) pupil contraction or dilation, (3) change in camera-to-eye distances. The effects of such elastic deformation on iris textures should be compensated before being sent for coding and matching. In addition, the non-uniform background illumination caused by complex capturing environment should also be eliminated in order to improve the system performance. Iris image normalization is the step which will reduce the effects of elastic deformation and background illumination, as shown in Figure 2-10.

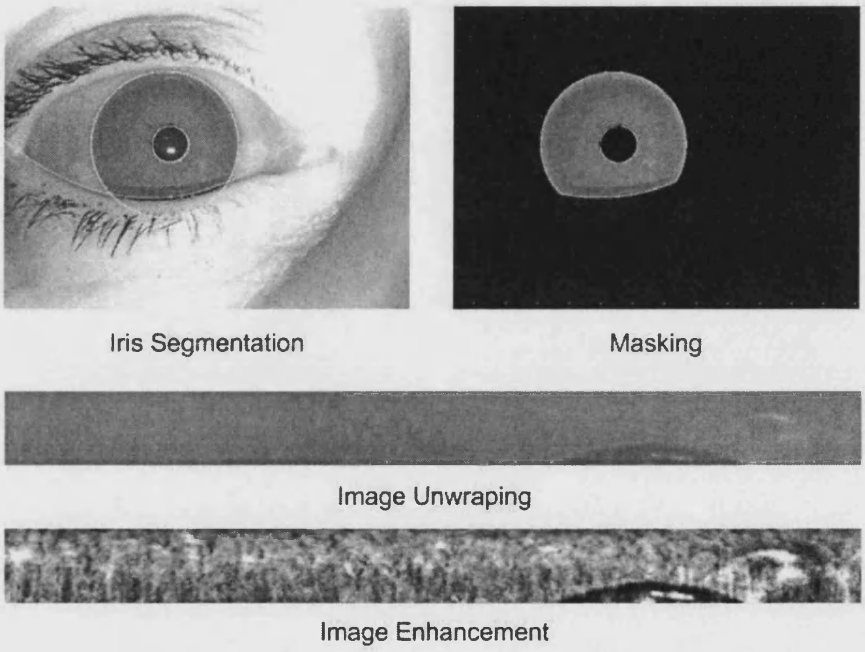

Figure 2-10 Iris Normalization

Uneven illumination removal is generally undertaken by common image enhancement techniques such as histogram equalization. And such technologies have so far satisfyingly met the system requirement. Thus the elastic deformation compensation becomes the research focus in iris normalization.

Daugman uses the rubber sheet model to compensate the iris deformation [31]. In radial direction, the texture is assumed to change linearly, thus the localized

iris in Cartesian coordinates (*x*, *y*) is linearly mapped into the dimensionless polar image coordinates (ρ, θ) according to:

$$\begin{aligned} x(\rho,\theta) &= (1-\rho)\times x_p(\theta) + \rho \times x_l(\theta) \\ y(\rho,\theta) &= (1-\rho)\times y_p(\theta) + \rho \times y_l(\theta) \end{aligned} \quad \text{(2-3)}$$

In which

$$\begin{aligned} x_p(\theta) &= x_{p0}(\theta) + r_p \times \cos(\theta) \\ y_p(\theta) &= y_{p0}(\theta) + r_p \times \sin(\theta) \\ x_l(\theta) &= x_{l0}(\theta) + r_l \times \cos(\theta) \\ y_l(\theta) &= y_{l0}(\theta) + r_l \times \sin(\theta) \end{aligned} \quad \text{(2-4)}$$

Where ρlies on [0, 1] and θis cyclic over [0, 2π], while (x_{p0}, y_{p0}) and (x_{l0}, y_{l0}) are the centre coordinates of the pupil and limbus.

Wildes et al. uses an image-registration technique to compensate for both elastic iris deformation and rotation [32]. An affine transform model is used to align a newly acquired image to an image in the database. This method is very time consuming and thus could only work in the verification mode (1 to 1 match).

The normalization methods used by Tan, Kim, Sanchez-Reillo, Kim, Monro, etc are generally similar [77, 35, 84, 85]. As shown in Figure 2-10, these methods will map the localized iris image into a fixed size rectangular image to ease the registration and coding steps.

In most iris normalization methods, the iris pixels are assumed to move only radially along the pupil radius and there are not any relative stretch or compression between iris pixels (e.g. move in a linear way). This assumption works quite well in practical applications. Some efforts have been done in non-linear iris normalization (or segmented linear normalization). Nonetheless, no obvious improvement in system performance has been seen from it.

The medical studies on iris structure movement could be used for reference in iris recognition research, some of which are summarized as follows:

- As far as one eye is concerned, the motion rules are always the same, no matter what the reason (Drug, Light, Emotion, Alcohol, etc) that caused the

movement could be. That is to say, the iris texture status is only connected with the radius of the pupil. The iris area in two images from the same eye should not have any relative stretch or compression as long as their pupil radiuses are equal to each other.

- Iris pixels at the same radius to the centre will always be at the same radius.
- Approved from clinical observation, iris structures generally move in a linear way. Nevertheless, when the iris structures are over stretched or compressed, they begin to move in a non-linear way, which does not often happen in daily life. This principle explains why linear normalization works quite well compensating for elastic deformations.

2.4.7 Iris Image Registration

Two normalized iris images need to be registered before they could be coded and matched. Image registration is the process of overlaying two or more images of the same scene taken at different times, from different viewpoints or by different sensors. It geometrically aligns two images—the reference and the sensed images. The majority of the registration methods consist of the following four steps:

- *Control points detection*: Salient objects in the image, such as closed-boundary regions, edge, contours, line intersection, are manually, or preferably, automatically detected. Some of the representative points, which are called Control Points (CPs) in the literature, will be used in further processing.
- *Feature Matching*: In this step, the correspondence of the Control Points between the sensed image and the reference image is established.
- *Transform Model Estimation*: Based on the correspondence of the CPs, the parameters of the mapping functions are calculated using specific mathematical mapping models.
- *Image Re-sampling and Transformation*: The sensed image is transformed by means of the mapping functions. The non-integer coordinates are calculated by certain interpolation techniques.

Due to the iris structure movement characteristics mentioned in section 2.4.6 and that the iris images have already been normalized, the iris image

registration problem is restricted to the translation compensation issue between the reference image and its sensed counterpart.

As mentioned in section 2.4.6, Wildes et al. uses an image-registration technique to compensate for both elastic iris deformation and rotation [32]. Thus both image normalization and registration problems have been solved in his affine transform model.

The most used iris image registration method is based on Mean Square Error (MSE). Due to the constraint of the capturing environment, the iris could not rotate much during capturing procedure, i.e. there could not be much horizontal shift between normalized rectangular images from the same eye. Assuming the maximum relative shift between two corresponding images is *n*, there should be *2n+1* aligning choices between them. Supposing $I_1(x,y)$ is the reference image and $I_2(x',y')$ is one of the *2n+1* aligning options for the sensed image, then the $I_2(x',y')$, which corresponds to the minimum MSE in equation (2-5) ,will be the registered candidate to the reference one. The normalized image size is supposed to be [*M, N*].

$$MSE = \frac{\sum_{x=1}^{M}\sum_{y=1}^{N}(|I_1(x,y)-I_2(x',y')|^2)}{(M*N)} \tag{2-5}$$

Based on the idea that the shift in the space domain corresponds to the phase shift in frequency domain, some correlation based methods are also employed in iris image registration. Assuming s_k and s_{k+1} are the reference and sensed images, their relative shift and correlation function are shown in equation (2-6).

$$\begin{aligned} s_k(n_1,n_2) &= s_{k+1}(n_1+d_1,n_2+d_2) \\ c_{k,k+1}(n_1,n_2) &= s_k(n_1,n_2)*s_{k+1}(-n_1,-n_2) \end{aligned} \tag{2-6}$$

And their corresponding Fourier transforms are:

$$\begin{aligned} S_k(f_1,f_2) &= S_{k+1}(f_1,f_2)\exp[j2\pi(d_1f_1+d_2f_2)] \\ C_{k,k+1}(f_1,f_2) &= S_k(f_1,f_2)S^*_{k+1}(f_1,f_2) \end{aligned} \tag{2-7}$$

Then the amplitude of the correlation in equation (2-7) is normalized so that the phase shift information is achieved:

$$\phi[C_{k,k+1}(f_1,f_2)] = \frac{S_k(f_1,f_2)S_{k+1}^*(f_1,f_2)}{|S_k(f_1,f_2)S_{k+1}^*(f_1,f_2)|} = \exp[-j2\pi(d_1f_1 + d_2f_2)] \quad \textbf{(2-8)}$$

Then the inverse Fourier transform is applied on equation (2-7):

$$c_{k,k+1}(n_1,n_2) = \delta(n_1 - d_1, n_2 - d_2) \quad \textbf{(2-9)}$$

The relative shift will be found on the biggest impulse in the correlation image, as indicted by equation (2-9).

2.4.8 Feature Extraction and Matching

Extensive work has been done on iris image feature extraction and matching through various directions. Generally these methods could be categorized into two areas: methods based on iris image structure analysis and methods based on local image variation analysis.

2.4.8.1 Methods Based on Local Image Variation Analysis

- Daugman uses a multi-scale Gabor wavelet filter to demodulate the iris texture [31]. 1024 complex-valued phasors are achieved by filtering an iris image at different scales using the designed filter. These phasors are then quantized into one of the four quadrants in the complex plane. The final 2048 bit iris code is accomplished by describing the local phasors variation on the complex plane. Hamming distance is employed for matching.
- Sanchez-Reillo implemented a low template size feature extraction and matching method, which is very similar to Daugman's. [35]
- Boles et al. applies a 1-D wavelet transform on all the concentric circles of the human iris image and the zero-crossing points are recorded to represent the local variations [59]. Two dissimilarity functions are used to measure the difference between two feature vectors.
- Sanchez-Avila's method is quite similar to Boles' method and more matching measures are utilized. [36]
- Tan generates a bank of 1D intensity signals from the iris image and filters these 1D signals with a special class of wavelet. The positions of local sharp variations are recorded as the features. The Hamming distance is measured to compare two different iris codes. [77] This is the most famous

method proposed by Tan. Recently, some new methods have been reported, such as ordinal measure based method. [96]

2.4.8.2 Methods based on Iris Image Structure Analysis

- Wildes et al construct a Laplacian pyramid at four resolution levels for iris images to be compared. The normalized correlation is used to compare two images. This method could only work in verification mode.[32]
- Lim et al use a 2-D Harr wavelet transform to decompose the iris image and the fourth level high frequency information is quantized to form the iris code. A modified learning neural network is adopted for matching.[41]
- Park et al decompose an iris image into 8 directional subband using a directional filter bank. The normalized directional energy is coded as feature vector. Euclidean distance is used in feature matching. [84]
- Kumar proposed a correlation based iris recognition method. The 2D Fourier transform is used to transfer the convolution process into product process. Then an inverse Fourier transform is utilized to output the correlation result. If the result shows a sharp peak, the two images are matched. [86]

There are also a lot of more efforts have been done on iris feature extraction and matching. Thus a comparison work for these current methods is highly desirable. Tan et al. conducted some comparison based on CASIA iris database for several leading feature extraction algorithms. These comparative studies mainly focused on academic area. The National Institute of Standard and Technology (NIST) has been conducting and managing the Iris Challenging Evaluation (ICE) project since 2005. The ICE 2006 is the first large-scale, open, independent technology evaluation for iris recognition This ICE project is open to both academic institutes and industrial companies.

The key question about feature extraction is: What is the essentially discriminating characteristic for one iris class to distinguish from others? Tan thinks the local variations, including both intensity variations and orientation variations, are the most distinguishing information for iris recognition. This conclusion could also be supported from the listed recognition methods above, in which the methods based on local image variation analysis generally perform

better than methods based on iris image structure analysis. Daugman's method utilizes the local phase variations to code the iris image and Tan captures the local intensity variations for feature vector. Both the two methods are leading algorithms in feature extraction and matching

The research in iris image feature extraction and matching focuses on two area recently: (1) How the local variation information could be extracted more effectively to represent the uniqueness of its structure. (2) How to speed up this feature extraction procedure to meet the requirement of real time recognition system.

2.4.9 Practical Applications

Iris recognition, as the most reliable biometrics, has been receiving unprecedented attention not only from the research institute, but also from industrial companies and governments. It is employed in more and more practical applications. The followings are some examples of the recent application of iris recognition systems.

- *Iris Recognition Immigration System (IRIS) in UK*: The automated IRIS control barrier is located at the immigration arrival halls as one part of the Immigration and Passport Control. Successfully enrolled passengers could enter the automated IRIS control barrier by looking into an iris recognition camera. The enrolment process takes approximately five to ten minutes, while crossing the IRIS barrier for the enrolled passenger would take 20 seconds. Similar equipments have also been adopted by Amsterdam Schiphol Airport and the United Arab Emirates border control.
- *Biometric Passport*: A number of countries or regions have proposed their biometrics passport plans. A biometric passport is a combination of paper and electronic identity document authenticating the citizenship of travelers by their biometrics, which generally includes faces, fingerprints and irises. The passport's critical information is stored in a tiny RFID chip. The biometrics algorithms are calculated outside the chip by electronic border control systems (e-borders). The International Civil Aviation Organization

(ICAO) defined the biometrics standards for biometric passports and recommended to its member countries.

- *Swiss Bank*: In a bid to better secure their headquarters building Pictet & Cie Bank of Geneva chose to install OKI's iris recognition cameras: IRISPASS-M. These cameras are connected to a central authentication server, which provides the access decision to each room. It is reported that the authentication process only takes two seconds.
- *Lancaster County Prison, Pennsylvania, USA*: A restricted access control system has been installed in this prison. All staff members have been registered in the system as well as some regular visitors on a voluntary basis. Also, this system is used on the booking and release of prison inmates. There are many documented instances where iris recognition has prevented an inmate from perpetrating identity fraud.
- *Pentagon Officer's Athletic Club, Washington, USA:* This system works in a recognition (1 to n) mode and a turnstile is installed to allow only one person through the entrance at a time. The system is integrated to a membership card and an accounting system. Iris recognition has successfully ensured that the membership card can not be abused by non-paying individuals who are not members of the club.
- *City Hospital of Bad Reichenhall, Bavaria:* Iris recognition is installed in the infant station of this hospital to secure access and prevent baby abductions, which is the first time iris recognition has been used for infant protections. Only the authorized person, such as mothers, nurses or doctors, will be enrolled into this system. Once the child is released from the infant station, the mother's registered information will be deleted and she will not be allowed to the station again.

With the price of iris cameras getting cheaper and the public is getting more familiar with the concept of iris recognition, this technology will be further deployed in an even wider area. Nevertheless, enormous research work needs to be done before iris recognition technologies meet the future requirements.

2.5 Research Difficulties and Emphases

As a newly emerging technology, although huge progress has been made in this area, a lot more needs to be done towards a widely suitable, real time iris

identification system. The following are the research difficulties in current iris recognition technologies and thus are also the studying emphases.

- *User Friendly Iris Cameras*: Iris capturing machine used to be the most challenging part in iris recognition research. With the involvement of large electronic & optical companies such as LG, Panasonic in recent years, many prototypes of distant, high resolution, self positioning iris cameras have been made, which greatly boosted the performance and convenience of current iris recognition systems. The research difficulties lie in the imaging process without the attention of the human user being captured. This requires some algorithms to be integrated into the camera such as automatic human face and eye detection, iris liveness detection, image quality assessment, etc.
- *Iris Image Pre-processing Techniques*: The difficulties in iris image pre-processing lie in the following parts: (1) Iris segmentation algorithm has to cope with images captured from different candidates, with different sensors and in various illumination environments. (2) Since iris segmentation occupies a huge amount of time of the whole process, improving the localization speed is very critical towards a real time identification system. (3) In future large, inter-connected and distributed iris recognition systems, the camera model one candidate registered with would not necessarily be the same with the verification camera model. So the two image formats need to be normalized to the same format and size for future coding and matching. In addition, the inter-operationability of different systems using different cameras will strongly depend on the unified iris normalization algorithm. (4) As stated in section 2.4.6, if the iris is excessively compressed or stretched, the iris structure deformation will be non-linear. Although it is not common in daily life, this trait could be abused by some malicious attackers (e.g. offenders using pupil dilating eye drops could be registered twice in a system). It is desirable to propose a non-linear iris normalization method based on physiological research and observation. (5) Effective iris texture is easily contaminated and occluded by eyelash and eyelids, thus greatly degrades the system performance. In order to improve the system

robustness against eyelids and eyelash degradation, an effective eyelid and eyelash detection and removal method is in urgent need.

- *Feature Extraction and Matching*: Feature extraction and matching is always one of the most important problems and therefore the hottest research topic since the emergence of automated iris recognition concept. As stated in section 2.4.8, the intensity and oriental variations of local iris texture is the essentially distinguishing information for recognition. Hence two questions come in this area: (1) How could these essentially distinguishing information be extracted effectively from the local variations in order to achieve higher performance such as higher EER? (2) How could the coding procedure be speeded up for real time applications?

This thesis will focus on the research difficulties in iris image pre-processing and feature extraction, as stated above. In iris localization, the research targets are the speed and accuracy. The aims of eyelash removal algorithm are based on the improvement in Equal Error Rate (EER). At last, a fast and robust iris feature extraction and matching scheme will be proposed and evaluated.

2.6 Summary

In this chapter, the state of the art in most aspects of automated iris recognition technologies has been reviewed. In each aspect, the leading theories and methods have been introduced.

The human iris is firstly introduced anatomically, which shows that iris is composed of several layers and the visual iris texture is the direct result of its multilayered structure. The evidences from clinical observation and developmental biology support that the iris texture is unique for each individual and stable with age. Some interesting biological characteristics, such as hippus, contraction with illumination, would be very useful in live specimen detection. Thus the physiological base for human iris recognition is built.

Then the iris recognition history, from bodily measurements in the beginning to the prototypes of automated iris recognition system, is briefly introduced.

High quality iris images and user-friendly capturing environment are the two key challenges for iris cameras. Some basic designing ideas for iris capturing machine are mentioned in the chapter, followed by the review of the leading iris cameras. Iris on the Move (IOM) by Sarnoff is mentioned in particular for its highly non-cooperative capturing environment.

Iris liveness detection techniques are highly desirable for recognition systems. Although it is under-researched, a lot of researching directions have been inspired by the iris recognition system properties such as Hippus, Pupillary light reflex, etc.

The current quality assessment method could be categorized in two: space domain based and frequency domain based. (1) The concepts often used by space domain based methods are: intensity, gradient, edge point distribution, etc. The methods proposed by Zhang et al. or Kee et al. are space domain based. (2) In frequency based methods, Fourier transform or wavelet transform are applied to the whole iris image or different local areas within this image. As the transformed image is concerned, the low frequency describes the general information of the image while the high frequency depicts the detailed minutiae. Thus, the clear images, which have many detailed iris structures, should contain much middle frequency or high frequency information in the transformed domain, while the defocused images should contain more low frequency information. The methods proposed by Daugman, Tan, Kalka, Jain are generally frequency domain based.

Iris segmentation occupies a huge portion of time within the whole iris recognition procedure. And thus it is the bottleneck for a practical real time identification system. The speed and accuracy are the two keywords for iris segmentation. The leading methods will be introduced, as well as a fast and robust segmentation method proposed in chapter four.

Iris image normalization copes with the iris elastic deformation and the non-uniform background illumination. Uneven illumination removal is generally

undertaken by common image enhancement techniques such as histogram equalization. Daugman uses the rubber sheet model to compensate the iris deformation. Wildes et al. uses an image-registration technique to compensate for both elastic iris deformation and rotation. The normalization methods used by Tan, Kim, Sanchez-Reillo, Kim, Monro, etc. will map the localized iris image into a fixed size rectangular image to ease the registration and coding steps. The medical study results of the pupil movement effect on iris structures are also listed in this chapter.

Due to the iris structure movement characteristics mentioned in this chapter and that the iris images have already been normalized, the iris image registration problem is restricted to the translation compensation issue between the reference image and its sensed counterpart.

Huge amount of work has been done on iris image feature extraction and matching through various directions. Generally these methods could be categorized into two areas: methods based on iris image structure analysis and methods based on local image variation analysis. Some algorithm evaluation and comparison work has been done yet further efforts are still required. The author agrees with the idea proposed by Tan that the local texture variations (including intensity variations and orientation variations) are the essentially distinguishing characteristic for one iris class to be different from others. Nevertheless, how to code such local variations more effectively in order to achieve a more robust and faster system is still under research. Chapter five will focus on this issue.

After stating the typical applications of iris recognition technology, the research difficulties and emphasis in this area are summarized. And this thesis will focus on the researching difficulties in image pre-processing, feature extraction and matching.

In order to fulfill the research targets in this project, an iris recognition researching platform is in need. Based on the extensive study and review on the literatures and standards, the Bath Iris Recognition Research Environment

is built in order to facilitate the research in Bath University. The next chapter will give an introduction to this environment.

3 Building Research Environment

3.1 Foreword

The Bath Iris Recognition Research Environment is the foundation for the research project to be carried out. Based on extensive literature and standards review, this platform is built. With the progress of our research, this platform will be upgraded accordingly and the research based on the platform will also be boosted by the platform upgrade. In this chapter, the environmental structure will be introduced briefly. Then the Bath iris image capturing machine will be illustrated, followed by the introduction of Bath iris image database established using the Bath iris image capturing machine. After that, an automatic image sorting algorithm used in Bath Research Environment is reported. At the end of this chapter, the basic iris image pre-processing techniques employed are illustrated.

3.2 Environment Structure

As shown in Figure 3-1, Bath Iris Recognition Research Environment could be divided into four parts: Iris Image Capturing System, Image Pre-processing system, Feature Extraction & Matching Scheme, Bath Iris Image Database. With the iris image capturing system, the dynamic video sequence of iris images could be seized and used for iris liveness detection. Based on the quality assessment and automatic sorting module, the Bath iris database is built and shared for with other researchers around the world. The software modules, like the image pre-processing module or the feature extraction and matching module, are upgraded with the research progress in these modules. Thus the research environment is getting better and better. The units surrounded by broken lines in Figure 3-1 are what the research will focus on in this platform.

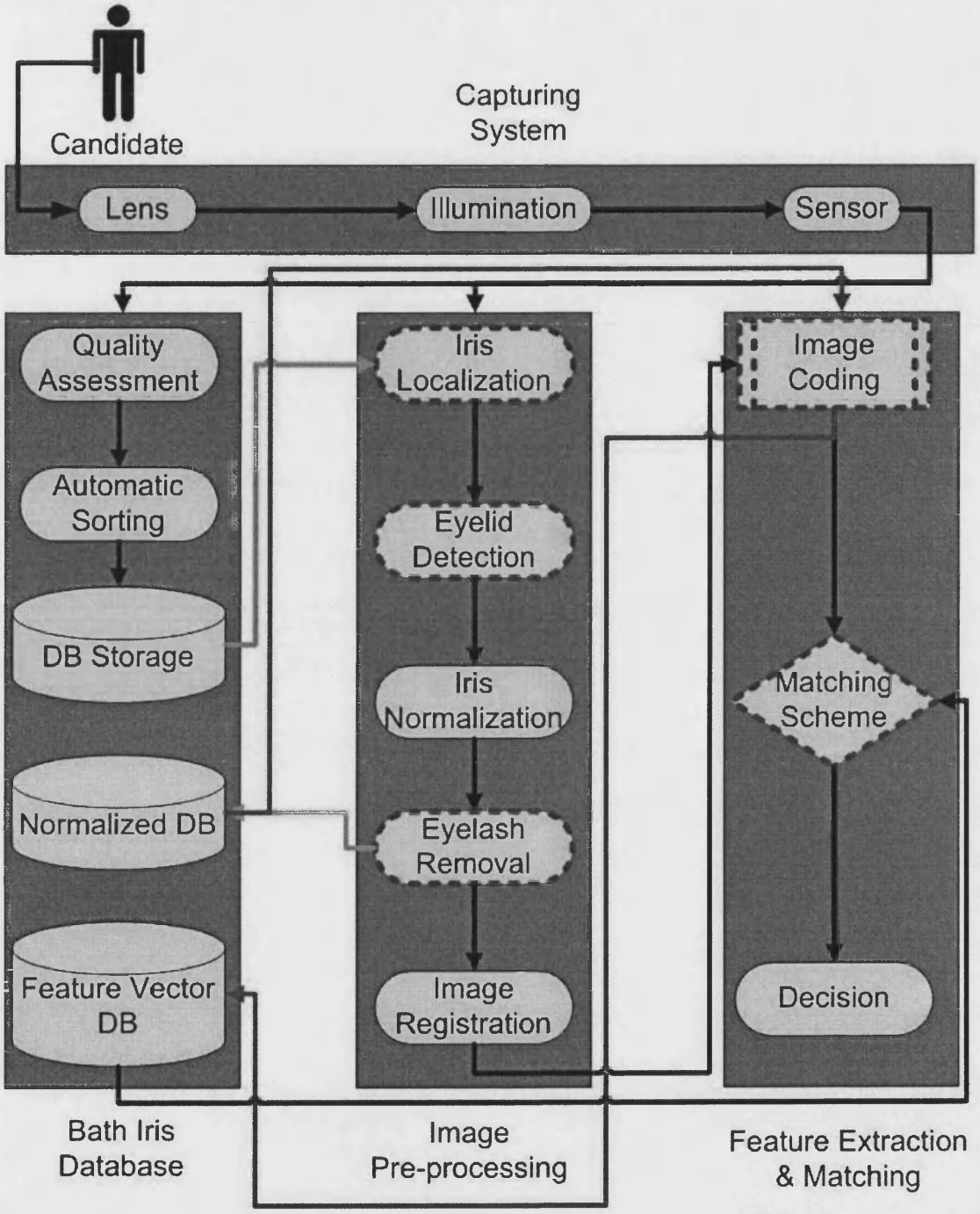

Figure 3-1 Bath Iris Recognition Research Environment Structure

3.3 Iris Camera Design

In order to assemble the iris image capturing machine, a high resolution machine vision camera is mounted on a height-adjustable camera stand equipped with a chinrest, with a set of infrared LEDs positioned below the camera, as shown in Figure 3-2 and Figure 3-3.

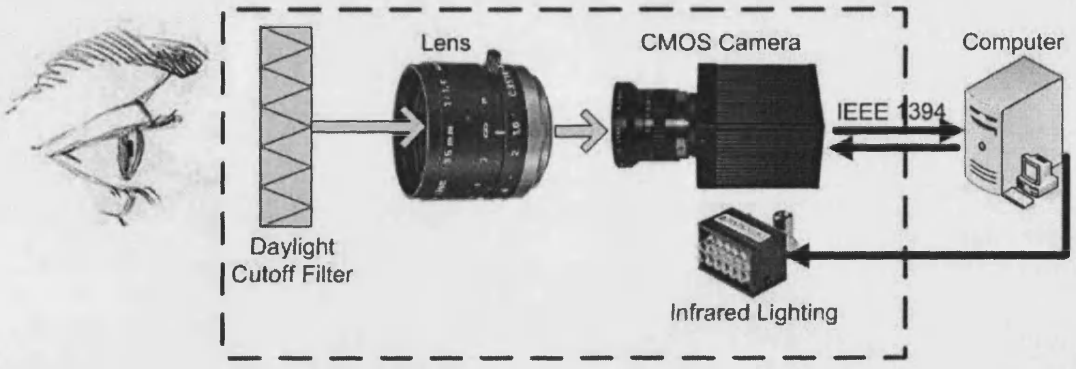

Figure 3-2 Iris Image Capturing Machine

Figure 3-3 Bath Iris Camera in Use

The ISG LightWise LW-1.3-S-1394 firewire camera is chosen for its good spectral response in the near-infrared region. It has a 1.3 mega-pixel CMOS sensor and the video output from the camera is fed to the computer through the IEEE 1394 port.

In order to maximize the use of the entire image resolution a Pentax C-3516 M, 35 mm lens with two extension rings is used to capture the iris image. In order to get a high-contrast image of the iris, the lens is focused on the iris and not any other part of the eye like the eyelashes or the pupil.

It is widely believed that iris textures will be imaged in high contrast under near-infrared (NIR) wavelength lighting. In the capturing system, an infrared LED array is used to illuminate the human iris to be captured from a distance of around 30 cm. The wavelength of the NIR light source peaks at 820nm. Some regulations prescribe the infrared radiation intensity on human eyes to protect the cornea, retinal from burn and possible delayed effects on the human lens, such as cataract. The International Commission on Non-Ionizing Radiation

Protection (ICNIRP) regulates that 10mW/cm^2 should be the limit. The British Standard Institute (BSI) suggests 0.77mW/cm^2 for LASER, which is widely accepted in Europe. Experiments confirm that the infrared radiation reaching the human eye in Bath iris capturing system is under 0.5 mW/cm^2 at its peak. Additional visible light LEDs are also aligned within the infrared light source to enlarge the iris area, by which the infrared light amount entering the eye will also be reduced. The light source is mounted below the camera in order to prevent shadows from appearing over the iris due to eyelashes.

A daylight cut-off filter RM-90 IR filter is chosen to remove reflections caused by daylight and other environmental light sources. The filter passes Infrared light without any attenuation and cut-off most of the visual light with wavelength below 780nm.

3.4 Bath Iris Image Database

A major hindrance to research in the field of iris recognition has been a shortage of publicly available images. With other biometrics such as face and fingerprints, there is access to thousands of images from various sources, but until recently the only readily available source of iris images has been the CASIA database. Although this dataset has proved to be invaluable, its lack of variety may have led to the design of somewhat biased systems. Recently, other iris image datasets have been assembled. As a contribution to this process, we are gathering high quality iris images from students and staff of The University of Bath comprising subjects from a variety of backgrounds. At the time of writing, over 800 classes have been collected. The images from each candidate were taken in the same session. The age, ethnicity and gender breakdown of a superset is tabulated in Table 3-1. When capturing the iris image, the subject is asked to place his chin on the chin-rest as the camera is focused onto his iris. Since the depth field is very small, the camera is then manually tuned to focus on the iris part instead of other parts like eyelid or eyelash. The subject is asked to blink or look aside to change their pupil size during the capturing procedure. Spectacles are suggested to be taken off in the capture process while hard or soft contact lenses will not be asked the same.

The whole capturing route will cost around five minutes for each subject averagely.

Age	%	Ethnicity	%	Gender	%
6 ~ 25	57.2	White	67.2	Female	48.3
26 ~ 35	22.5	Black	8.0		
36 ~ 45	8.7	Southern Asian	3.6		
46 ~ 55	5.1	Oriental	15.3	Male	51.7
56 ~ 65	6.5	Others	5.9		

Table 3-1 Breakdown of Bath Iris Image Database

Unique identification token (Student Library ID Card, Driving License, etc.) is asked to be shown prior to image capture in order to avoid duplicate registration. Before image capture, the subjects are made aware that their personal information will not be divulged to the third party unless specifically asked to do so by the court.

3.5 Automatic Image Sorting

A video sequence consisting 200 images will be seized for each eye during one capture action with Bath iris image capturing system. During the capturing procedure, the candidate will be asked to blink or look away in order to get a variety of pupil sizes. Therefore, inevitably some bad quality images would exist within the 200 frame video sequence. Occlusion, motion-blur, defocus and off-angle are four types of most common image problems under Bath iris image capturing system. Occlusions are generally caused by eyelid, which occur when the candidate blinks during capturing procedure. Since the depth-of-field of the camera is quite small, a small move for the candidate from the focal plane would cause serious defocus in the captured images. The eye movement or the head tilt on the focal plane could result in motion blur. When the candidate's eye looks away from the direct line of sight of the camera-lens, the off-angled images would have a distorted iris shape and partial out-of-focus. Thus an automatic image sorting algorithm is in need.

The automatic image sorting method employed in Bath system is based upon the analysis of specular reflection in the pupil. (1)The images first should be down sampled to 160X120 to reduce the computational complexity without information loss for image screening. (2) Then a horizontal line gray scale difference analysis is carried out, summed over a 5-pixel-wide region. If the biggest intensity change is smaller than a threshold, the specular reflection is deemed to be outside the pupil. Thus this image is rejected. (3) The candidate specular reflection is scanned in rows to find its width. If the width is not within the pre-assumed range, go back to step 2 and check the second biggest intensity change. The maximum times jumping back to step is 5. (4) The light-to-pupil change in graylevel, over a 5 pixel region, is evaluated and compared against a minimum cutoff to check if the light is at the edge of the iris. (5) The height of the specular reflection is also checked to be within the proper range. This method is simple yet quite robust. Also its low computational complexity meets the requirement for real time image sorting. Figure 3-4 lists various bad quality images rejected by Bath iris image sorting software.

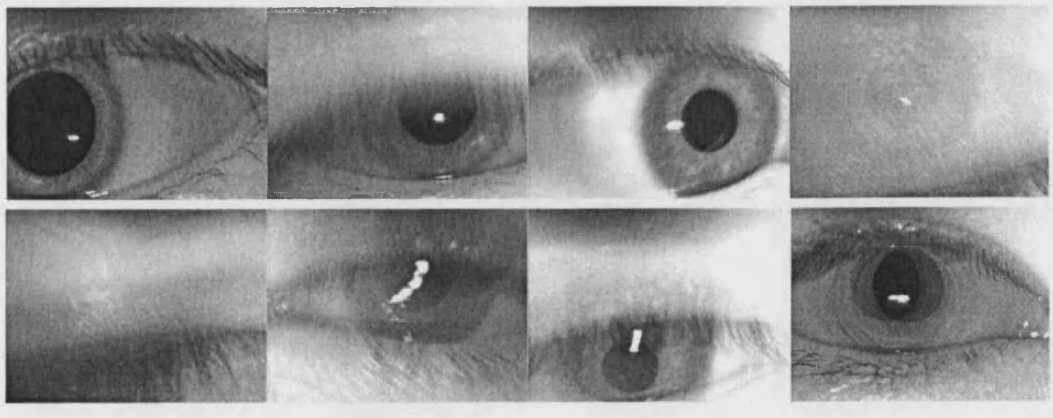

Figure 3-4 Rejected Images

3.6 Iris Image Pre-processing

A preliminary iris pre-processing method should be implemented first, based on which the future research could be carried out. The initial pre-processing scheme includes iris boundary localization and iris image normalization (image

unwrapping and image enhancement). Figure 3-5 illustrates different steps in our preliminary iris image pre-processing method.

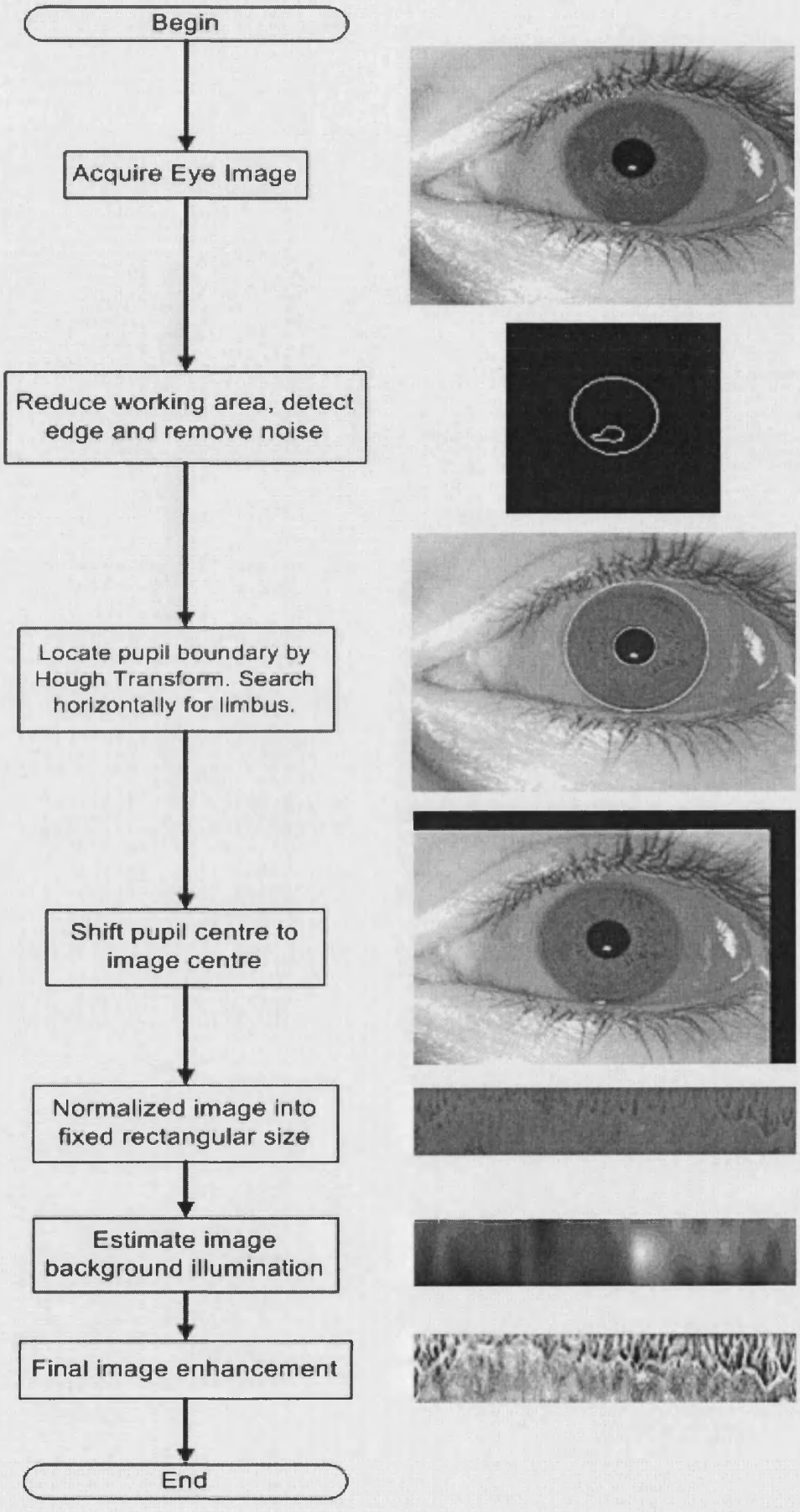

Figure 3-5 Preliminary Iris Image Pre-processing

3.6.1 Iris Localization

The iris is an annular portion between the pupil and the sclera. Both the inner and outer boundaries of a typical iris can approximately be taken as circles. As mentioned in section 2.2, the two circles are usually not concentric.

Location of the pupil and outer iris boundaries starts with the removal of the bright spot in the pupil caused by the reflection of the infrared light source. This reduces the influence of high gray level values on the gray scale distribution. Then the image is scanned to isolate a region containing the pupil and iris. This is done based on the assumption that the majority of image rows and columns passing through the pupil will have larger gray level variance than those not passing through the pupil. It is assumed that the pupil is circular and because the pupil boundary is a distinct edge feature, a Hough transform is used to find the centre and radius of the pupil. To locate the outer boundary of the iris (limbus) a horizontal line through the pupil centre is scanned for the jumps in gray level on either side of the pupil. Chapter four will propose a fast and effective iris segmentation method.

3.6.2 Iris Image Unwrapping

Since the pupil and the limbus are not concentric, *P* and *I* are assumed to be the centres of the pupil and iris respectively, as is shown in Figure 3-6. Each radius *MN* on the iris annulus should be mapped linearly onto the fixed sized rectangular iris. Due to the non-concentricity, the length of *MN* varies with the angle θ. The calculation of the MN length is illustrated as follow:

$$\begin{aligned} MN &= PN - PM \\ &= PN - R_p \\ &= \sqrt{R_i^2 + PI^2 - 2 * PI * R_i * \cos \measuredangle PIN} - R_p \end{aligned} \tag{3-1}$$

$$\cos \measuredangle PIN = -\cos(\theta + \measuredangle PNI) \tag{3-2}$$

$$\measuredangle PNI = \arcsin\left(\frac{\sin\theta * PI}{R_i}\right) \tag{3-3}$$

In practical implementation, the intensity value of each pixel on the normalized iris is calculated by mapping back linearly to a position on the original image. This position will not be always exactly with integral coordinates, so the normalized gray value is obtained by bilinear interpolation from its four nearest neighbours.

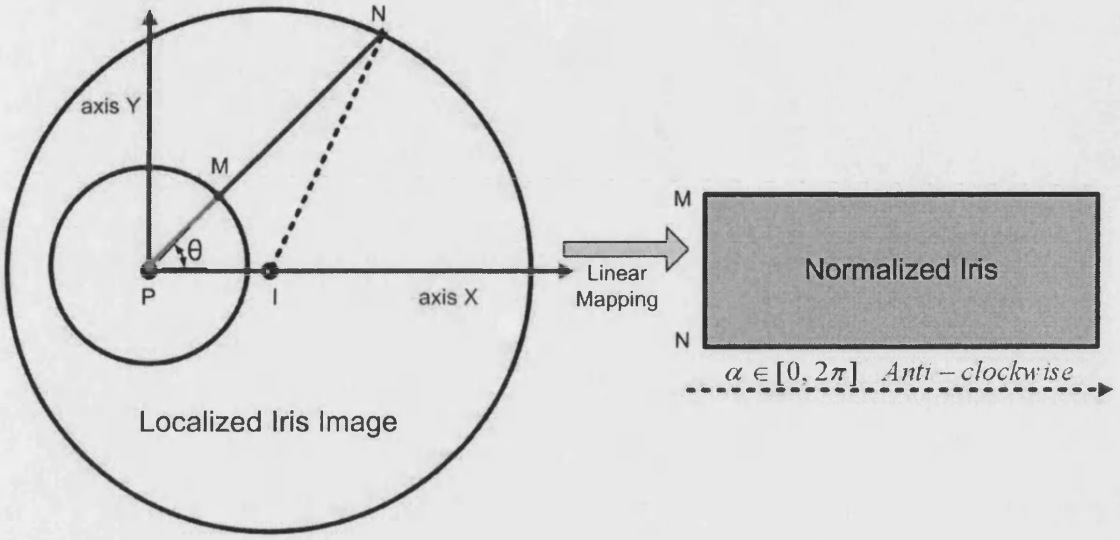

Figure 3-6 Iris Unwrapping Model

3.6.3 Iris Image Enhancement

Iris image enhancement has been mentioned specifically in few literatures. The method employed in Bath Iris Research Environment is quite similar to Tan's method [77]. This method first estimates approximately the background illumination on the normalized iris image. The normalized image is first divided into small blocks and the mean intensity value of each block is calculated. Then the background illumination is achieved through interpolation. After that the estimated background illumination was subtracted from the normalized image to compensate for a variety of lighting conditions. Then the local histogram equalization is applied to the lighting corrected image. The visual effects of such operation could be seen in Figure 3-5.

3.7 Summary

Based on extensive literature and standards review, the Bath Iris Recognition Research Environment is built as the foundation for the research project to be

carried out. This environment could be divided into four parts: Iris Image Capturing System, Image Pre-processing system, Feature Extraction & Matching Scheme, Bath Iris Image Database.

In order to assemble the iris image capturing machine, a high resolution machine vision camera is mounted on a height-adjustable camera stand equipped with a chinrest, with a set of infrared LEDs positioned below the camera.

Using the iris camera assembly in Bath, A high quality Bath Iris Image Database is established. This high quality database will make the image coding research purely focus on the distinguishing information extraction.

A robust and low complexity iris image sorting method based on the analysis of specular reflection is employed. By studying the position, width and height of the specular reflection, the received amount of images from the camera is greatly reduced, and thus the system load and false recognition rate will be evidently decreased.

A preliminary iris pre-processing method should be implemented first, based on which the future research could be carried out. The initial pre-processing scheme includes iris boundary localization and iris image normalization (image unwrapping and image enhancement).

The methods for better iris segmentation, feature extraction, matching and eyelash removal will be the research emphasises based on the researching environment.

4 Robust and Time Efficient Iris Segmentation

4.1 Foreword

Iris segmentation includes iris localization and eyelid removal. Iris segmentation locates the iris portion in the eye image by finding the parameters of the iris boundaries and the eyelid shape occluding the iris area. To make the depiction easier, the inner iris boundary is called pupil and the outer iris boundary called limbus. Pupil and limbus are generally approximated as circles, yet they are not concentric. If the iris area is also occupied by eyelid, these occluded areas should also be detected and eliminated. Generally, parabolic curves are used to fit the eyelid shape.

Iris segmentation is one of the research difficulties and considered as the bottleneck in real time iris recognition systems because of the following reasons: (1) Correct and accurate segmentation is the precondition for image coding and matching, and thus is the premise of the success of the whole iris recognition system. (2) Many iris image pre-processing methods, such as image quality assessment, iris normalization, also need the segmentation results to carry on. (3) Iris segmentation is generally the most time consuming stage in the whole recognition procedure. Thus it is the bottleneck in building the real time iris identification system. (4) Iris segmentation has to cope with pictures taken by enormous numbers of iris cameras under different illumination circumstances.

Iris segmentation is the key stage for the success of the whole iris recognition system. Speed and accuracy are the two key evaluating points for iris segmentation methods. In this chapter, some leading localization methods will be introduced first. Then a robust and time efficient iris segmentation method will be proposed and compared with the current leading solutions.

Compared with eyelid removal, iris localization is more important. Iris localization is essential to any iris recognition systems, while eyelid removal is only necessary for severely occluded images. For some iris recognition algorithm, eyelid removal is not performed for the interest of low computational complexity. In the description of the proposed iris segmentation method, the iris localization method will be illustrated in detail and tested thoroughly at first. Although eyelid removal is not necessary in Bath system for its high quality input images, a fast and effective eyelid removal method will still be presented after the description of iris localization.

4.2 Current Solutions

4.2.1 Daugman's Segmentation Method

Daugman uses an integrodifferential operator to fit the circular contours of both pupil and limbus [31].

$$\max_{(r,x_0,y_0)} \left| G_\sigma(r) * \frac{\partial}{\partial r} \oint_{r,x_0,y_0} \frac{I(x,y)}{2\pi r} ds \right| \qquad \textbf{(4-1)}$$

Where $I(x,y)$ is an iris image and the algorithm will search over the image domain (x,y) for the maximum in the blurred partial derivative with respect to increasing radius r, of the normalized contour integral of $I(x,y)$ along a circular arc ds of radius r and center coordinates (x_0,y_0). $G_\sigma(r)=(1/\sqrt{2\pi}\sigma)e^{-(r^2/2\sigma^2)}$ is a Gaussian filter with scale σ that smoothes the image to select the spatial scale of edges under consideration. The symbol $*$ denotes convolution. Daugman's method starts with a set of centroids (x_0,y_0) and searches iteratively for a maximum contour integral derivative along the changing radius r. It is a searching of 3D parameters space (x,y,r).

Since the images Daugman copes with have more obvious limbus than pupil. The outer boundary of iris is found before the inner counterpart. Both boundaries are found using equation (4-1).

In eyelid detection, the path of contour in equation (4-1) is changed from circle to arc, with spline parameters fitted by standard statistical estimation methods to describe optimally the available evidence for each eyelid boundary.

4.2.2 Hough Transform Based Methods

Hough transform is a quite effective method detecting shapes in images, noted for its insensitivity to missing parts of curves, to image noise, and to other structures co-existing in the image. Considering an example of circle detection, the 3 parameters of a circle form an integral parameter space, where one point corresponds to a circle in the original image. First the edge detector is applied to the original image and all the pixels with edge magnitude exceeding some threshold will be set value 1 while other pixels 0. To each edge point in the original binarised edge image, in the parameter space will be corresponded to a cone surface. Each point within the cone surface corresponds one circle passing through that edge point and thus would be added by one. The whole parameter space works as an accumulator and the maximum point in the parameter space will be picked out. Its 3D coordinates in the parameter space are the three parameters defining the circle in the original image.

The robustness of Hough transform is caused by the robustness of transformation from the image space into the parameter space. A missing part of the circle will cause only a lower local maximum because smaller number of edge pixels contributes to the corresponding points in the parameter space. Even though the Hough transform is a very powerful technique for curve detection, exponential growth of the parameter space data with the increase of the number of curve parameters restricts its practical usability to curves with few parameters, such as lines or circles.

The iris segmentation methods utilized by Wides et al, David Zhang, Tisse et al and Tan et al are generally Hough transform based [32, 2, 37, 77]. These methods normally consist of two steps: edge detection and Hough transform voting. Wides' method will be illustrated here as an example.

The edge-map is recovered via gradient-based edge detection and magnitude thresholding.

$$\left|\nabla G(x,y) * I(x,y)\right| \tag{4-2}$$

Where

$$\nabla \equiv (\partial/\partial x, \partial/\partial y) \tag{4-3}$$

$$G(x,y) = \frac{1}{2\pi\sigma^2} e^{-\frac{(x-x_0)^2+(y-y_0)2}{2\sigma^2}} \tag{4-4}$$

Equation (4-4) is a 2D Gaussian smoother with center (x_0, y_0) and standard deviation σ, which could define the spatial scale of edges under consideration. The horizontal edge information is mainly used to avoid the influence of eyelid boundaries.

Assuming (x_j, y_j), $j = 1,2,...,n$, is a set of edge points, the Hough transform voting procedure could be described using the following equations:

$$H(x_c, y_c, r) = \sum_{j=1}^{n} h(x_j, y_j, x_c, y_c, r) \tag{4-5}$$

Where

$$h(x_j, y_j, x_c, y_c, r) = \begin{cases} 1, & if \ \ g(x_j, y_j, x_c, y_c, r) = 0 \\ 0, & otherwise \end{cases} \tag{4-6}$$

$$g(x_j, y_j, x_c, y_c, r) = (x_j - x_c)^2 + (y_j - y_c)^2 - r^2 \tag{4-7}$$

For each parameter set (x_j, y_j, x_c, y_c, r), $g(x_j, y_j, x_c, y_c, r) = 0$ represents that the circle (x_c, y_c, r) passes through the edge point (x_j, y_j). The parameter set (x_c, y_c, r) maximizing H is chosen as the iris boundary.

In implementation, the parameter space is structured as a 3D array accumulator, which is indexed by the discretized values for x_c, y_c and r. Once the accumulation is done, this 3D array is scanned for the maximum value.

Similar techniques would be utilized in eyelid detection. The vertical edge information is utilized for eyelid boundaries instead of horizontal edge information. Then these vertical edge points would be used to voted in the parameter space in Hough transform, modeled as parabolic arcs.

4.2.3 Research Difficulties in Iris Segmentation

Both the integrodifferential based method and the Hough transform based methods have achieved good performance. However, as mentioned earlier, the iris segmentation step is still the most time consuming stage in the whole iris recognition procedure. In many systems, it could almost take half of the time. Thus the time efficiency of iris segmentation algorithms is still the hot research topic in iris recognition systems. In order to promote the research in real time iris recognition systems, a new iris segmentation algorithm with low computational complexity and high accuracy is proposed in this thesis. The iris localization method will be illustrated in detail and tested thoroughly at first, followed by the description of an effective eyelid removal method.

4.3 Proposed Iris Localization Method

4.3.1 Reduce Working Area to Pupil Area

Taking one image sample from the Bath database as an example, shown in Figure 4-1, the proposed iris localization method would be illustrated based on it.

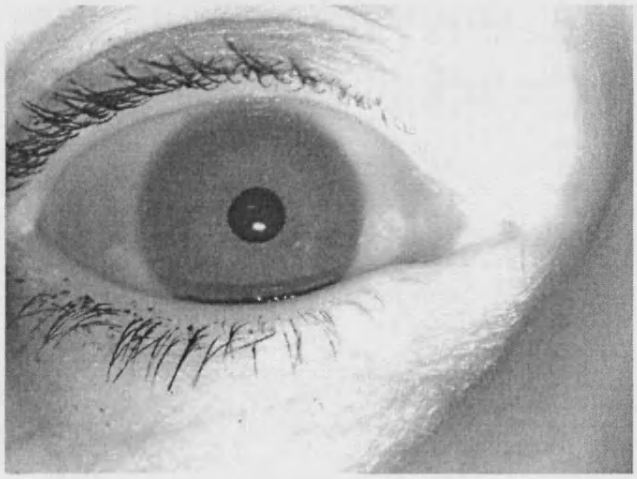

Figure 4-1 Example Image

The input iris images captured by different cameras could have different size, gray scale depth or colors. These variables should all be normalized in order to

make the algorithm parameter setting easier. In this case, every input image would be converted into a 640X480, 8 bits grayscale image.

The illumination status will also be checked before further process. If the average grayscale intensity is lower than 80 or higher than 240, this image would be rejected because it is too dark or bright.

The vital issue for accurate iris localization is to find the pupil area correctly. In all the images which have been coped with through Bath iris recognition software, the pupil boundaries are generally much more obvious than the limbuses. Thus pupils are firstly localized before limbuses. Provided that pupil is a fairly small area within the eye image, interfered by strong eyelashes, heavy eye brows and environmental illumination, it could be quite difficult to find the pupil area for some images.

According to literature, the leading method for pupil area finding is by projecting the whole image vertically and horizontally, the darkest point in each axis is supposed to be the coordinate of the rough pupil center. This method is based on the idea that the pupil is the biggest dark area in the image and the projection line across its center contributes least intensity compared with its other parallels. Yet in practical applications, huge eyelash block, artificial eyelashes, heavy eyebrows, etc, will form even bigger dark area than the pupil. In this thesis, a new pupil area finding method based on the standard deviation analysis for each projection line is proposed. Based on the wide test on different image databases such as CASIA, Bath, LG, NIST, Sarnoff, Retica, UBIRIS, SecurimMetrics, this pupil area finding method could work reliably, thus found the basement for successful iris localization. The iris localization results will be shown later in this chapter, which could prove the performance of this pupil area finding method.

Firstly, the margin area for the re-sampled iris image would be masked as shown in Figure 4-2, in order to eliminate the influence of eyebrows, irregular illumination noise, which could disturb future detection.

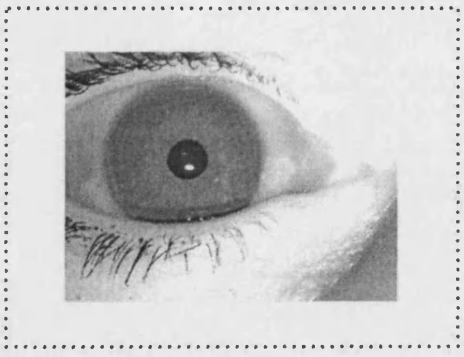

Figure 4-2 Margin Masked Image

Then the standard deviation of each image column is calculated and the top 50 columns are chosen, as shown in Figure 4-3. The blue curve shows the standard deviation distribution, among which the top 50 are shown by red lines.

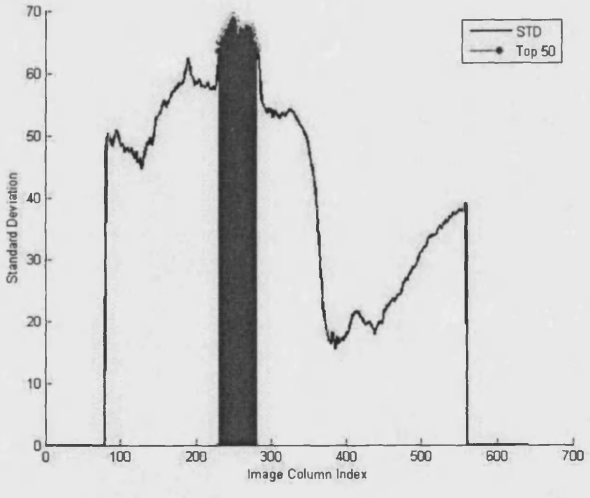

Figure 4-3 Standard Deviation Analysis

The median index of the top 50 columns is calculated as *Median_x*. Then for the top 50 columns near the *Median_x*, Their mean value is supposed to be x-coordinate of the rough pupil centre. If the rough x-coordinate is too far away from the rough pupil centre, Mask these local columns and re-do this step. Then the working area in reduced accordingly, as shown Figure 4-4.

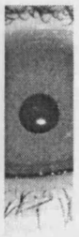

Figure 4-4 Horizontally Reduced Image

Now, the horizontally reduced image will be projected to the y axis and the top 40 darkest rows will be chosen and their median calculated as *Median_y*. Then for the top 40 rows near the *Median_y*, Their mean value is supposed to be y-coordinate of the rough pupil centre. If the rough y-coordinate is too far away from the centre, Mask these local rows and re-do this step. Thus the pupil area is found. The contrast of the pupil area image is enhanced in order to give prominence to the pupil boundary, as is shown in Figure 4-5.

Figure 4-5 Original & Enhanced Pupil Area

4.3.2 Adaptive Canny Filter

A threshold adaptive canny edge detector is designed to make the number of edge points in a certain amount using a self-adaptive threshold variable. In implementation, the threshold of a normal canny edge detector will adjust itself according to the numbers of edge points, until the number is within a range. The 8-connected areas are labeled, where areas containing less than 50 pixels are

removed to reduce noise. The example binarised edge point image is shown in Figure 4-6.

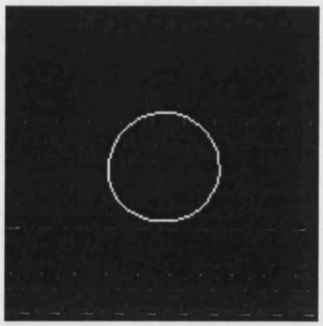

Figure 4-6 Binary Image for Pupil Area

The contrast of the pupil area image is enhanced in order to give prominence to the pupil boundary. The biggest 8-connected continuous area is chosen and all of its edge points are stored in a 2D array. The edge points in this 2D array will be used to calculate the pupil boundary parameters. If it failed, the second biggest 8-connected continuous area will be the substitute, as so on.

Hough Transform is utilized most often in this situation. In order to reduce the complexity in Hough Transform method, some improved algorithms, such as Connective Hough Transform (CHT), Random Hough Transform (RHT), have been proposed. Inspired by RHT, random picking became a new way to speed up the curve fitting procedure. Tan mentioned a circle fitting method for iris localization by random picking four pixels each time, but this method has not been described in detail. Enlightened by Tan's method, this thesis will propose an iris localization scheme based on Random Sample Consensus (RANSAC).

4.3.3 RANSAC Introduction

The RANSAC algorithm is an algorithm for robust fitting of models, introduced by Fischler and Bolls in 1981. It is robust for its good tolerance to outliers in the experimental data and capability of interpreting and smoothing data containing a significant percentage of gross errors. [87, 88, 89]

The basic idea for RANSAC is very straightforward. First, samples are picked randomly from the input data set, in which each point has the same probability of selection. Then a model hypothesis is constructed by computing the model parameters using the sample data. The size of the sample depends on the model parameters. For example, in pupil boundary fitting, the circle model only has 3 parameters. Thus the sample size is consequently 3. Next, the hypothetical model quality is evaluated on the full input data, in which a cost function is needed to compute the model quality. Generally, the number of data points agreeing with the model within an error tolerance (inliers) is calculated by cost function. Normally, the model parameters estimated by RANSAC is not very accurate. Thus a finer estimation using for example a least-square fit based on the inliers is utilized to get a precise result. If the input data set contains several distinct curves, the model parameters for the first model are estimated and the inliers points for this model will be removed from the input data set. Then the algorithm is simply repeated with the remainder of the input data set to find the next model.

Here the RANSAC algorithm will be described step by step:

1. The input data set is X and its size is x. The curve model has n parameters, which means the random sample should have n points as well.
2. From the random sampled set $S(S_1, S_2, \cdots\cdots, S_n)$, the hypothetical model is calculated as $P(P_1, P_2, \cdots\cdots P_n)$.
3. If an input data point is within the distance L from the hypothetical model, this point is regarded as an inliers point to this model, i.e. L is the distance tolerance for inliers. In this way, the inliers data set M is selected from X according to L. The size of M is m.
4. Assume t is the inliers threshold for a hypothetical model to be approved as a real curve.
   - If $m \geq t$, the hypothetical model $P(P_1, P_2, \cdots\cdots P_n)$ is approved to be the real model.
   - Else, go to step 2, re-sample n points and repeat the above process.
5. Some optimization techniques could be used based on the inliers data set to get a optimized model $P^*(P_1^*, P_2^*, \cdots\cdots P_n^*)$.

6. Each time a random sample is selected, the accumulator *count* will self increase till exit when $count = k$.

Figure 4-7 is the flowchart for a typical RANSAC algorithm.

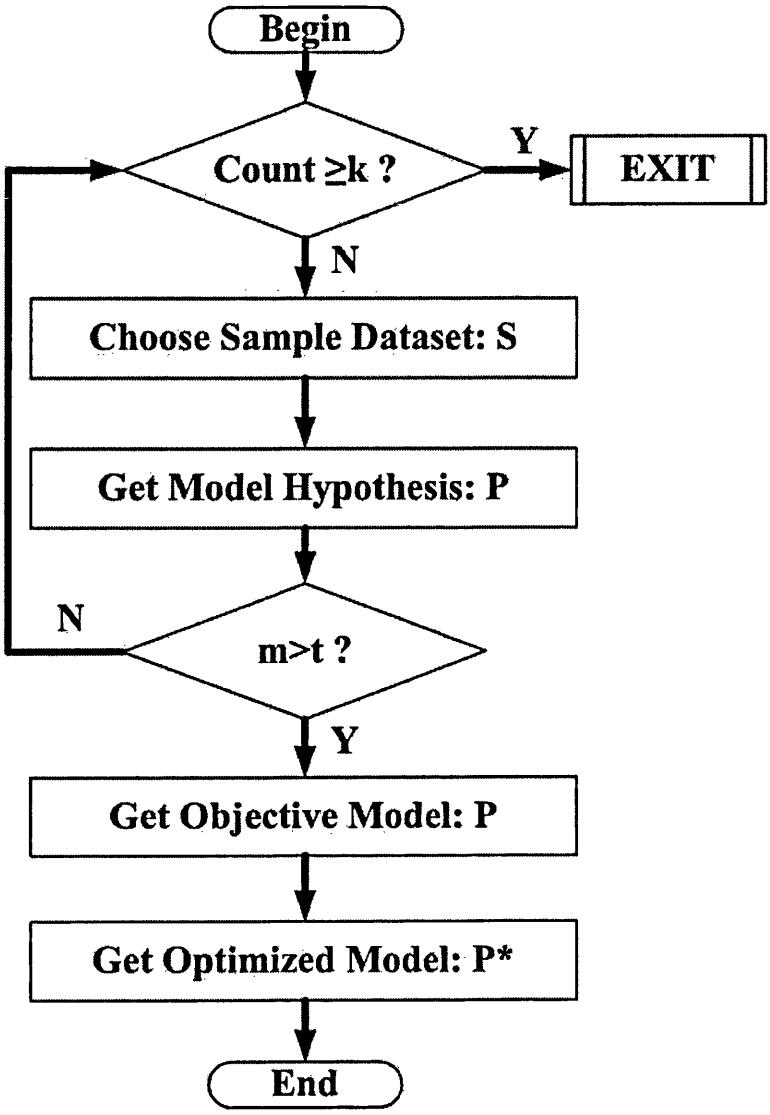

Figure 4-7 RANSAC Flow Chart

4.3.4 Pupil Boundary Fitting Based on RANSAC

4.3.4.1 RANSAC Control Parameters

Based on the general RANSAC idea, the pupil boundary is localized as shown in Figure 4-11. Before implementing the RANSAC algorithm, two control parameters need to be decided.

- ***Sample Iteration Limit*** k **:** Assume g is the probability that denotes success objective model finding after k sample iterations, then

$$(1-g)=(1-v^n)^k \quad \text{(4-8)}$$

$$\Rightarrow k=\frac{\log(1-g)}{\log(1-v^n)} \quad \text{(4-9)}$$

Where

$$v=m/x \quad \text{(4-10)}$$

Normally, the noise ratio in the pupil area won't be higher 40%, thus generally v will be bigger than 60%. Assuming $v=0.6$, after k sampling iterations the objective model find probability g should be equal to 99.99%. According to equation (4-9)(4-9)(4-9), k is calculated as 37.85. $k=37.85$ is only a theoretical value. In its implementation in Bath, we choose $k=600$ in order to increase the algorithm reliability.

- ***Inliers Point Threshold*** t**:** For model hypothesis, its inliers data set is found as M with the size m. If $m>t$, this hypothetical model is regarded as the object model. Otherwise, another sample set is chosen to repeat the RANSAC procedure.

Supposing P is a hypothetical model yet not the real object model, m_P is its inliers number and $y=m_P/x$. The real value for y is unknown, but generally $y<v$. Assuming $v=0.6$, the threshold t should make y^{t-n} equals to a very small value. y^{t-n} would be very small when t equals to 20.

In Bath system implementation, t is not a fixed value. The adaptive canny edge detector could only constrict the edge point number into the same order to magnitude. Thus for some images having more edge points, threshold t could authorize some false model. While for images with less edge points, t would be too high for a real object model. A dynamic decreasing t is adopted in Bath system, in which t first starts with a maximum value. If the real object model is not found after $k=600$ times samples, the inliers point threshold t would decrease and re-do $k=600$ times samples, and so on till the real object model is found or t reaches its minimum value and exit.

4.3.4.2 Additional Checks for Objective Model Confirmation

The RANSAC algorithm only requires the inliers point number to be checked after the hypothetical circle is found, which is not enough to eliminate the false model according to the practice in Bath system. In this thesis, some more practical checks have been proposed and achieved very good performances. These checks are generally based on the reduced 8-bit grayscale image instead of the edge point binary image.

- ***Average Pupil Intensity Check:*** All the pixels within the hypothetical pupil circle will be collected and their average intensity will be calculated as $Pupil\_Intensity$. Generally, $Pupil\_Intensity$ should be smaller than 80.

- ***Pupil Pixel Intensity Distribution Check:*** Find all the pixels within the hypothetical circles. Get the histogram of these pixels and bin them as shown in Figure 4-8. If the hypothetical model is the real pupil boundary, most of these pixels should be in one bin (Bin1). Otherwise, the hypothetical circle would contain areas with different intensity values and the pixels in it would be categorized into two or three bins. In Figure 4-8, Bin1 contains the pupil related pixels and Bin2 contains the iris related pixels. The hypothetical model is considered as a false model if equation (4-11) is satisfied.

$$\left\{\frac{size(Bin2)}{size(Bin1)} > 0.3\right\} \;\&\&\; \{index(Bin2) > 2 * Pupil\_Intensity\} \qquad (4\text{-}11)$$

Where $Pupil\_Intensity$ is the average intensity value for pixels within the pupil. $size(Bin)$ is the number of pixels in the Bin and $index(Bin)$ is the gray scale index for this bin. Because the average gray scale of iris pixels is generally twice higher than pupil pixels, equation (4-11) would eliminate the hypothetical circles containing two or more different areas with different gray scale intensities, as Figure 4-9 shows.

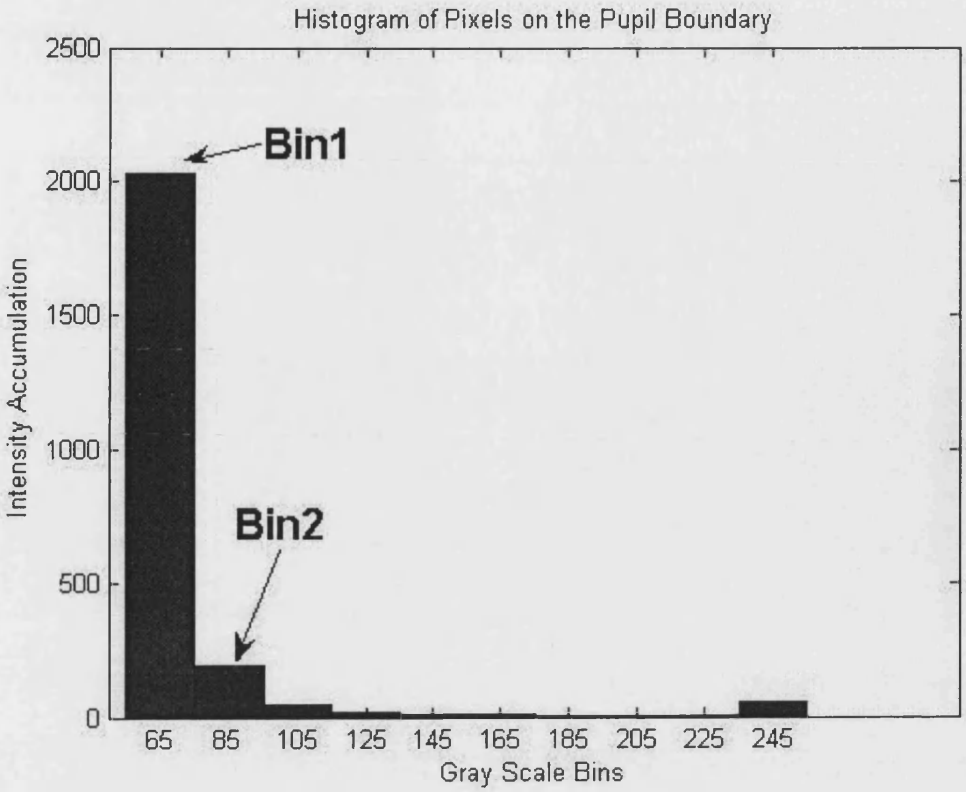

Figure 4-8 Histogram of Pixels on the Pupil Boundary

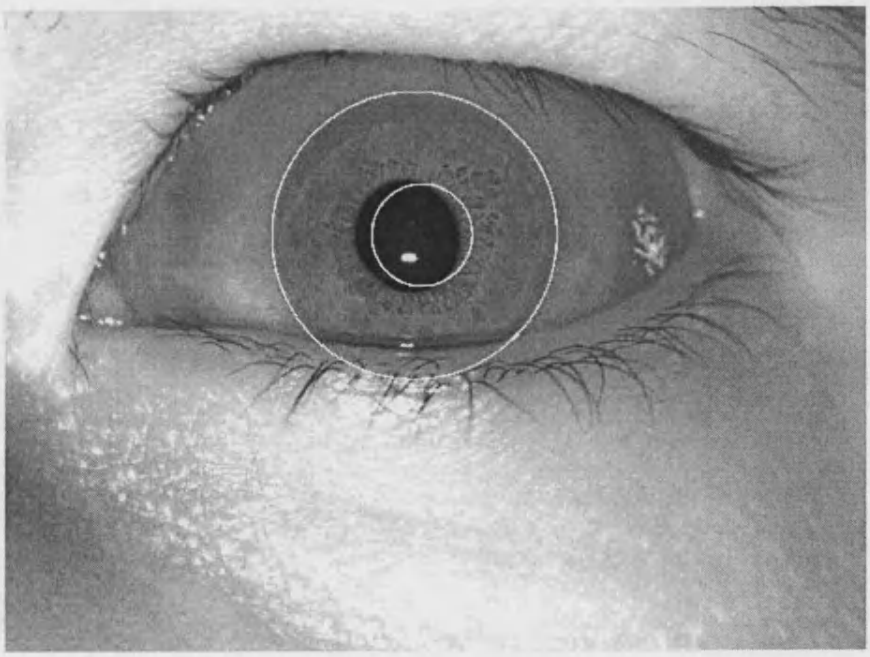

Figure 4-9 Hypothetical Circle across the Iris Region

- ***Pupil Outskirt Intensity Distribution Check:*** In some cases, the hypothetical boundary could be found far within the real pupil boundary and still could pass the RANSAC check, as shown in Figure 4-10. In Bath system, all the pixels within 10-pixel distance from outside the hypothetical circle would be chosen and stored into a 2D array called *Iris_Pixel,* in which the pixels darker than $1.2 * Pupil\_Intensity$ will be stored into another 2D array named *Dark_Iris_Pixel.* If too many dark pixels are in this supposed iris area as equation (4-12) shows, this hypothetical model is considered as a false model.

$$\frac{length(Dark\_Iris\_Pixel)}{length(Iris\_Pixel)} > 0.2 \qquad \textbf{(4-12)}$$

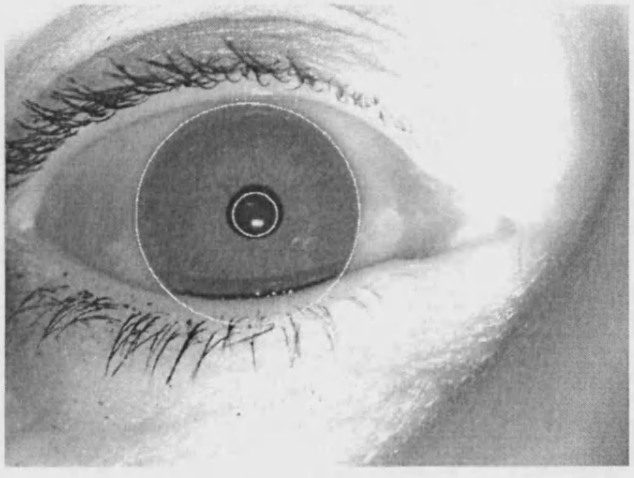

Figure 4-10 Hypothetical Circle within the Pupil

- ***Pupil Boundary Pixel Intensity Consistency Check:*** All the pixels within 1-pixel distance to the hypothetical model from both sides are collected as pixels on the model hypothesis. The gray scale intensity of these pixels should not change much in a good curve fitting. Thus the standard deviation of these intensities is set to be limited under 50. And the difference between the darkest and the brightest pixel should be within 150.

- ***Cross Pupil Boundary Intensity Change Check:*** The average intensity value should change dramatically across the pupil boundary. All the pixels within 1-pixel distance to the hypothetical model from outside will be chosen

and their intensities summation will be calculated as $sum\_intensity\_outer$. The corresponding $sum\_intensity\_inner$ comes from the sum of pixels between 2-pixel and 3-pixels distance to the hypothetical model from inside. The ratio between them should accord to equation (4-13). This will make the location more precise.

$$\frac{sum\_intensity\_outer}{sum\_intensity\_inner} > 1.2 \qquad \textbf{(4-13)}$$

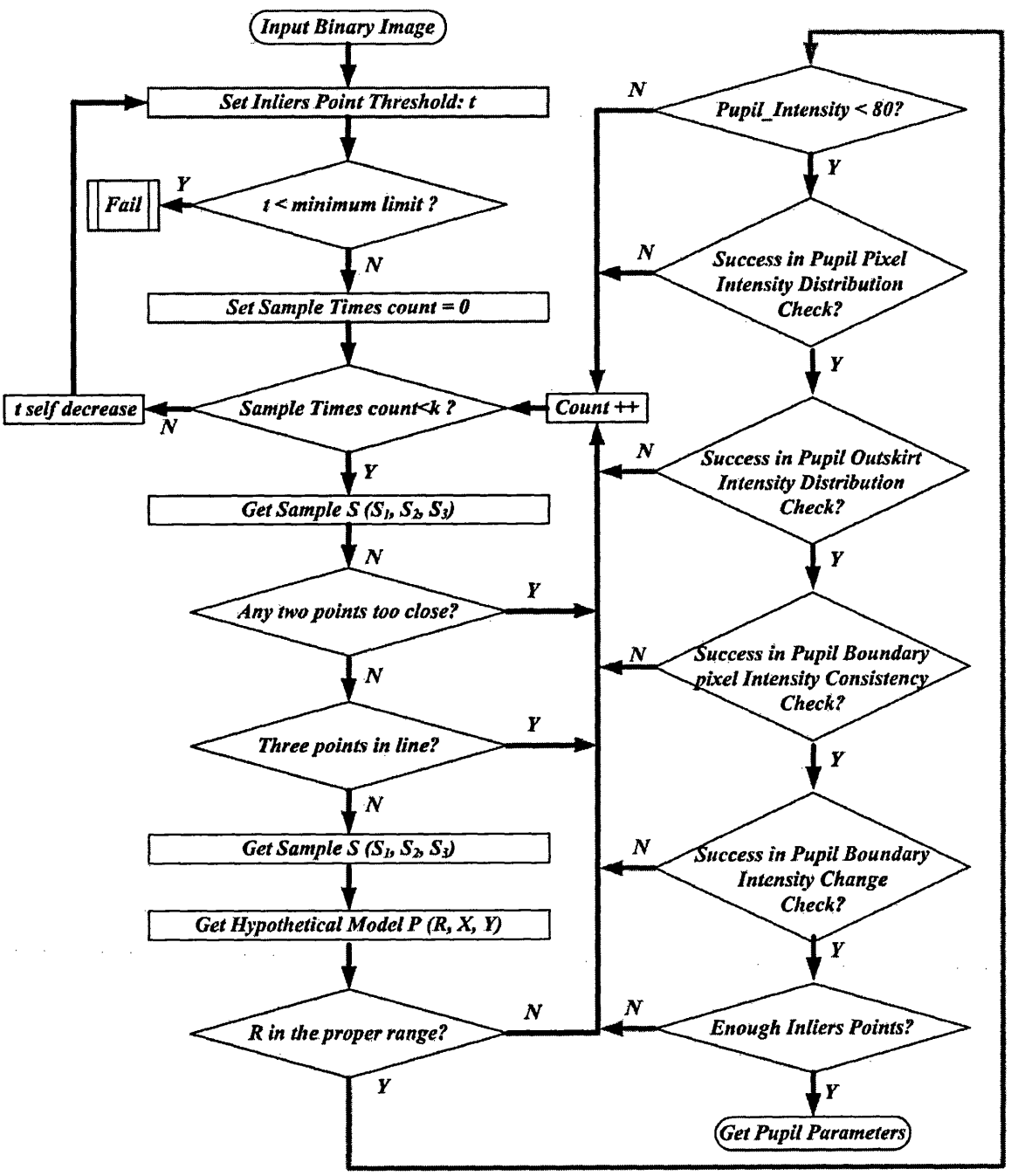

Figure 4-11 Proposed Pupil Finding Flow Chart

Till now, the pupil has been located as $P(Pupil\_X, Pupil\_Y, Pupil\_R)$. The pupil localization is the most difficult part in iris segmentation. The searching of the iris boundary could be based on the pupil parameters and thus becoming much easier.

4.3.5 Finding the iris Boundary

Although the pupil and the limbus are non-concentric, their centroids are very close. In software implementation practice, the pupil center and the limbus center are considered sharing the same vertical coordinate, that is, $Pupil\_Y = Iris\_Y$, where $Iris\_Y$ is the vertical coordinate of the limbus. The difficulty about limbus searching is that the limbus is not as obvious as the pupil. And many irises have annular textures, which could be easily confused with limbus. The integral differential operator idea is utilized by many people in searching the limbus. The method proposed in this thesis is also based on this idea.

First, the pupil parameters $P(Pupil\_X, Pupil\_Y, Pupil\_R)$ derived from the reduced image should be transformed into the original full size image in order to carry on subsequent calculation.

Then, starting from the pupil centroid $(Pupil\_X, Pupil\_Y)$, the limbus boundary will be searched in two opposite directions along the x axis. Let us take the searching in the left direction as an example.

1. The limbus radius searching range $Iris\_R\_Range$ is set to be $[Pupil\_R+40,\ Pupil\_R+140]$ in Bath system.
2. The searching angle range is set to be $[-15^o,\ 15^o]$. This searching angle range could effectively avoid the influence of eyelid and is still able to provide enough gradient information.
3. Along with the increasing of the searching radius, the summation of pixel intensity on each arc is saved in a vector $Intensity\_Sum\_Vector$.
4. A median filter is used to smooth the values in vector $Intensity\_Sum\_Vector$. Then the integral differential idea is utilized as in equation (4-14).

$$\begin{aligned} Intensity\_Sum\_Diff(k) = & Intensity\_Sum\_Vector(k+3)+\ldots \\ & Intensity\_Sum\_Vector(k+4)+\ldots \\ & Intensity\_Sum\_Vector(k+5)-\ldots \\ & Intensity\_Sum\_Vector(k-3)-\ldots \\ & Intensity\_Sum\_Vector(k-4)-\ldots \\ & Intensity\_Sum\_Vector(k-5) \end{aligned} \quad \text{(4-14)}$$

Where $Intensity\_Sum\_Diff$ is a vector containing the gradient information of $Intensity\_Sum\_Vector$, $k \in [Pupil\_R+45,\ Pupil\_R+135]$.

5. The maximum value in $Intensity\_Sum\_Vector$ is thought where the limbus is.
6. If the detected limbus is too close to the pupil, find the index of the second biggest value in $Intensity\_Sum\_Vector$ as where the limbus is. Then check if the pupil and limbus are too close, and so on.

After the limbus radiuses in two directions have been found, their relative length would be compared. If difference between them is too long, the longer part will repeat step 6 above. This is because the longer part is often caused by specular reflection on the sclera.

4.4 Experiments with the Proposed Localization Method

The two key issues about iris localization are speed and accuracy. Thus the two issues will be tested on the PC based MatLab 7 environment with 2.4G Hz CPU. The following databases are chosen to test the performance of the proposed iris localization method: NIST, Plymouth, Retica, Sarnoff, CASIA and Bath. The results will be shown in the rest of this section.

The impartiality of algorithm comparison is always under discussion. A just comparison demands two conditions: (1) Good software implementation of each algorithm. (2) Identical evaluating platforms. In iris recognition algorithm research, the leading algorithms of others is generally implemented by the researcher and compared with his proposed method. In this way, the other leading algorithms could not be implemented as well as it should be, thus a biased comparison results would easily be achieved. The iris localization

algorithms proposed by Daugman and Wildes were also realized by the author in the interest of comparison. In order to make these two algorithms perform as well as our approach, the speeds of both have been slowed to an amazing extent after tuning the parameters. This is obviously not a fair comparison. Luckily, a paper published by CASIA contains the experimental results of the two algorithms based on the same test environment as us [90]. Since CASIA is the leading research institute in iris recognition, the comparison with their results should be more convincing. These comparison results will be given by the end of this section.

It is hard to determine whether or not the localization is correct or not by computer. Thus all the results are subjectively judged by the researchers, who are supposed to have enough experiences in the judgment process.

4.4.1 Results based on NIST Database

This database is provided by the National Institute of Standard and Technology (NIST) and captured using LG IrisAccess 4000. It has 2953 images in different qualities. Localization results on this database are shown in Table 1-1 and some example images with different qualities are also given in the following.

DB Name	Total Number	Numbers of Correct Loc	Average Loc Time
NIST	*2953*	*2953*	*0.922 (s)*

Table 4-1 Localization Results on NIST Database

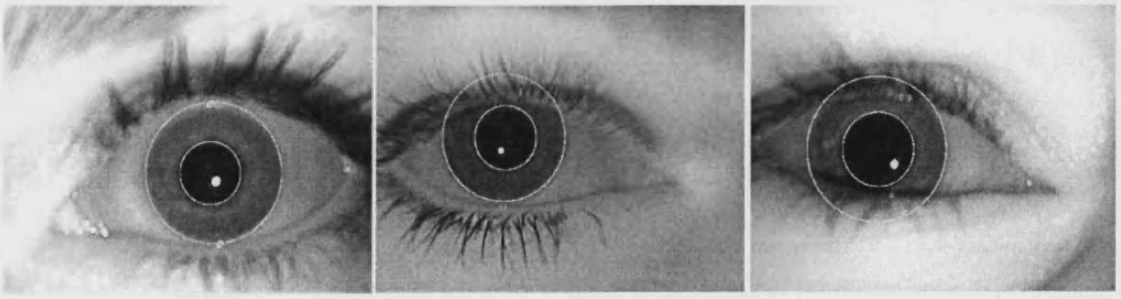

Figure 4-12 NIST Blurred Images

Figure 4-13 NIST Uneven Illuminated Images

Figure 4-14 NIST Heavy Eyebrow or Hair Images

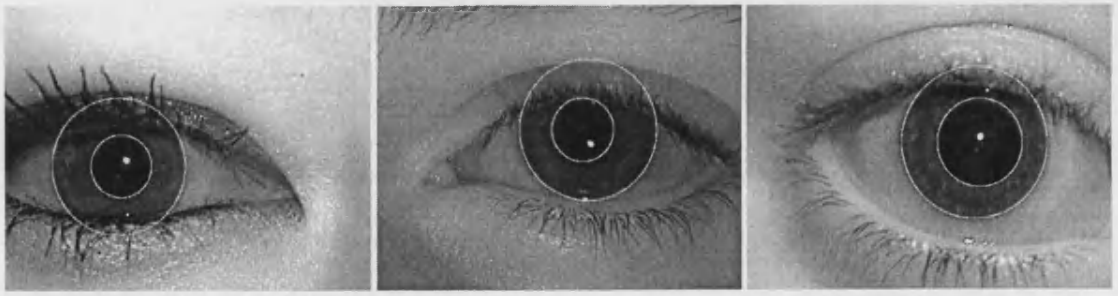

Figure 4-15 NIST Dark Iris Images

Figure 4-16 NIST Heavy Eye black Images

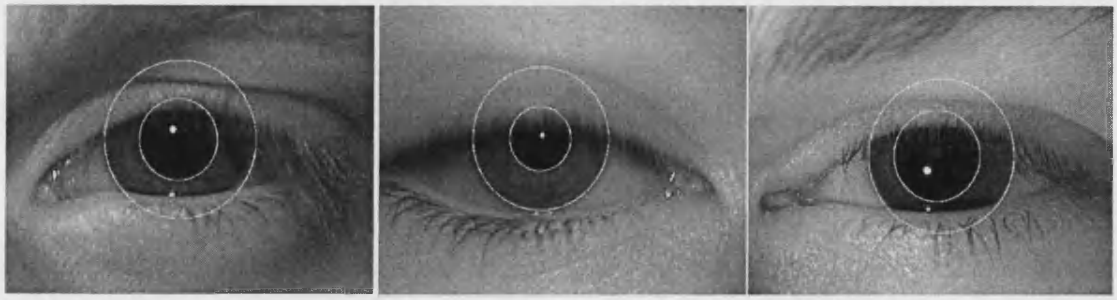

Figure 4-17 NIST Heavily Occluded Images

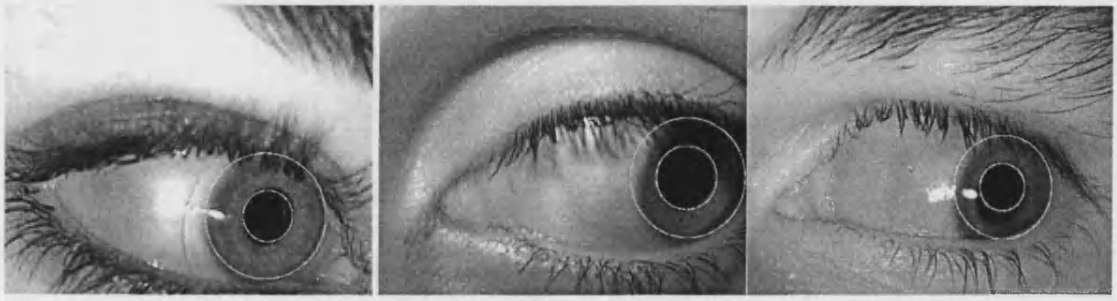

Figure 4-18 NIST Off Angle Images

The proposed algorithm could localize all the images in different qualities in a very fast speed, as shown in the tables and figures above. One issue needs to be pointed out is that the iris boundaries in those off angle images could not be exactly fitted using the circle model. These images could generally be treated in two ways: (1) These images could be picked out by quality assessment module and rejected. (2) Some non-circular model could be used to fit the boundary and normalized into fixed size using non-linear mapping method.

4.4.2 Results based on Plymouth Database

These images came from a joint project between Bath University and Plymouth Royal Eye Infirmary. In order to research on how huge pupil dilation and cataract operation affect the performance of our iris recognition algorithm, some iris images were taken from the cataract patients using Bath Iris Capture Machine. Their iris images were first taken before the cataract operation, and after 15 days these eyes were re-imaged when the patients came to get their eyes examined. In each capturing session, the eye images were captured

before and after the usage of eye dilating drops. The results are shown in the following of this section.

DB Name	Total Number	Numbers of Correct Loc	Time of Average Loc
Plymouth	108	108	0.562 (s)

Table 4-2 Localization Results on Plymouth Database

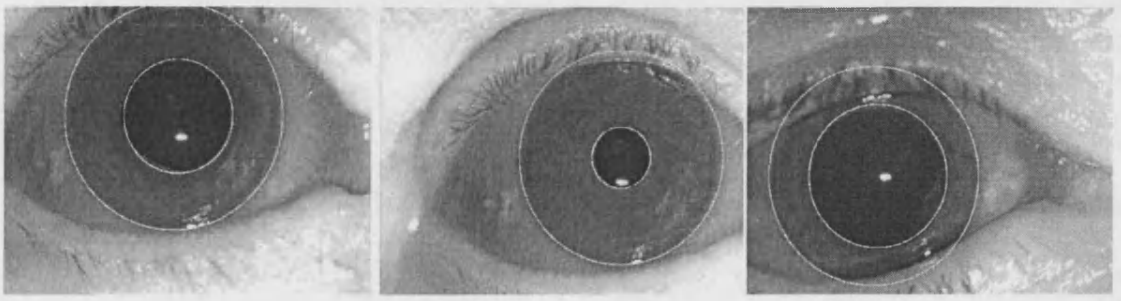

Figure 4-19 Plymouth Images

4.4.3 Results Based on Retica Database

DB Name	Total Number	Numbers of Correct Loc	Time of Average Loc
Retica	1100	1038	1.272 (s)

Table 4-3 Localization Results on Retica Database

The reason there are so many wrongly localized images is that Retica database deliberately contains some bad quality images and non-iris images, as shown in Figure 4-20.

Figure 4-20 Retica Bad Images

4.4.4 Results Based on Sarnoff Images

Sarnoff database is built based on the system named Iris on the Move (IOM). IOM can capture the iris images while the subject walks through the capturing portal at a normal walking pace. These images are generally blurred and contaminated by many specular reflections. Although the proposed the localization algorithm could easily find the pupil boundaries, the contaminated iris area will bring a lot of difficulties in future iris image coding and matching. Thus the IOM system still needs to be improved.

DB Name	Total Number	Numbers of Correct Loc	Time of Average Loc
Sarnoff	*63*	*63*	*0.484 (s)*

Table 4-4 Localization Results on Sarnoff Database

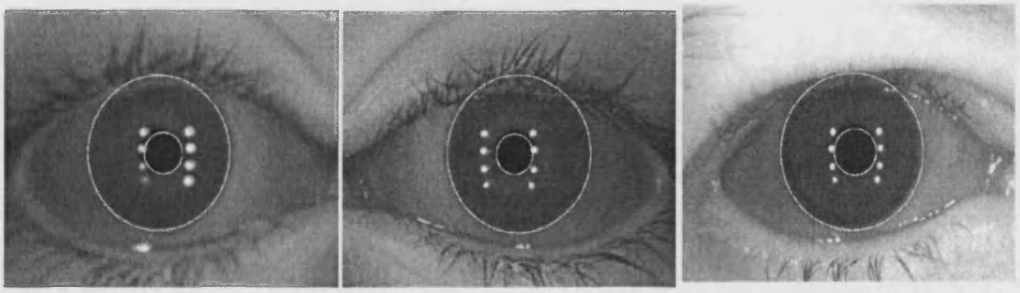

Figure 4-21 Sarnoff Images

4.4.5 Results Based on Bath Database

Since the Bath Iris Database is of high quality and this algorithm is designed based on it, the localization is quite fast and accurate.

DB Name	Total Number	Numbers of Correct Loc	Time of Average Loc
Bath	*8000*	*8000*	*0.432 (s)*

Table 4-5 Localization Results on Bath Database

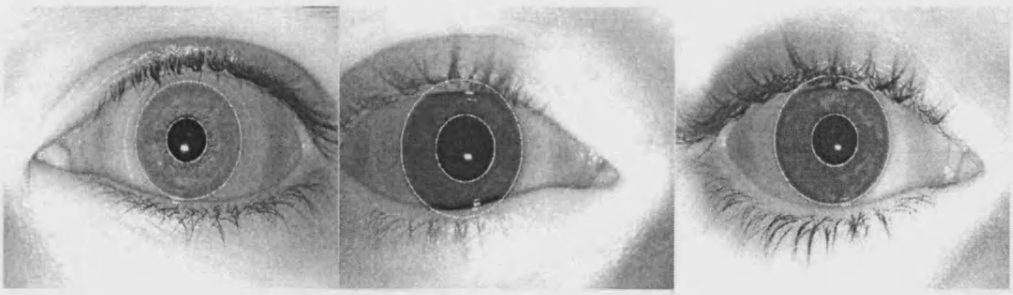

Figure 4-22 Bath Images

4.5 Localization Algorithms Comparison

As discussed earlier, the impartiality of algorithm comparison needs good software implementation of each algorithm and identical evaluating platforms. The implementation results for Daugman and Wildes' methods are from the publication by Dr Cui from CASIA. Provided CASIA is the leading institute in iris recognition research, the results from Dr Cui's paper should be very convincing.

756 images from CASIA database were chosen in Cui's paper to be tested in a Matlab environment based on 2.4GHz CPU. In our experiment, 2000 images were chosen from CASIA database using the Matlab environment with a 2.4GHz CPU. The image size we use is 640*480, which should be more time consuming than images sized at 320*280, which were used in Cui's paper. Although it is still not a very fair comparison, it gives some idea how the proposed method works against other algorithms.

Methods	*Total Number*	*Image Size*	*Correct Loc Rate*	*Time of Average Loc*
Proposed	***2000***	***640*480***	***100%***	***0.718 (s)***
Daugman	***756***	***320*280***	***98.6%***	***6.56 (s)***
Wildes 1	***756***	***320*280***	***99.9%***	***8.28 (s)***
Wildes 2	***756***	***320*280***	***99.5%***	***1.98(s)***

Table 4-6 Localization Algorithms Comparison

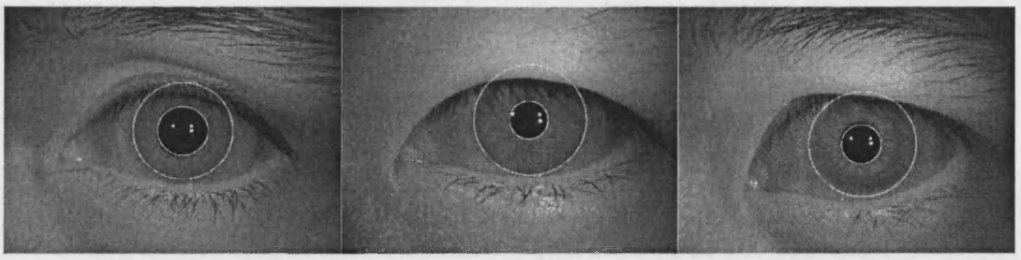

Figure 4-23 CASIA Images

4.6 Proposed Eyelid Removal Method

Although eyelid detection is not as important as iris localization, it is necessary for iris images seriously occluded by eyelids. Daugman and Wildes mentioned the eyelid detection methods similar to their iris localization algorithms, but no detailed description and experiment have been reported. This section will propose a fast and robust eyelid detection method and encouraging performance has been achieved through experiments.

Generally, parabolic curves are used to model the shapes of the upper and lower eyelids. The eyelid boundaries are always contaminated by eyelashes, which increases the computational complexity and decreases the detection accuracy. Thus the speed and accuracy is still the key issue for eyelid detection. The iris localization results are generally used in searching the eyelid boundaries. Taking Figure 4-1 as example, the following will illustrate in detail the proposed eyelid removal method.

4.6.1 Preliminary Image Processing

Based on the localization results, the working area is reduced to around the iris area. The image is then enhanced in order to improve the contrast within the iris area, as shown in Figure 4-24.

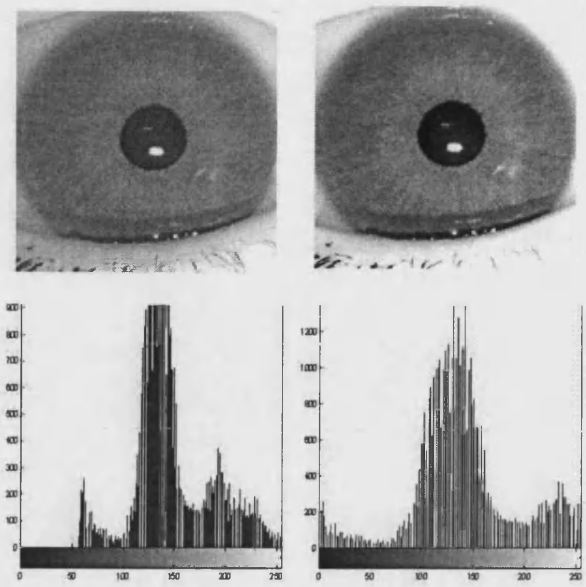

Figure 4-24 Reduced Image Enhancement for Eyelid Detection

Edge points fitting is the common technique for boundary searching and the speed of the edge detector is important to real time system. Although Roberts operator is fastest, Sobel operator is chosen for its larger convolution kernel, which could smooth the input image to a greater extend and so makes the operator less sensitive to noises. Compared with iris boundaries and eyelashes, the intensity gradient directions along the eyelid boundaries are generally vertical. Thus a vertical Sobel operator S_v is utilized for edge detection. A Gaussian filter is used before edge detection to reduce the noise level, as shown in Figure 4-25.

$$S_v = \begin{bmatrix} +1 & +2 & +1 \\ 0 & 0 & 0 \\ -1 & -2 & -1 \end{bmatrix} \qquad \textbf{(4-15)}$$

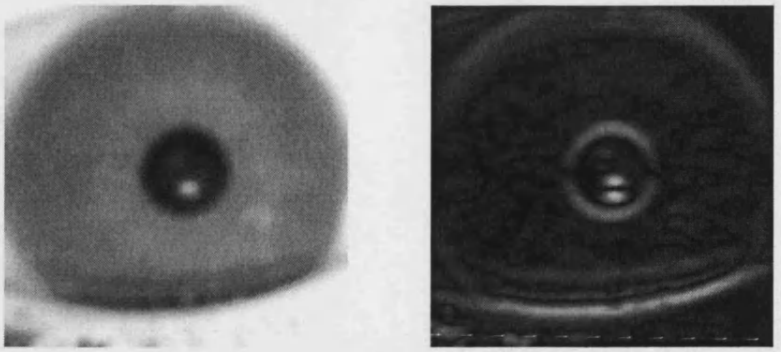

Smoothed Image Vertical Gradient

Figure 4-25 Vertical Gradient Image

4.6.2 Edge Point Selection

Figure 4-25 shows all the edge points achieved from vertical Sobel operator. Apart from the eyelid boundary edge points, edges from the limbus, pupil, specular reflection, etc have also been introduced. The introduction of these unrelated edge points could increase the computational complexity as well as deteriorate the accuracy. This thesis will propose an effective and fast edge point selection program, which could effectively eliminate uninterested edge points while still keeping enough eyelid boundary edge points.

Assuming the iris center as the benchmark point, the eyelid edge points would only be picked up from two annular areas along the iris radius: $[1.5 * Pupil\_R \sim Iris\_R - 5]$ and $[Iris\_R + 5 \sim 1.1 * Iris\_R]$. Thus an eyelid mask is made and applied to the gradient image, as shown in Figure 4-26.

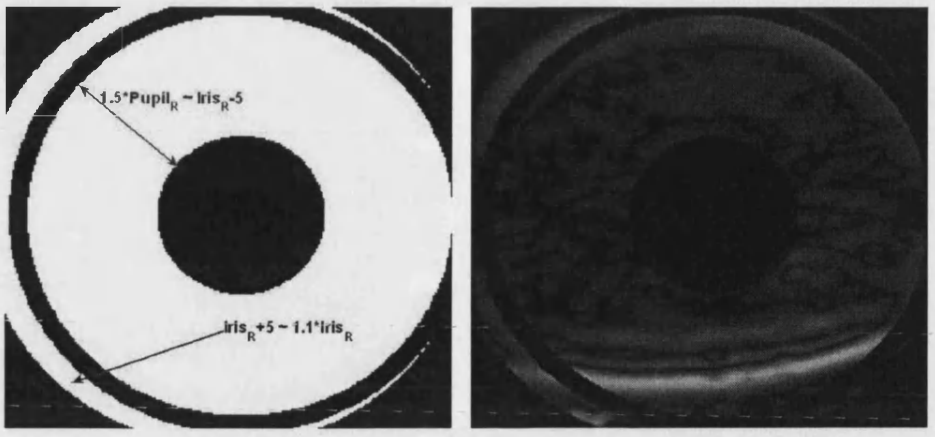

Eyelid Mask Masked Gradient Image

Figure 4-26 Masked Gradient Image

The image is then changed back to the original size. Since the pixel intensity in the eyelid is generally greater than the iris, the edge points with positive gradient larger than a threshold are regarded from the upper eyelid boundary and the edge points with negative gradient lower than a threshold are regarded from the lower eyelid boundary. Thus the two gradient images are generated for upper and lower eyelid detection separately, as shown in Figure 4-27.

(a) (b)

Gradient Image for Upper Eyelid Gradient Image for Lower Eyelid

Figure 4-27 Gradient Images for Upper and Lower Eyelid

For image (a) in Figure 4-27, the lowest edge point in each column is used to fit the upper eyelid, while for image (b) in Figure 4-27, the highest edge point in each column is chosen for lower eyelid fitting. Some curvature checking is applied after afterwards to eliminate the false fitting results (e.g. Figure 4-27 (a)). The example results and flow chart are shown in Figure 4-28 and Figure 4-29 separately.

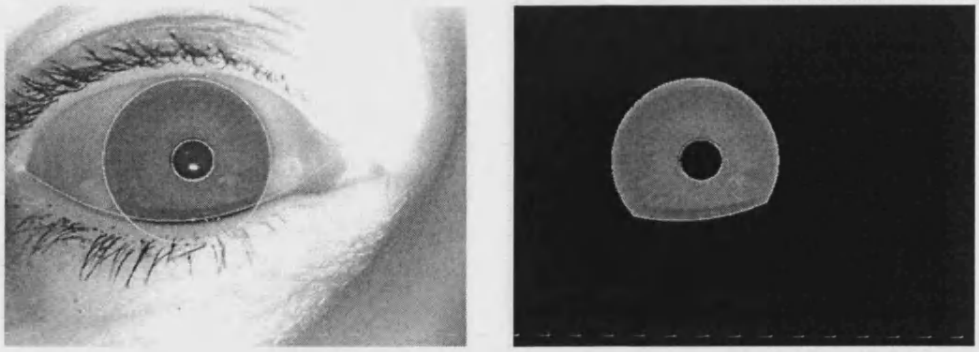

Figure 4-28 Eyelid Detection & Removal

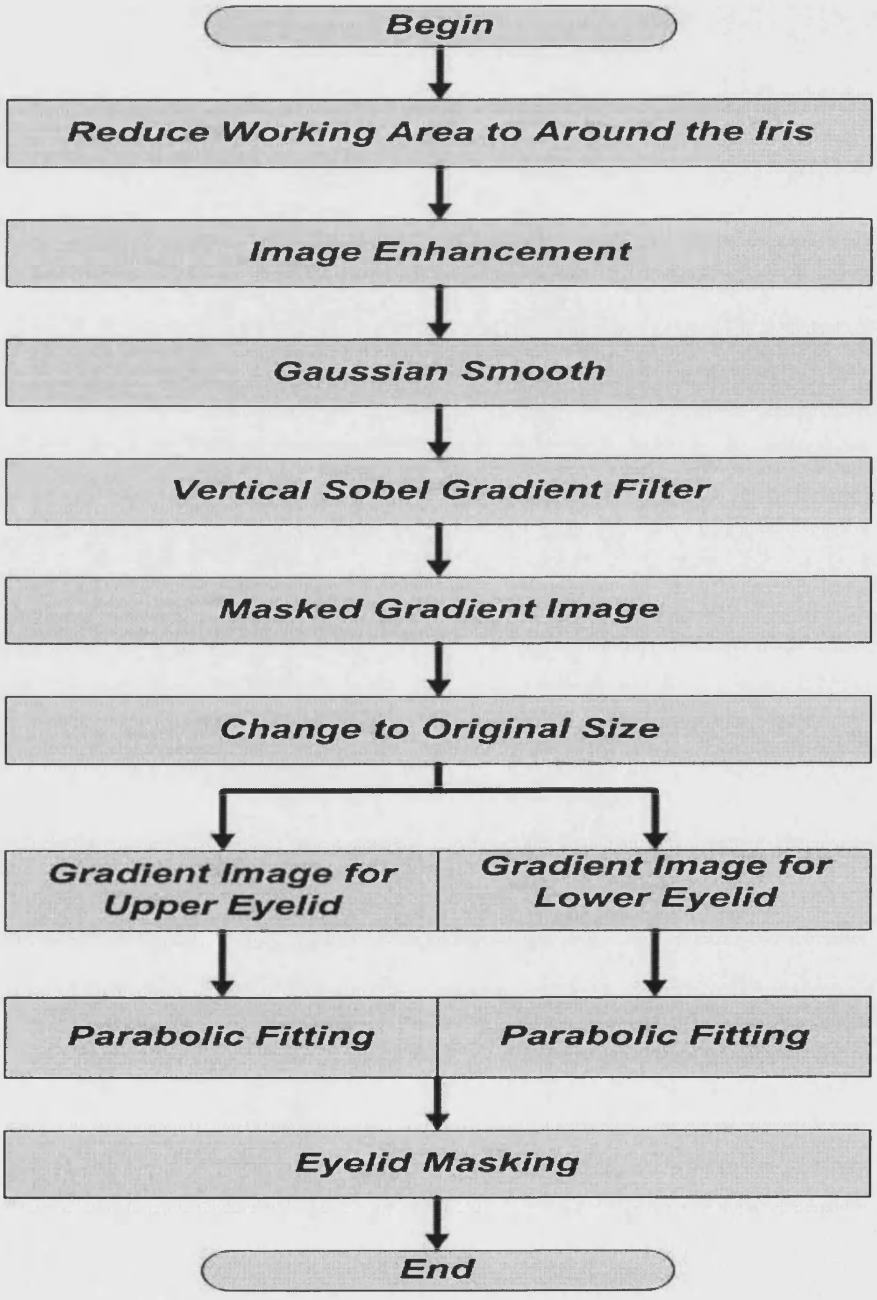

Figure 4-29 Eyelid Removal Flow Chart

4.7 Eyelid Removal Experiments and Comparison

4.7.1 Results on Bath Database

150 classes, 3000 images are chosen to test the eyelid removal algorithm proposed in this thesis. Manual check is carried out afterwards. No eyelid is missed in the results, while few images without eyelids occlusion are masked due to heavy noises. These wrongly masked images are regarded as false. The researchers will check through the whole results to decide if the removal is correct or not. The eyelid removal results are shown in Table 4-7. Some sample images are given in Figure 4-30.

DB Name	Total Number	Number of Correct Removal	Time of Average Removal
Bath	3000	2982	0.235 (s)

Table 4-7 Eyelid Removal Results on Bath Database

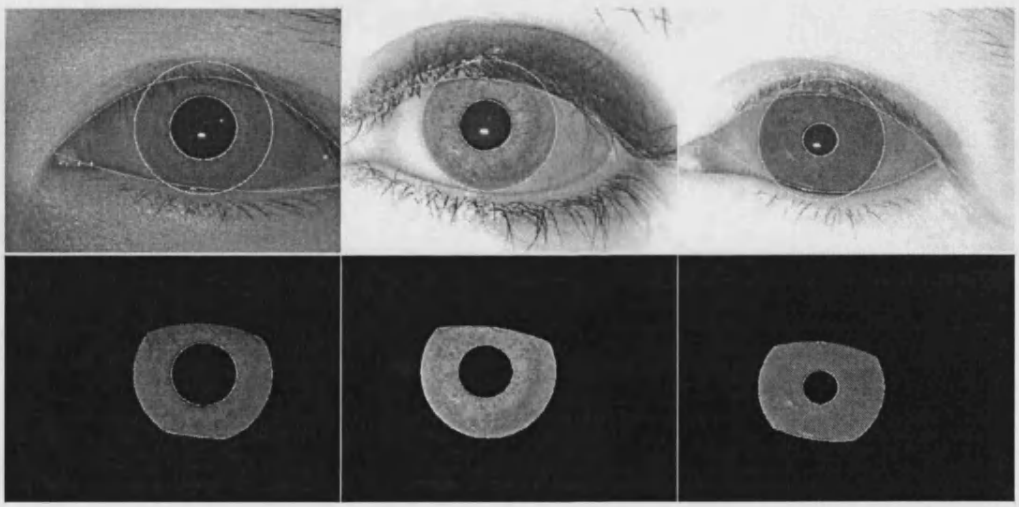

Figure 4-30 Eyelid Removal Results on Bath Database

4.7.2 Results & Comparison on CASIA Database

As stated in section 4.5, a fair comparison is very difficult under current research situation. J. Cui proposed an eyelid detection method and tested on the same database as stated in section 4.5 [90]. In order to make a comparison, we choose 1000 images from the CASIA database and tested the proposed algorithm on the same platform (2.4GHz CPU, Matlab). The test results are

shown in Table 4-8. Figure 4-31 shows some sample images for eyelid removal on CASIA Database.

Methods	Total Number	Image Size	Rate of Correct Removal	Time of Average Removal
Proposed	*1000*	*640*480*	*96.7%*	*0.234 (s)*
Cui	*756*	*320*280*	*93.39%*	*0.9527 (s)*

Table 4-8 Eyelid Removal Results on CASIA Database

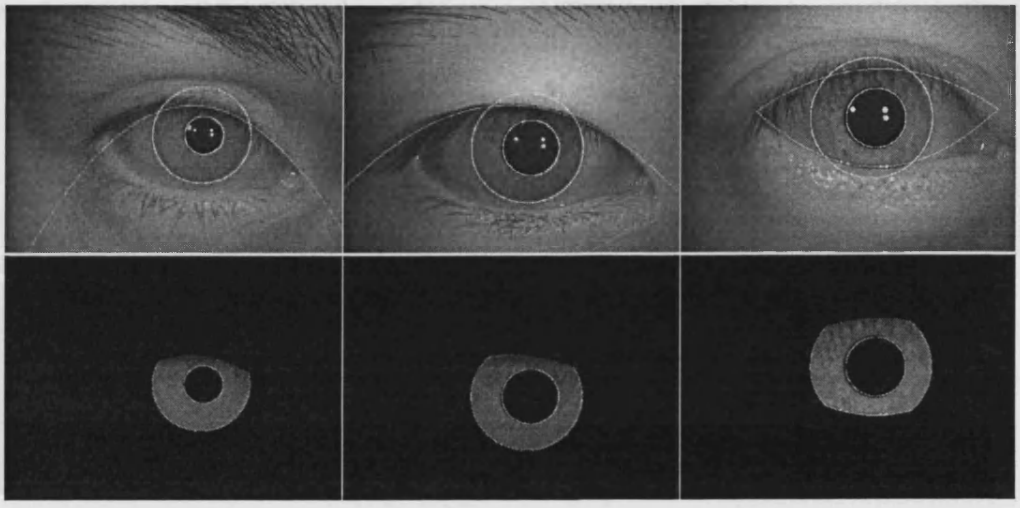

Figure 4-31 Eyelid Removal Results on CASIA Database

As we can see from the results, the proposed eyelid removal method could be carried out at a very high speed while still keeping satisfying correct removal rate. In practical applications, if the input images are generally of good quality, the eyelid removal module would be disabled to speed up the system. In this case, the eyelid occluded image could be eliminated by the iris image quality assessment module.

4.8 Summary

Iris segmentation includes iris localization and eyelid removal. Iris segmentation locates the iris portion in the eye image by finding the parameters of the iris boundaries and the eyelid shape occluding the iris area. Iris segmentation is the

key stage for the success of the whole iris recognition system. Speed and accuracy are the two key evaluating points for iris segmentation methods. In this chapter, some leading localization methods were introduced first. Then a robust and time efficient iris segmentation method has been proposed and compared with the current leading solutions. The proposed iris segmentation method consists of two steps: iris localization algorithm and eyelid detection algorithm.

The thesis proposed a fast and robust iris localization algorithm based on Random Sample Consensus (RANSAC). Experiments have been done on the image databases from NIST, Plymouth, Retica, Sarnoff, Bath and CASIA. The results showed that the proposed algorithm could not only maintain a high localization rate, but also perform the procedure much faster than the leading algorithms proposed by Daugman or Wildes. Within the proposed iris localization algorithm, the contributions could be summarized as follows:

- A new pupil area finding method based on the standard deviation analysis for each projection line is proposed. According to the experiments, this method could greatly enhance the pupil finding accuracy.
- In edge point detection, a threshold adaptive canny edge detector is designed to make the edge point number in a certain amount using a self-adaptive threshold variable.
- The RANSAC method is applied to the iris boundary fitting and the encouraging performance is achieved.
- A lot of additional checking criterions were proposed based on the 8 bit gray scale image.

This chapter also reported a fast and robust eyelid removal algorithm, which could be carried out in a very high speed while still keeping satisfying correct removal rate. The main contributions in this method are the effective edge point selection method, which could effectively eliminate uninterested edge points while still keeping enough eyelid boundary edge points.

5 Image Coding Based on Local Frequency Amplitude Variation

5.1 Foreword

A great amount of work has been done on iris image feature extraction and matching through various directions. Daugman filters iris image with a family of multi-scale Gabor filters and their phase structure is demodulated into a sequence of complex-valued phasors. These phasors are then projected onto a four quadrant complex plane and a binary iris code is generated from these phasors. Tan generates a bank of 1D intensity signals from the iris image and filters these 1D signals with a special class of wavelet. The positions of local sharp variations are recorded as the features. Generally these methods could be categorized into two areas: methods based on iris image structure analysis and methods based on local image variation analysis. Both Tan and Daugman's methods belong to the local image variation analysis based methods.

The key question about feature extraction is: What is the essentially discriminating characteristic for one iris class to distinguish from others? Tan thinks the local variations, including both intensity variations and orientation variations, are the most distinguishing information for iris recognition. This conclusion could also be supported from the listed recognition methods above, in which the methods based on local image variation analysis generally perform better than methods based on iris image structure analysis. Daugman's method utilizes the local phase variations to code the iris image and Tan captures the local intensity variations for feature vector. Both the two methods are leading algorithms in feature extraction and matching

Focusing on the question above, this chapter will propose a feature extraction method based on local frequency amplitude variation.

5.2 Proposed Iris Coding Technique

The image of a human iris is highly specific to the individual, whose two eyes are also unique. In order to represent this information, Daugman uses local phase variation and Tan captures local intensity variation. Also based on the idea of extracting the image local variation analysis, this thesis will exploit the local frequency variation as another novel method for coding the iris image. The proposed iris coding method is called Monro Iris Transform (MIT) to make it easy to remember. The input image for MIT is an 8 bit grayscale rectangular image with the size 512*80, as shown in Figure 5-1.

Figure 5-1 Normalized Image to Be Coded

5.2.1 Segmentation Into Patches

In order to exploit the local information, the input iris image is divided into rectangular patches, as shown in Figure 5-2, in which the parameter set denotes in the following way:

- ***Patch*** denotes the local area that generates the sub-feature of MIT.
- ***Width*** denotes the width of a Patch.
- ***Length*** denotes the length of a Patch.
- ***Centroid*** denotes the centre coordinates of the Patch.
- ***Angle*** represents the rotation of the Patch.
- ***V_Space*** denotes the vertical distance between two Patches.
- ***H_Space*** denotes the horizontal distance between two Patches.

In one parameter set, all the patches have the same size, orientation, overlapping and spacing. The proposed MIT will be applied to these patches. The patch size controls the scale of the coded local information while the orientation balances the ratio of the circumferential feature information and the radial feature information. If the spacing is too close, namely overlapping, the

marginal information between patches could be utilized. Otherwise increasing the spacing could reduce the feature vector length.

The patch is the basic fragment used in our method. To obtain optimum performance we tune the length, width, orientation (angle) and the relative position of a series of patches.

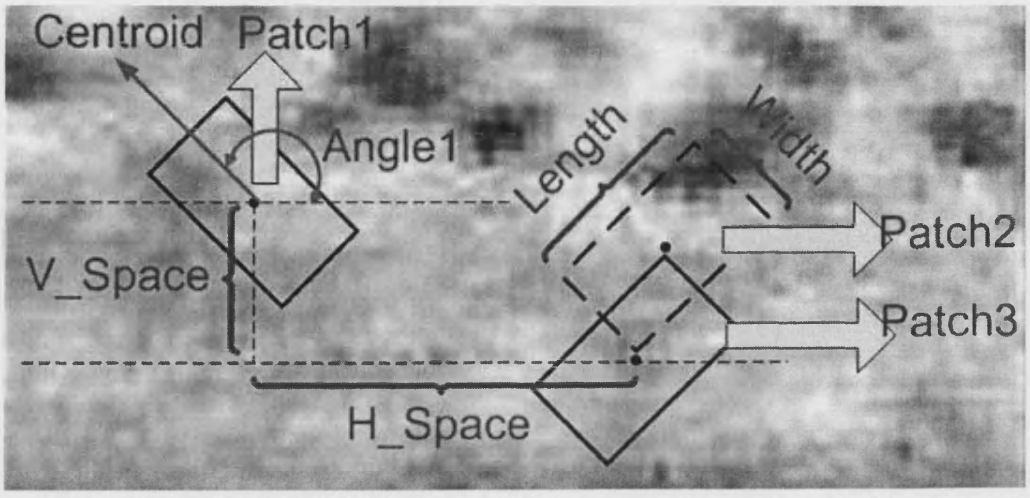

Figure 5-2 Diagram showing some parameters of the proposed iris coding method

5.2.2 Patch Coding

The procedure for coding a patch is shown in Figure 5-3. First a 1D intensity signal is obtained by averaging the patch across its width to reduce noise. Using broad patches also makes iris image registration easier, which is important for rotation invariant iris recognition. The FFT is then applied to this 1D signal to obtain spectral coefficients. In order to reduce the spectral leakage during the FFT, a window is employed before the FFT. The Frequency Magnitude Differences between adjacent patches are calculated and a short binary code is generated from the zero crossings of each difference. These constitute the feature vectors of our iris code. The following section will illustrate the feature vector generation procedure in detail.

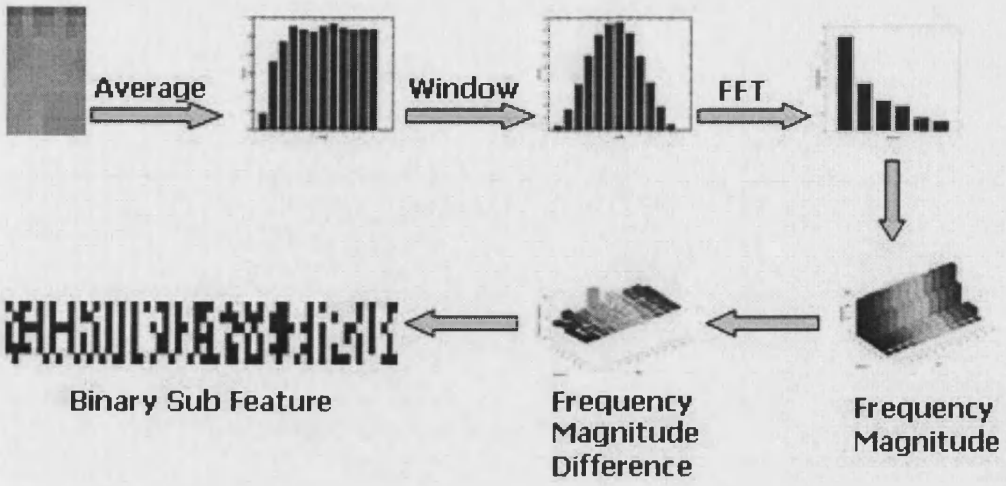

Figure 5-3 Procedure of Patch Coding

5.2.3 Feature Vector Generation Procedure

The input image Figure 5-1 is first divided into several overlapped bands and the length of each band equals to the length of the patch. These bands will then be rotated to a certain angle, as shown in Figure 5-4. If the rotation angle equals to 90^0, only the feature information along the circumference will be exploited, while when rotation angle is equal to 180^0, only the radial feature information can be used. Thus the rotation angle should be tuned to balance between the two directional information classes and achieve the optimum. As we can see from the iris image, the bands closer to the pupil have more iris texture than the bands near the sclera. Thus these near-pupil bands are more important in iris recognition than others. In our algorithm, the closer the band to the pupil is, the more it will be weighted. In Monro Iris Transform (MIT), there are two kinds of weighting scheme. One is the space weighting as stated above, the other is the frequency weighting, which will be introduced in the following. Both weighting systems are tested extensively and the optimum parameters have been chosen.

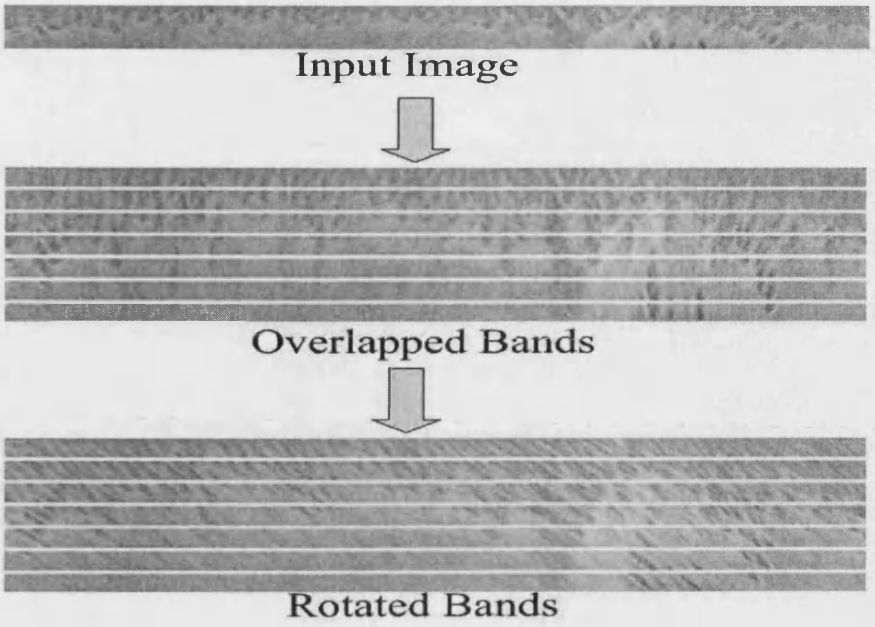

Figure 5-4 Band Operation on Input Image

Then every band is divided into patches according to the patch width and a series of 1D intensity signal is obtained by averaging the patch across its width to reduce noise. Also, this operation would make the iris image registration easier. In order to reduce the spectral leakage in the coming FFT operation, a specially designed Hanning window is applied to each of these 1D signals. This procedure is shown in Figure 5-5.

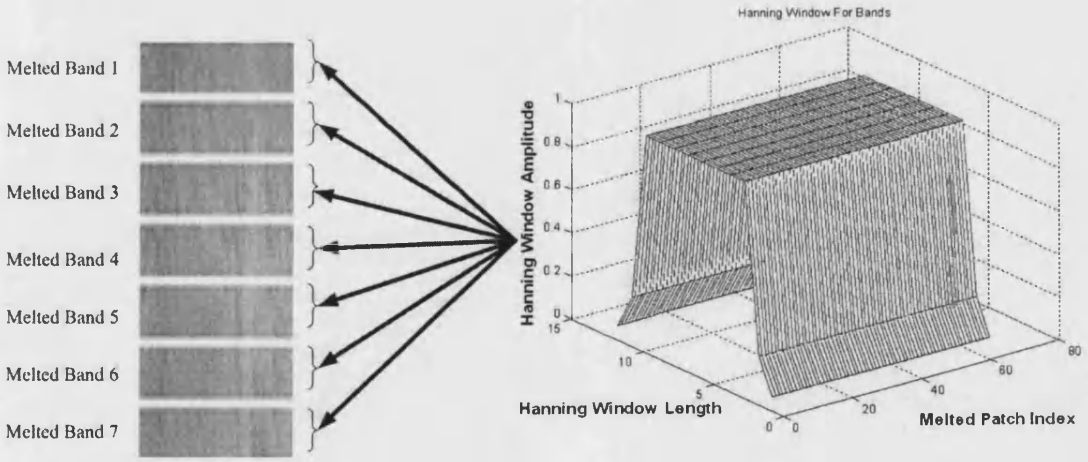

Figure 5-5 Hanning Window for Melted Bands

Then Fourier Transform is a linear operator that decomposes a function into a continuous spectrum of its frequency components. The Fast Fourier Transform

(FFT) is an efficient algorithm to compute the Discrete Fourier Transform (DFT) with great speed. Thus the 1D FFT algorithm is applied to every windowed 1D signal achieved above to get the local frequency information fast. The accomplished frequency domain spectrum is symmetrical in amplitude as shown in Figure 5-6. The DC is generally thought as the local illumination and thus only the spectrum within the range (2~7) is chosen to represent the local frequency information. We name this truncated 1D spectrum as *Am_FFT_AvgB*.

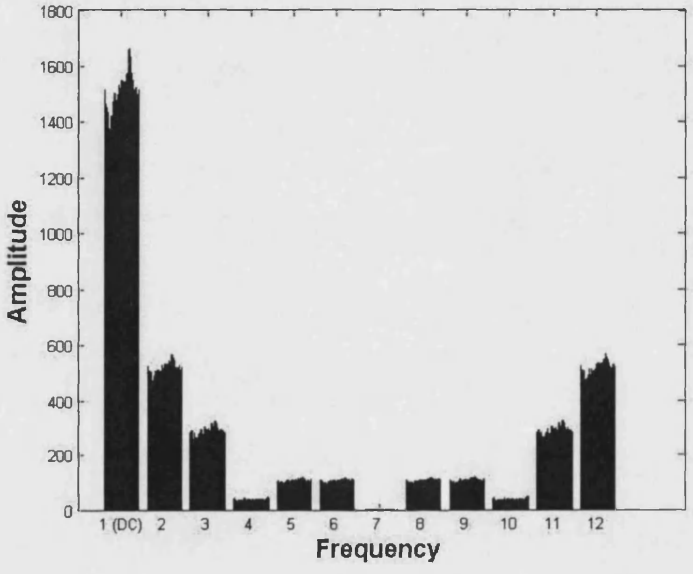

Figure 5-6 FFT Amplitude of 1D Signals

For each band, the former *Am_FFT_AvgB* would be subtracted by its adjacent latter to get the local variation in each frequency level. Thus the amplitude variation matrix is achieved as shown in Figure 5-7. The information in different frequency level should have different distinguishing capability between iris image classes, thus these levels should be weighted in accordance. The best parameters form frequency weighting are found through extensive parameter exploration. We also found that the medium frequencies are more distinctive than the low and high frequencies. We assume the reasons are: (1) The low frequency generally describes the universal texture structures, which are quite similar to all iris images. (2) The high frequency are normally caused by random noise, which does not contain much unique information of the iris image.

The amplitude variation matrix is then binarised to record the zero crossing points as the sub-feature vector. The feature vector of our iris code is constituted by these sub-feature vectors.

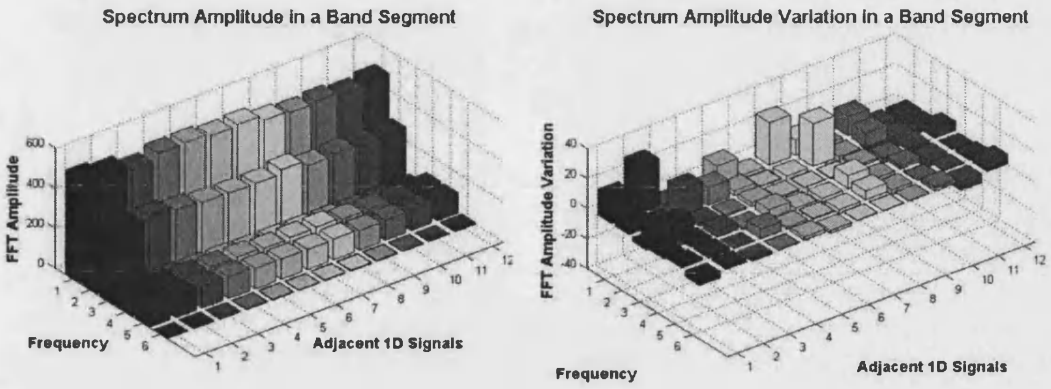

Figure 5-7 Local Spectrum Amplitude Variations

5.3 Classifier Design

The classifier design of a typical iris recognition system is a supervised learning procedure, which includes the following aspects:

- First, the training set has to be decided. In Bath system, three images have been randomly picked from each class as the training set.
- The training and testing images would be coded by MIT and then saved as binary feature vectors.
- In feature vector comparison, the distance between different iris feature vectors is measured by the weighted Hamming distance, which can be defined as follows:

$$Dis = \frac{1}{A}\sum_{i=1}^{N}\alpha_i[\frac{1}{B}\sum_{j=1}^{M}[\beta_j Feature1_{(i,j)} \oplus \beta_j Feature2_{(i,j)}]] \qquad (5\text{-}1)$$

$$B = \sum_{j=1}^{M}\beta_j \;; \qquad A = \sum_{i=1}^{N}\alpha_i$$

Where α_i denotes the weighting coefficient of different patches, with those nearer to the pupil weighted more heavily. β_j is a weight applied to different frequencies, with mid frequencies emphasized. $Feature1$ and $Feature2$ are two sub-features to be compared, and $\oplus$ denotes the XOR operation. M is the number of patches in each band and N is the number

of bands in each normalized image. B and A are the normalization coefficient respectively for the band and image.

In order to make the iris recognition system rotation invariant, we code every registered iris image from several initial positions around the circumference. Seven 'slip' templates are thus made from one registered iris image. An iris to be recognized will be matched to each slip template of the registered iris image and the minimum distance taken as the matching distance.

5.4 Experiment Description

The experiments will be taken in a PC Matlab environment with 2.4GHz CPU. The iris database we use to test the performance comes from the CASIA iris database. It has 308 classes of irises and 2174 images. For each class of iris, three images are selected arbitrarily as a training set, and the others used for testing.

The following metrics would be used in algorithm performance evaluation:

1. Correct Recognition Rate (CRR): Compare one test image to all the stored templates. If closest match in the stored templates belongs to the same class with the test image, it is called a correct recognition. The CRR is achieved from the experiments on the whole testing set.
2. ROC Curve: The criterion tests in the verification mode. If we tune the threshold for one test image to be accepted or rejected by one stored template, the False Acceptance Rate (FAR) and False Rejection Rate (FRR) will change accordingly. If the testing image number is T and the stored model number is S, the maximum false rejection number is T and the highest false acceptance number is $T*(S-1)$. If one image is false rejected, *FRR= 1/T*. If one image is false accepted, the *FAR= 1/T*(S-1)*. The closer the ROC is to the coordinate origin, the better the algorithm performance.
3. Equal Error Rate (EER): In order to evaluate the ROC curve quantitatively, a point in the ROC curve is used when FAR=FRR. This point is called the equal error rate point: EER=FAR=FRR.
4. Matching & Non-matching Distribution Graph: In evaluating performance, comparison between stored images and test images can be divided into

matching and non-matching categories and the Hamming distances displayed for each. If these sets are well separated, the system will work well on verification and recognition. The EER of an iris recognition system is the probability at which the two distributions intersect.

5. Decidability Index: A decidability index d is often used to measure the separation of two distributions:

$$d = \frac{|\mu_1 - \mu_2|}{\sqrt{\frac{(\sigma_1^2 + \sigma_2^2)}{2}}} \quad \text{(5-2)}$$

Where μ1 and μ2 are the means of the distributions and σ1 andσ2 are their standard deviations. The bigger the decidability is, the better the algorithm.

In the next section, we describe the tuning of the parameters used in the method for optimal performance, using two metrics to evaluate the performance: (1) CRR and (2) FAR at first False Rejection.

5.5 Finding the Optimal Parameters

5.5.1 Patch Width and Length

The size of the patch increases with local frequency information scale. The width corresponds to the circumferential scale and the length indicates the radial scale. Table 5-1 shows the CRR achieved with different length and width parameters with vertical patches and no windowing. Figure 5-8 shows the effect of different patch lengths and widths on the FAR at First False Rejection in Verification Mode. We can see that when (Width, Length) equals (8, 12), the system performance is the best both for maximum CRR and minimum FAR. This is chosen as the fundamental patch for the exploration of other parameters.

Width \ Length	8	12	16	24
4	95.20	96.48	96.40	93.92
8	96.96	96.88	96.88	96.16
16	92.40	92.16	89.12	85.28
32	79.20	75.04	70.08	57.60

Table 5-1 CRR (%) Tuned by Patch Width & Length

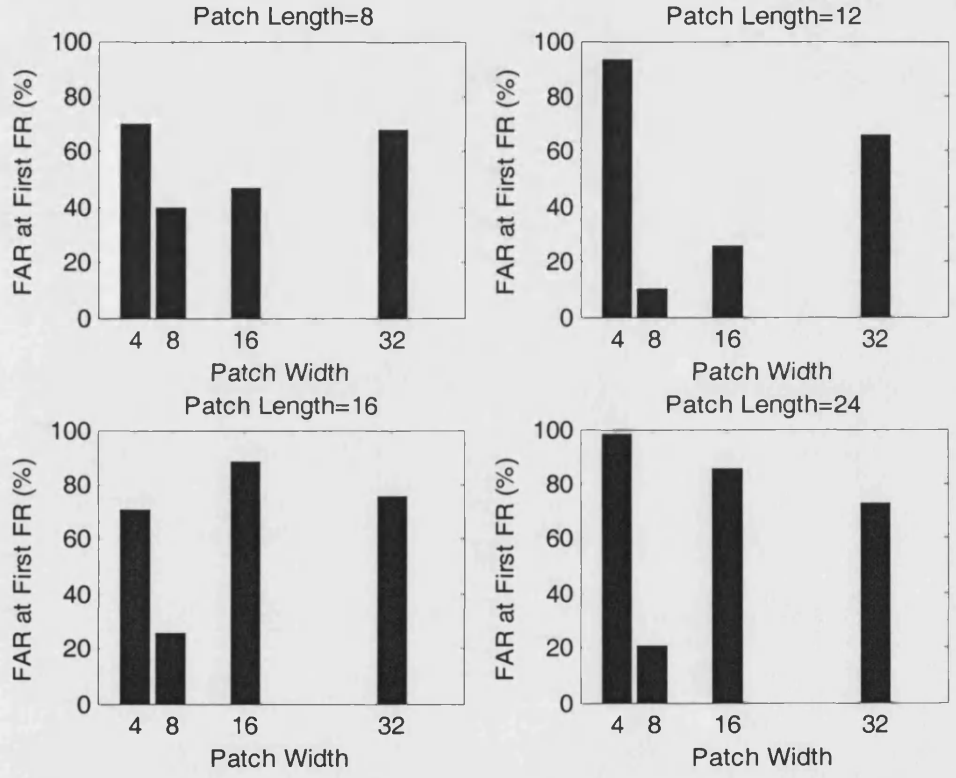

Figure 5-8 Effect of Patch Length & Width on FAR at First False Rejection

5.5.2 Patch Spacing

The feature vectors are formed from differences between patches. The number of feature vectors possible depends on the spacing of the patches. If the spacing is close or overlapping, many feature vectors will be obtained but they may be similar, so their codes will not be well distributed. If they are too far apart, insufficient vectors may be obtained. It could be seen from Table 5-2 that The selection of Vertical Spacing is 6 for the best CRR, at which patches overlap. The H_Space was chosen the same way as the V_Space. Huge

amount of parameter exploration has been done on the combination of $[V\_Space,\ H\_Space]$ and the best combination is achieved as (6, 8).

V_SPACE	2	4	6
CRR (%)	99.04	99.92	99.92
V_SPACE	8	10	12
CRR (%)	99.20	98.96	96.88

Table 5-2 CRR Tuned by Patch Space

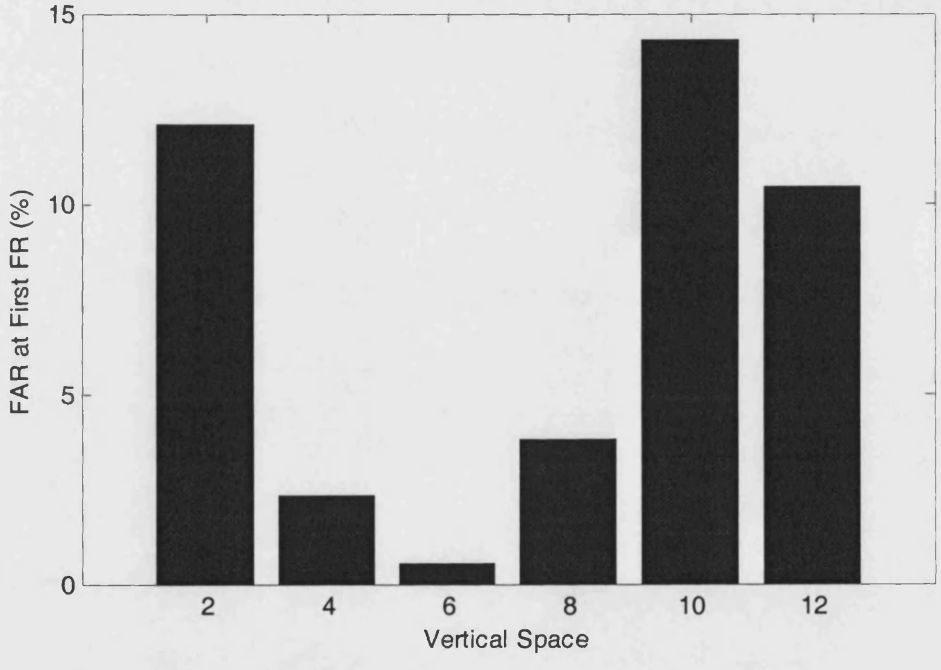

Figure 5-9 Effect of Patch Space on FAR at First False Rejection

5.5.3 FFT Window

In order to reduce FFT aliasing, a number of Hanning windows truncated in the middle were applied to the ends of the data prior to the FFT. The truncated middle values in the Hanning window are set as 1 and the values on the two sides will keep the same as the Hanning window. The tapered pixels on each side could be 6, 4, 3, or 2. Their corresponding windows are shown Figure 5-10. In Table 5-3, it is seen that the best window affects 2 pixels at each end of the data.

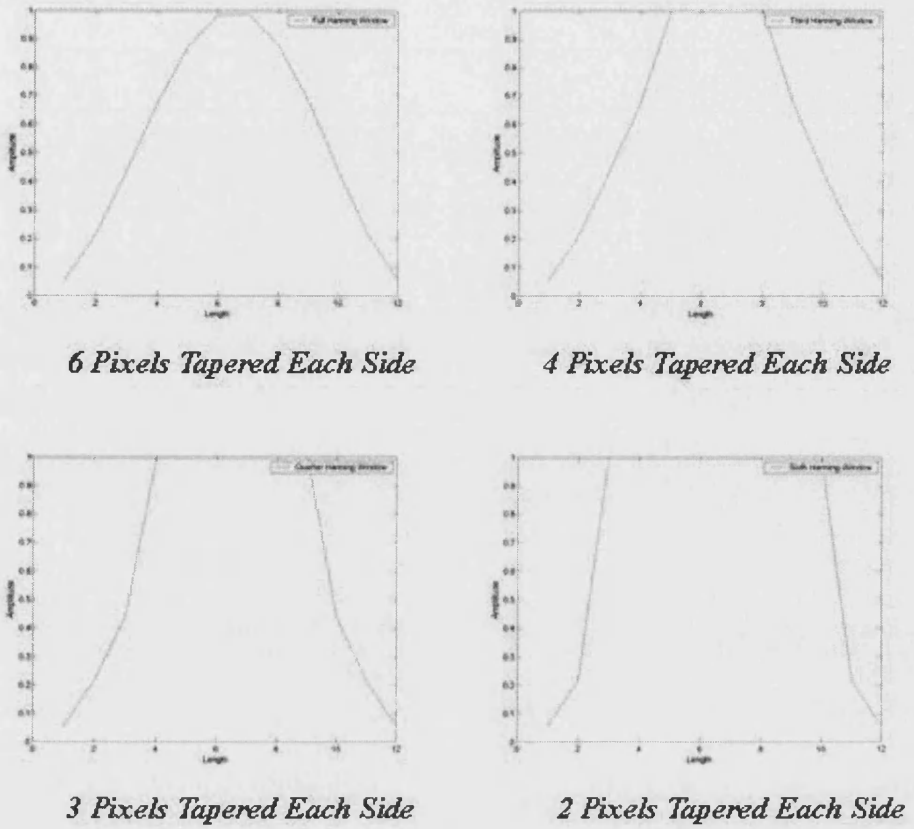

Figure 5-10 Truncated Hanning Window

6	4	3	2	Pixels Tapered
96.96	99.60	99.84	99.92	CRR (%)
26.47	3.24	0.39	0.29	FAR at First False Rejection (%)

Table 5-3 Performance Tuned by Truncated Window

5.5.4 Patch Angle

Both Daugman and Tan apply their transforms circumferentially. We have investigated the use of circumferential, radial and diagonal patches. At the 512x48 resolution used, a diagonal patch gives better performance that either circumferential or radial. This is shown by Table 5-4, in which we achieve 100% CRR. The FAR at First Rejection is also best for the diagonal patch.

0	45	90	Angle
99.92	100.00	92.40	CRR (%)
0.2889	0.0039	46.6510	FAR at First False Rejection (%)

Table 5-4 Performance Tuned by Patch Angles

If $Angle = 0$, the algorithm only utilize the circumferential information. When $Angle = 90$, only the radial information could be used for recognition. To apply the transform diagonally, which is the combination of the above two, could achieve a better performance. Also, we could see that local variation is more distinctive along the circumference than along the radius. That is why Daugman and Tan both apply their transforms circumferentially.

The above briefly introduced the extensive parameter exploration procedure and gave some parameter exploring examples. The best parameter set are achieved as:

$$\begin{aligned} &Width = 8, \quad Length = 12, \quad Angle = 45, \\ &V\_Space = 6, \quad H\_Space = 8 \end{aligned} \tag{5-3}$$

Then an extensive exploration around the best parameter set (5-3) was done in the 5-D parameter space ($Width$, $Length$, $Angle$, V_Space, H_Space), which also proved parameter set (5-3) is the local best. Strictly speaking, parameter set (5-3) could be best only when the five dimensions are independent. Further research needs to be done in this area.

5.6 Performance Evaluation and Comparison

As stated in section 5.4, the experiments will be taken in a PC Matlab environment with 2.4GHz CPU. The iris database we use to test the performance comes from the CASIA iris database. It has 308 classes of irises and 2174 images. For each class of iris, three images are selected arbitrarily as a training set, and the others used for testing. In order to make the iris recognition system rotation invariant, we code every registered iris image from

several initial positions around the circumference. Seven 'slip' templates are thus made from one registered iris image. An iris to be recognized will be matched to each slip template of the registered iris image and the minimum distance taken as the matching distance. The implementation of Daugman's method and Tan's method are got from Dr Li Ma from CASIA, which are regarded as good implementations of these two algorithms. The comparison between these three algorithms is implemented under the same environment and the evaluating metrics proposed in section 5.4 are used for comparison.

5.6.1 Correct Recognition Rate (CRR) Comparison

Daugman	*Tan*	*Monro*	*Method*
100	*100*	*100*	*CRR (%)*

Table 5-5 CRR Comparison

Since the algorithms of Daugman and Tan are well implemented by Dr Li Ma, these three algorithms have all achieved 100% correct recognition rate. It also proved that the methods based on local image variation analysis could describe the essential iris feature.

5.6.2 Receiver Operating Characteristic (ROC) Curve Comparison

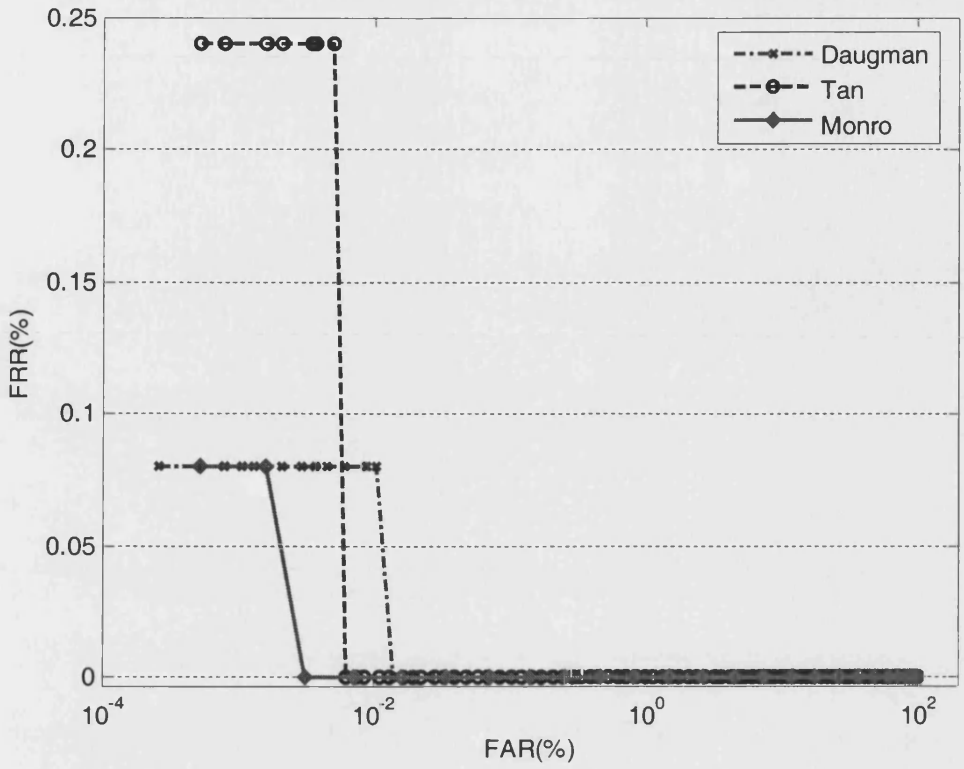

Figure 5-11 ROC Curve Comparison

The horizontal axis denotes the false acceptance rate and the vertical axis indicates the false rejection rate. For one algorithm, the increasing of FAR always comes with the decreasing of FRR. It is a trade off. Low FAR threshold could be used in high security places, such as bank, intelligence agency, etc. While Low FRR could be applied to daily life area, in order to make the system less troublesome. The closer the ROC curve to the coordinate origin is, the better the algorithm is. We can see from Figure 5-11 that the proposed Monro Iris Transform is the closest to the coordinate origin.

5.6.3 Comparison in Practical Application Situation

In many applications an acceptable FAR would be 0.00003. For example in cash point machines (ATMs) using a four digit PIN, the FAR would be no better than 0.0001 (assuming that PIN numbers and guesses are random which is probably not the case.) Table 5-6 is a comparison of FRR when FAR=0.00003.

Daugman	Tan	Monro	Method
0.08	0.25	0.00	FRR (%)

Table 5-6 Comparison in Practical Application Situation (FAR = 0.00003)

5.6.4 Equal Error Rate (EER) Comparison

The tuning of the threshold value determines its false acceptance rate and its false rejection rate, and when the rates are equal, the common rate is referred to as the equal error rate. The value indicates that the proportion of false acceptances is equal to the proportion of false rejections. The lower the equal error rate value, the higher the accuracy of the biometric system. The proposed MIT (Monro Iris Transform) has achieved the lowest EER.

Daugman	Tan	Monro	Method
0.76674	0.23795	0.15864	EER (%)

Table 5-7 EER Comparison

5.6.5 Decidability Index Comparison

In evaluating performance, comparisons between stored images and test images can be divided into matching and non-matching categories and the Hamming distances displayed for each. If these sets are well separated, the system will work well on verification and recognition. A decidability index d is often used to measure the separation of two distributions, as described in equation (5-2). The match and non-match distribution graphs for the methods of daugman, Tan and Monro are all drawn and their corresponding decidability indexes are calculated in the following. The mean and standard deviation of each distribution are also shown in the graphs.

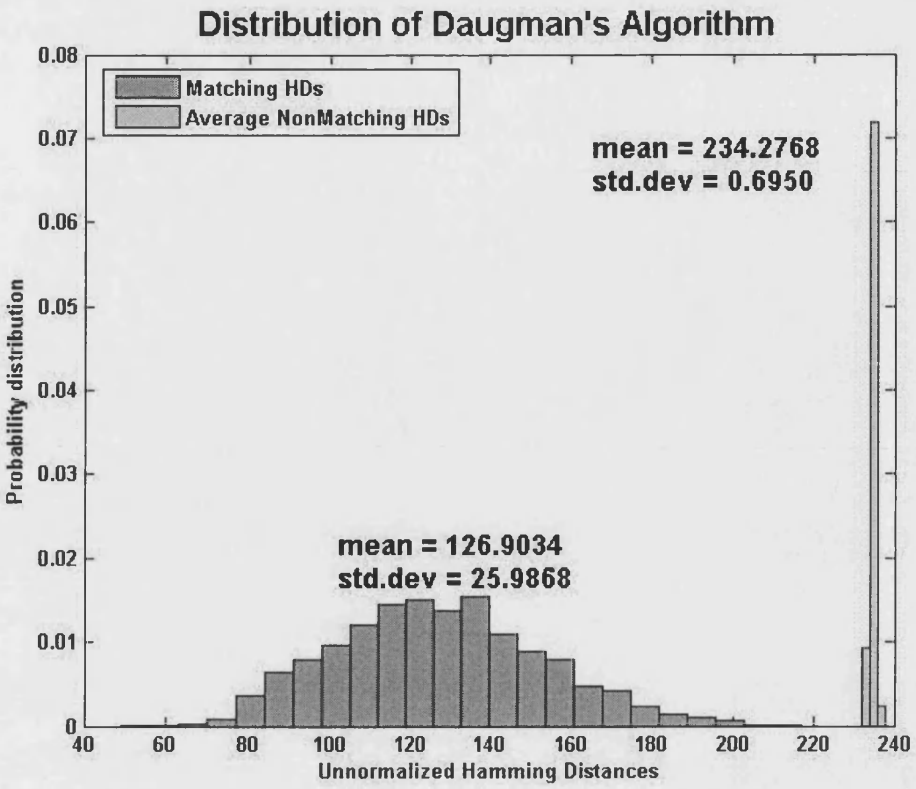

Figure 5-12 Distribution of Daugman's Algorithm

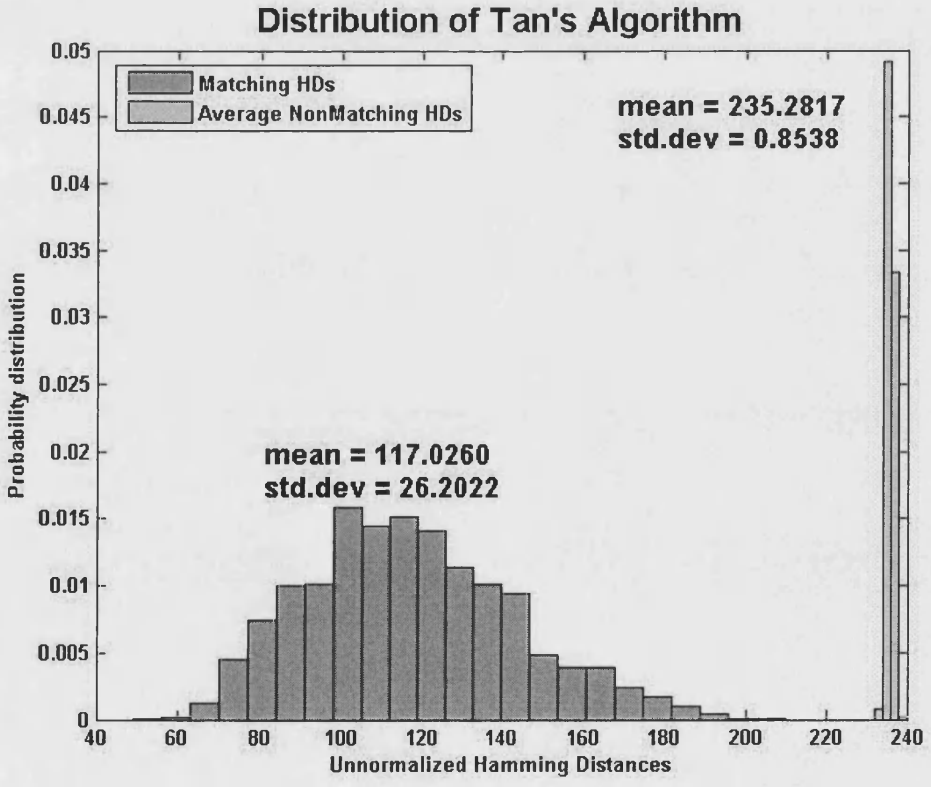

Figure 5-13 Distribution of Tan's Algorithm

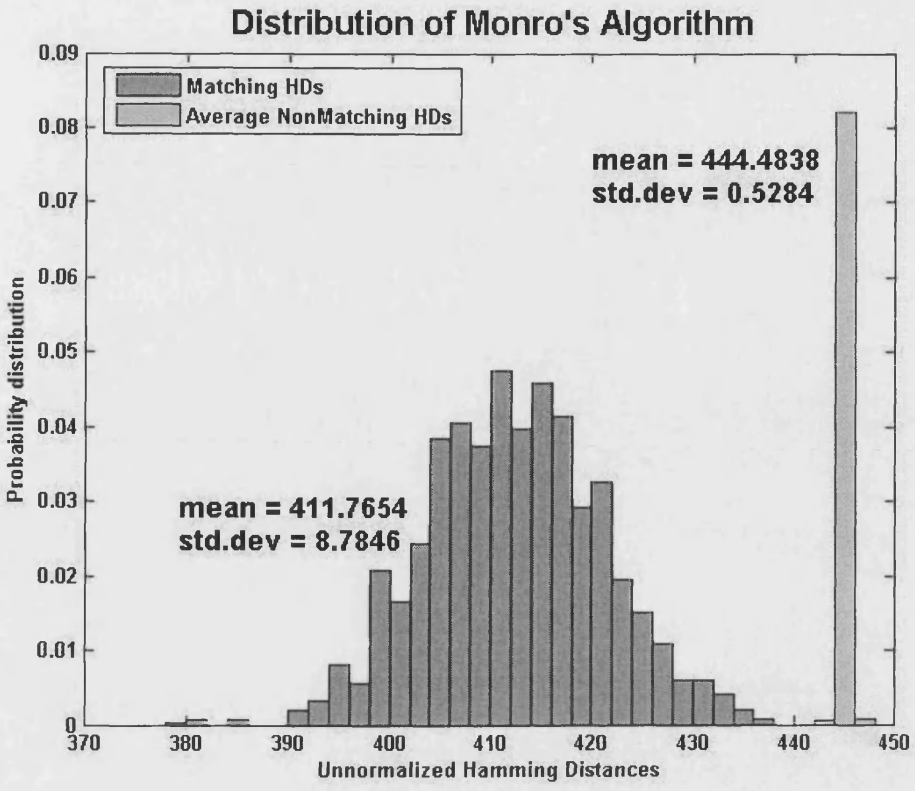

Figure 5-14 Distribution of Monro's Algorithm

Daugman	Tan	Monro	Method
5.8412	6.3792	5.2578	Decidability Index d

Table 5-8 Comparison on Decidability Index

It could be seen from the three distribution graphs that all the three algorithms could well separate the match-distribution and the non-match-distribution. As the Decidability Index d is concerned, Tan's algorithm is slightly better than Daugman's and Monro's algorithms. Although the difference is quite small, this result is not consistent with the rest. This needs to be further researched.

According to the testing software, the total Hamming distance should be 1000. Thus the average Hamming distance between two un-related binary feature vectors should be 500. Among the three graphs above, the mean of the average non-match distribution of Monro's algorithm is the closest to 500. This means the Monro Iris Code has less redundant information than the other two.

5.6.6 Complexity Comparison

Complexity is a very important factor in practical applications of iris recognition methods, especially for systems with large databases and real time queries. One of the aims for the research is to reduce the computational complexity and thus contribute to the real time system. In Table 5-9 the speed of the three methods is compared in the Matlab environment with a 2.4GHz CPU. The proposed iris coding and matching method is the fastest.

Item / Method	Feature Extraction (ms)	Match (ms)	Feature Extraction + Match (ms)
Daugman	422	31	453
Tan	125	68	193
Monro	89	31	120

Table 5-9 Complexity Comparison

Obviously, the speed of the algorithm highly depends on the programming implementation. Thus a bad realization of a good algorithm could lead to terrible results. Since Dr Li Ma is the implementer of Tan's algorithm and we got Tan's implementation from Dr Li Ma, this comparison should be reasonable to some extent.

5.7 Summary

A lot of work has been done on iris image feature extraction and matching through various directions. Generally these methods could be categorized into two areas: methods based on iris image structure analysis and methods based on local image variation analysis. Normally local image variation analysis based methods perform better than iris image structure analysis based methods. Both Tan and Daugman's methods belong to the local image variation analysis based methods. Daugman utilizes the local phase variation and Tan adopts the local intensity variation to represent the iris image feature.

The research in iris image feature extraction and matching focuses on two area recently: (1) How the local variation information could be extracted more effectively to represent the uniqueness of its structure. (2) How to speed up this feature extraction procedure to meet the requirement of real time recognition system.

In an attempt to solve the above two questions, this thesis proposed a local frequency amplitude variation based iris coding algorithm, following the research direction of local image variation analysis. Extensive experiments showed that the proposed algorithm could greatly reduce the processing time while still maintain a very high distinguishing capability.

Through the research in this chapter, two possible answers to the questions proposed at the beginning of this chapter could be given: (1) The local image variation is the essential unique information for one iris class to be differentiated from another. Apart from utilizing the local phase or intensity variations, this thesis used the local frequency variation, which is also proved to be very effective. (2) The adoption of Fast Fourier Transform (FFT) makes the feature extraction procedure very time efficiency. Thus the fast representation of local feature information is a very effective way to speed up the coding process.

The future work in feature extraction and matching will focus on the following aspects: (1) The combination of local phase, intensity and frequency feature. (2) Introducing more weighting schemes, such as different weighting for different bit in a sub-feature vector. (3) Exploring more transform methods to represent the local feature, such as 2D FFT, DCT, 2D DCT, etc.

6 Eyelash Removal Algorithm Based on Local Area Analysis

6.1 Foreword

A typical iris recognition system includes iris capture, image pre-processing, feature extraction and matching. While early work has focused primarily on feature extraction with great success, the pre-processing task has received less attention. However, the performance of a system is greatly influenced by the quality of captured images. Amongst the various factors that could affect the quality of iris images, one of the most commonly encountered is eyelash occlusion, which can degrade iris images either during enrolment or verification. Examples of iris images with eyelash occlusion are shown in Figure 6-1. Such strong 'eyelash textures' obscure the real iris texture, and hence interfere seriously with the recognition capability of any recognition system. Reducing the influence of the eyelash on recognition is therefore an important problem.

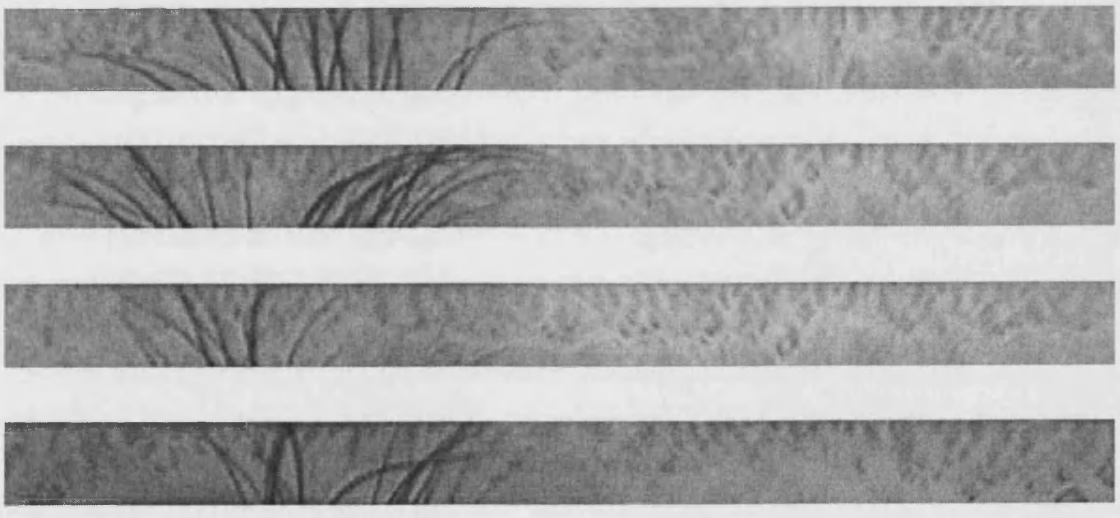

Figure 6-1 Iris Images Occluded by Eyelashes

Early efforts to mitigate the effects of eyelash tried to ignore parts of the iris to avoid eyelash contamination. Later some researchers tried to detect and mask the eyelash pixels from the image. Zhang et al classified the eyelashes into two categories, separable and multiple [91]. They then used an edge detector to find separable eyelashes, and recognized multiple eyelashes by intensity variance.

Daugman detects eyelashes using wavelet demodulation and masks them in iris coding [31]. Both of these methods locate the eyelash pixels in the image and exclude the iris code bits generated from these pixels. Although these two methods successfully detect and mask eyelashes, the improvements in system performance are quite modest. In this chapter we will develop a method for removing eyelashes and restoring the underlying iris texture as much as possible.

In this work, we recreate iris pixels occluded by eyelashes using information from their non-occluded neighbours. Briefly, for every pixel in the iris image, we first decide if the pixel is in an area contaminated by eyelashes, and if so we determine the direction of the eyelash. We then filter the image locally along a direction perpendicular to the eyelash because we have the best chance of finding uncontaminated pixels along this direction. To avoid incorrectly filtering non-eyelash pixels, no pixel is altered unless the change in that pixel exceeds a certain threshold. The iris coding algorithms proposed by Daugman and Tan and our own method have been tested in the same environment as last chapter and encouraging improvements are shown. The preferred metric for iris recognition performance is the Equal Error Rate (EER), where False Acceptance Rate (FAR) and False Rejection Rate (FRR) become equal. Our proposed eyelash removal method reduces the EER greatly for all the three methods proposed.

6.2 Eyelash Removal

Our work is done using images from the CASIA database, images in which are normalized into a rectangular 512 x 80 image. For processing we use the 48 rows of pixels nearest the pupil, which are at the top in Figure 6-1. This operation could eliminate some eyelashes occluding the outer iris area, but still many truncated normalized images suffer from heavy eyelash. Figure 6-2 summarizes the proposed eyelash removal algorithm based on nonlinear conditional directional filtering.

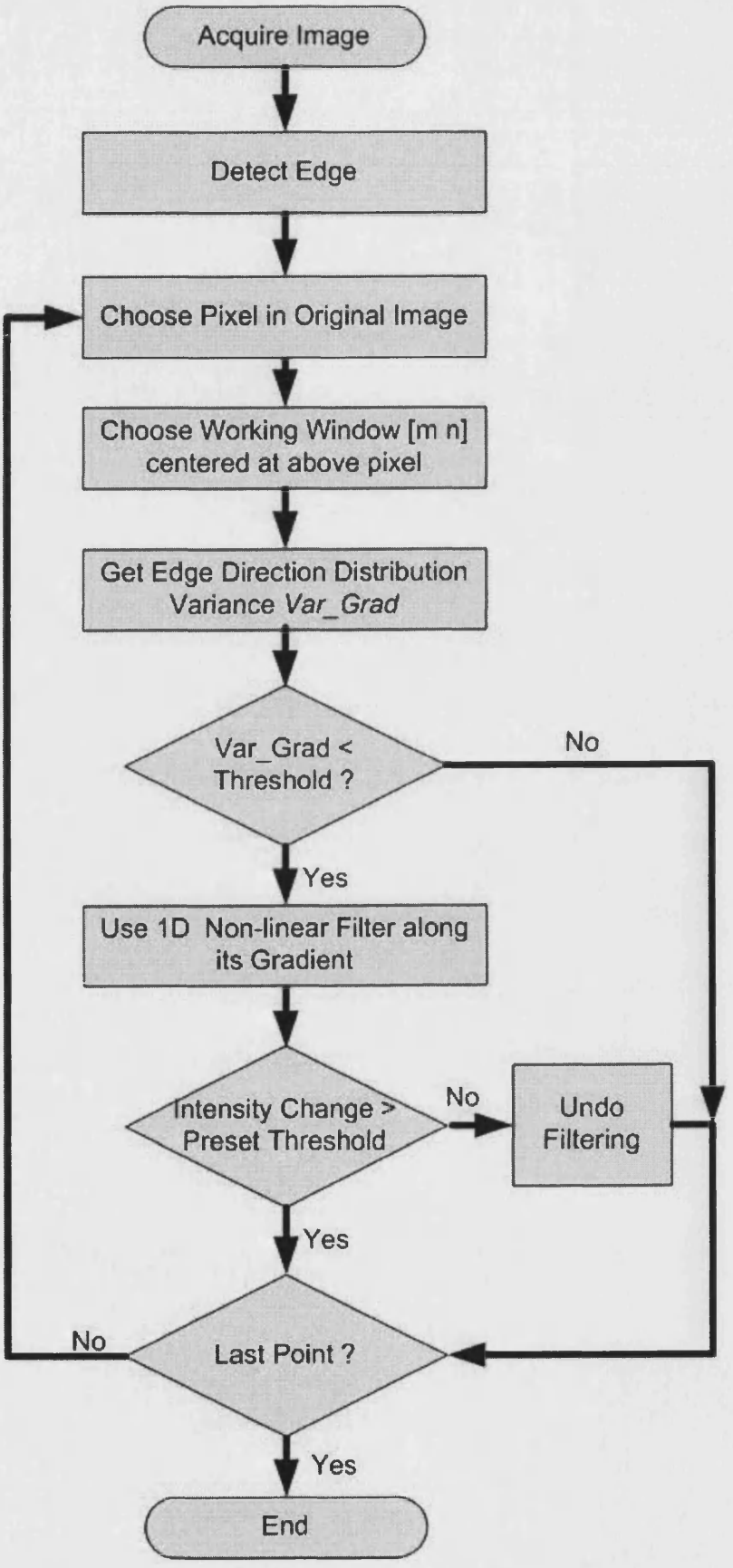

Figure 6-2 Proposed Eyelash Removal Method

The following of this chapter will take Figure 6-3 as an example to illustrate the proposed eyelash removal algorithm.

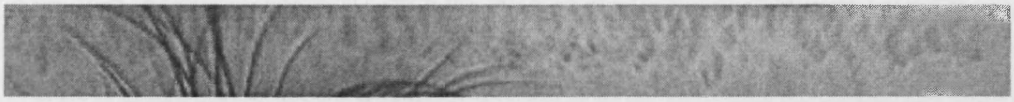

Figure 6-3 One Example of Eyelash Occluded Image

6.2.1 Edge Detection

An eyelash causes a discontinuity along its edges, so to detect an eyelash and estimate its direction, a 3 x 3 Sobel edge filter is applied to the normalized image, as shown in Figure 6-4.

-1	-2	-1
0	0	0
1	2	1

(a) X Derivative

z_1	z_2	z_3
z_4	z_5	z_6
z_7	z_8	z_9

(b) Image Region

-1	0	1
-2	0	2
-1	0	1

(c) Y Derivative

Figure 6-4 Sobel Edge Filter

For every pixel, the estimated gradients in the X and Y directions are [Gx ,Gy] and the magnitude of the gradient at the center point of the mask, called Grad, are computed:

$$G_x = (z_7 + 2z_8 + z_9) - (z_1 + 2z_2 + z_3) \quad \textbf{(6-1)}$$

$$G_y = (z_3 + 2z_6 + z_9) - (z_1 + 2z_4 + z_7) \quad \textbf{(6-2)}$$

$$Grad = \left(G_x^2 + G_y^2\right)^{1/2} \quad \textbf{(6-3)}$$

The local gradient direction (perpendicular to the edge) is:

$$\theta = \arctan(G_y / G_x) \quad \textbf{(6-4)}$$

After the 3×3 Sobel operator is applied to the image, the 8-connected areas in the binary image are labeled and those less than 6 pixels long will be removed from the image to reduce the noise. The results are shown in Figure 6-5. We can see that the Sobel operator could pick out the eyelash edges quite well and the noises are effectively removed.

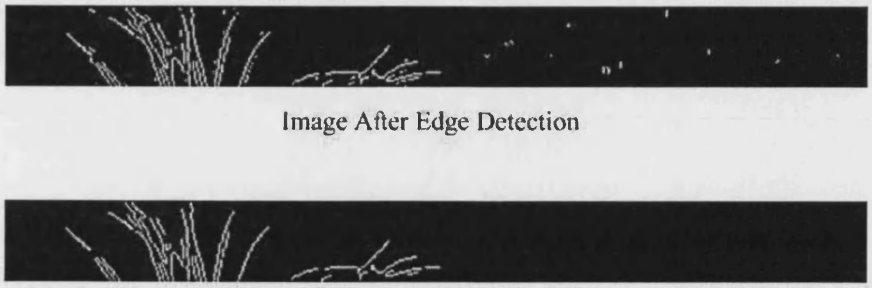

Figure 6-5 Results After Edge Detection

6.2.2 Extended Image for Filtering

In order to implement the eyelash removal filter, the original image and the binarised edge image should be extended to a larger size as shown in Figure 6-6. The extended parts should be large enough for the convolution kernel to filter the margin pixels in the original image. The extended parts along horizontal boundaries are the mirror symmetries of their corresponding interior parts along the same boundaries. Since the normalized image was mapped from an annular iris, the extended end comes from the beginning with the same size and vice versa. Also the gradient orientation image for the binarised edge image should be extended for the convenience of calculation.

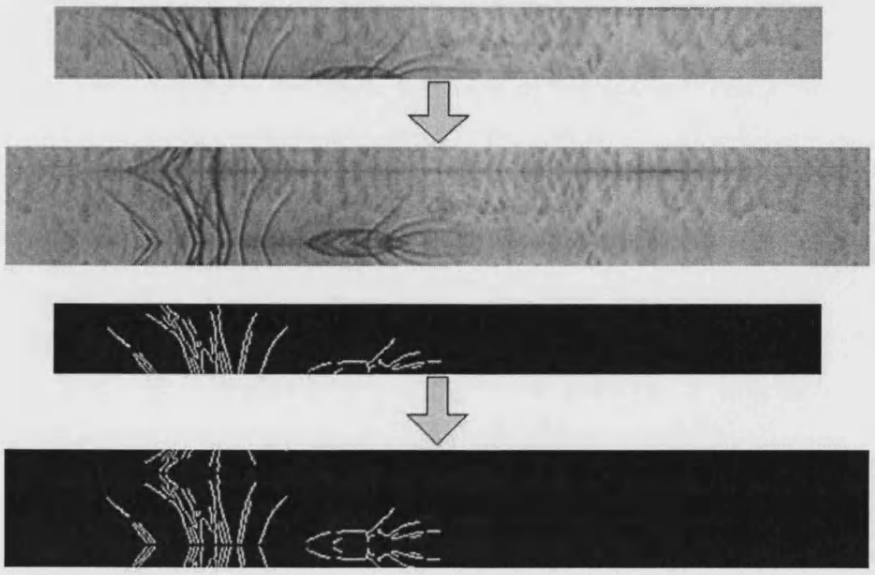

Figure 6-6 Extended Image

6.2.3 Eyelash Area Decision

To decide if a pixel is occluded, we define a window of size [m n] centered at the pixel and compute a gradient direction variance over those r pixels for which Grad > 15:

$$Var\_Grad = \frac{1}{r-1}\sum_{i=1}^{r}\left(\theta_i - \bar{\theta}\right)^2 \quad \textbf{(6-5)}$$

If the gradient direction has a small variance, a strong edge is indicated, as can be seen in Figure 6-7, and this pixel is classified as being affected by eyelash. Otherwise, this area is considered as non-eyelash area and will not be filtered.

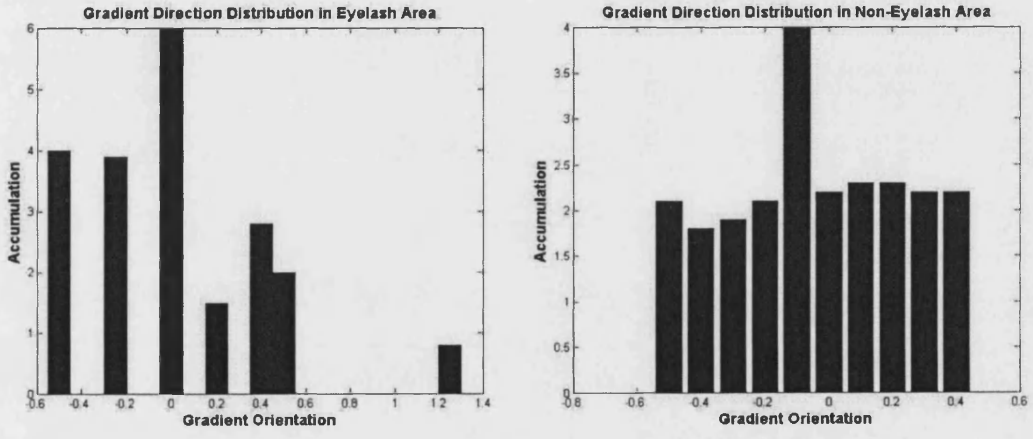

Figure 6-7 Gradient Direction Distribution

6.2.4 Non-linear Filtering

For each pixel classified as an eyelash pixel, a 1D median filter of length L is applied along the direction θ to estimate the value of the image with the eyelash removed. In general the direction does not pass exactly through pixels, so the median filter is applied to values equally spaced by the distance between actual pixels, which are calculated using bilinear interpolation of the four nearest pixels.

Not every pixel in the eyelash window is occluded by eyelash, so we only change the intensity if the intensity difference after filtering exceeds a threshold. Specifically we compute:

$$Recover = Diff - k * Var(Image) \quad (6\text{-}6)$$

Diff is the difference in intensity between the filtered and unfiltered pixel and Var (Image) is the intensity variance of the whole (unfiltered) image. K is the parameter used to tune the threshold. If Recover is positive, the pixel is replaced by the filtered value, otherwise the filter is not applied.

6.2.5 Visual Results

Figure 6-8 and Figure 6-9 show the effect of the eyelash removal method on normalized human iris images with and without filtering. It is seen that visually the filter has little effect on an image with no eyelash occlusion, while in the occluded case the eyelashes are replaced by pixels representative of underlying iris texture. It is not perfect; the positions of the eyelashes are visible.

(a) Image without eyelash occlusion

(b) The effect of the eyelash removal filter

Figure 6-8 Filter Effect for Non-Eyelash Images

(a) Image affected by eyelash

(b) The effect of the eyelash removal filter

Figure 6-9 Filter Effect for Eyelash Images

6.3 Experiments and Comparison

6.3.1 Experimental Environment

The experimental environment is the same as that in the last chapter. The experiments were taken in a PC Matlab environment with 2.4GHz CPU. The iris database we use to test the performance comes from the CASIA iris database. It has 308 classes of irises and 2174 images. For each class of iris, three images are selected arbitrarily as a training set, and the others used for testing. In order to make the iris recognition system rotation invariant, we code every registered iris image from several initial positions around the circumference. And the nearest 'slip' template is the matching template between the test image and the registered image.

The parameters of the filtering process are tuned using the Monro Iris Transform (MIT). Because 100% Correct Recognition Rate (CRR) is achieved on this data before eyelash removal was applied, we tune the filter for minimum Equal Error Rate (EER).

6.3.2 Parameter Tuning

There are five parameters affecting the performance of the proposed directional filter: Window_Size [m n], 1D median filter length L, normalized edge point gradient direction variance Var_Grad, and intensity change k. Experimentally the best parameters are:

$$[m\ n\ L\ Var\_Grad\ k] = [16\ 32\ 33\ 0.5\ 0.3] \quad \textbf{(6-7)}$$

Strictly speaking, this requires the five parameter dimensions to be independent to each other, which would be researched further. Table 6-1 to Table 6-5 show some EER results by varying each of the parameters in turn around this chosen operating point. It is seen that the performance is quite sensitive to all parameter settings except Var_Grad.

8	12	16	24	m
1.72	0.53	0.26	0.40	EER (10^{-3})

Table 6-1 Parameter m Tuning

8	16	32	64	n
0.93	3.44	0.26	3.17	EER (10^{-3})

Table 6-2 Parameter n Tuning

9	17	33	65	L
3.17	0.39	0.26	1.06	EER (10^{-3})

Table 6-3 Parameter L Tuning

0.01	0.2	0.5	1	Var_Grad
0.40	0.26	0.26	0.26	EER (10^{-3})

Table 6-4 Parameter Var_Grad Tuning

0.1	0.2	0.3	0.4	k
0.40	0.40	0.26	0.40	EER (10^{-3})

Table 6-5 Parameter k Tuning

6.3.3 Results on the Monro Iris Transform (MIT)

With the Monro algorithm, the CRR remains 100% after eyelash removal. However the EER is reduced significantly, from 1.59×10^{-3} to 2.6×10^{-4}, almost six times smaller than before the eyelash removal. Figure 6-10 shows the Receiver Operating Characteristic (ROC) before and after eyelash removal. This is obtained by altering the weighted Hamming distance threshold to achieve a desired FAR. Without eyelash removal there is one False Rejection at a FAR of about 10^{-2}.

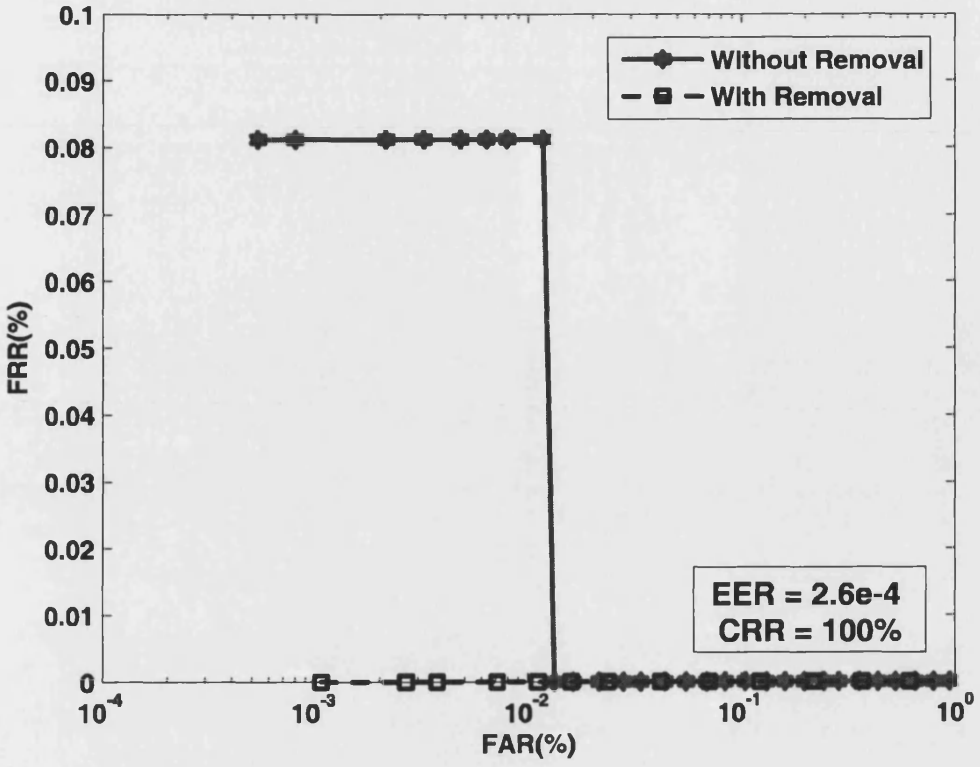

Figure 6-10 ROC Curves with the Monro Iris coding method, with and without eyelash removal

The match and non-match distributions are also graphed and their decidability indexes are calculated. Figure 6-11 and Figure 6-12 show that the matching distribution is shifted towards lower Hamming distances, as would be expected. And the decidability shifts from 5.2578 to 5.6671, indicating an improvement in the performance of the system, which could also been seen from inspection of the two distributions

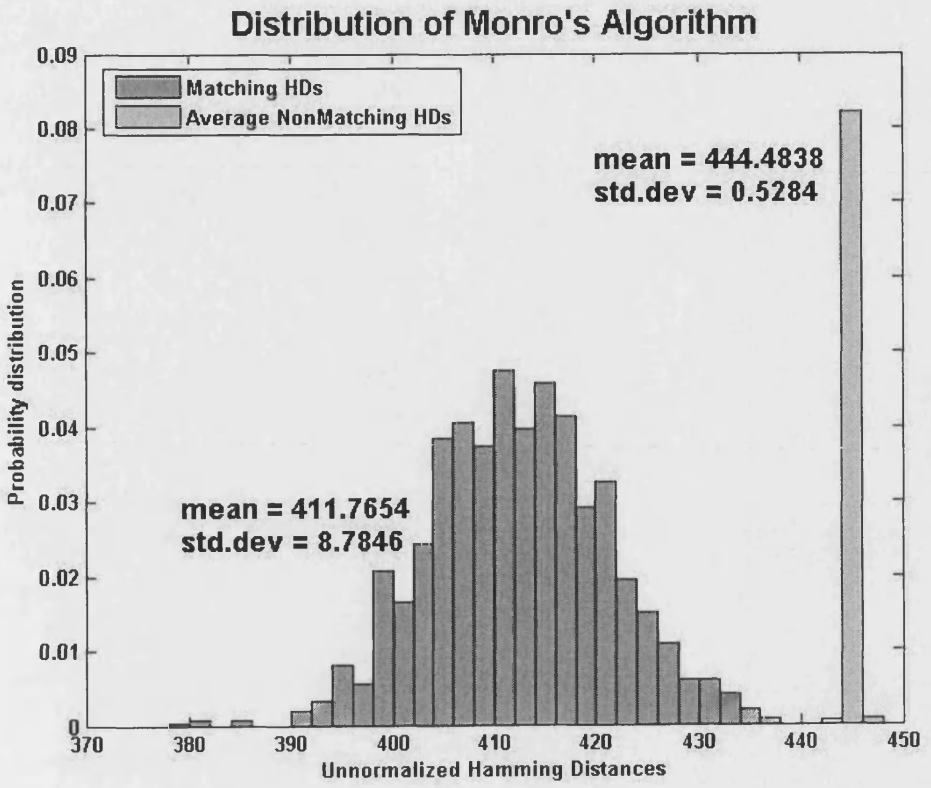

Figure 6-11 Distribution of Monro's Algorithm Without Filter

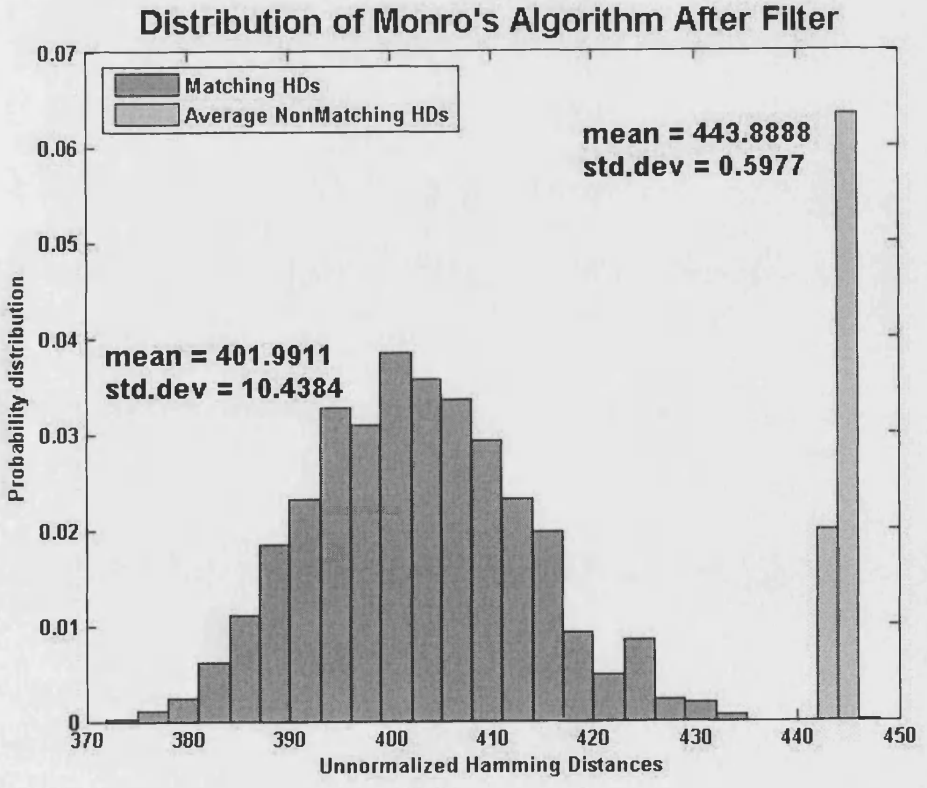

Figure 6-12 Distribution of Monro's Algorithm After Filter

Stage / Criterion	Without Filter	With Filter
EER (10^{-3})	1.59	0.26
Decidability Index	5.2578	5.6671

Table 6-6 Results Comparison on Monro's Algorithm

6.3.4 Results on Daugman's Iris Transform

Daugman's iris coding algorithm is also utilized to test the proposed eyelash removal method based on the same CASIA database and in the same Matlab environment with a 2.4GHz CPU. The CRR is also 100% after the eyelash removal filter. All the other evaluating criterions (ROC curve, EER, Decidability index, Distribution Graph) are all got improved after the eyelash removal filter, as will be shown in the following tables and figures. Since Daugman's iris coding method is widely accepted and applied to many industrial products, the effectivity of the proposed eyelash removal algorithm with Daugman's coding method gives it a wider future for practical application.

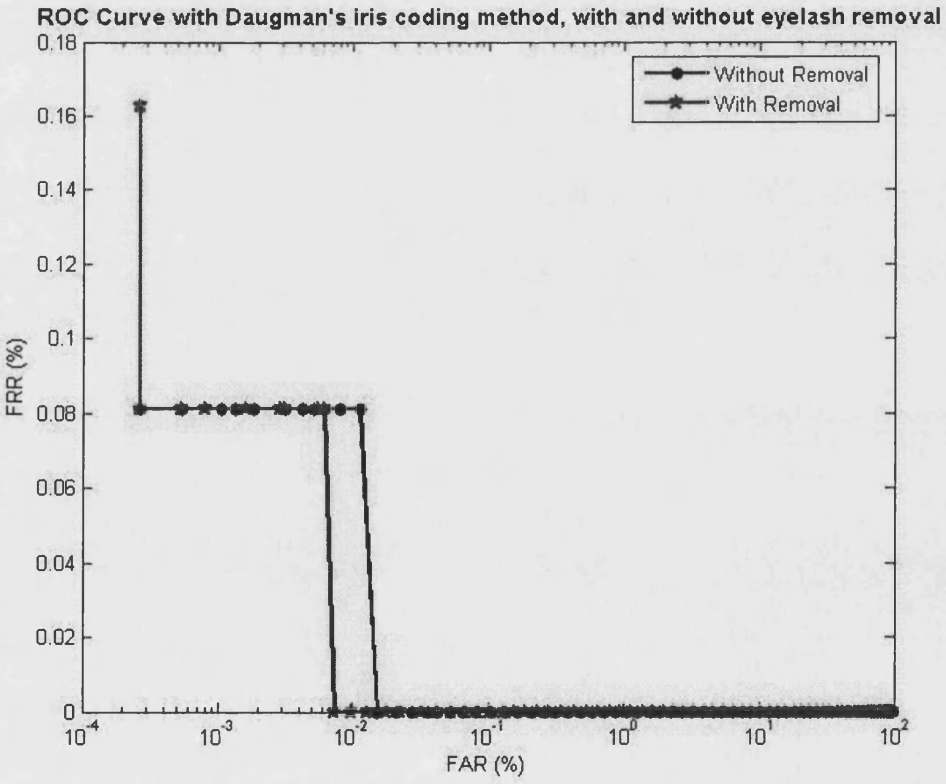

Figure 6-13 ROC Curve with Daugman's Iris Coding Method, With and Without Eyelash Removal

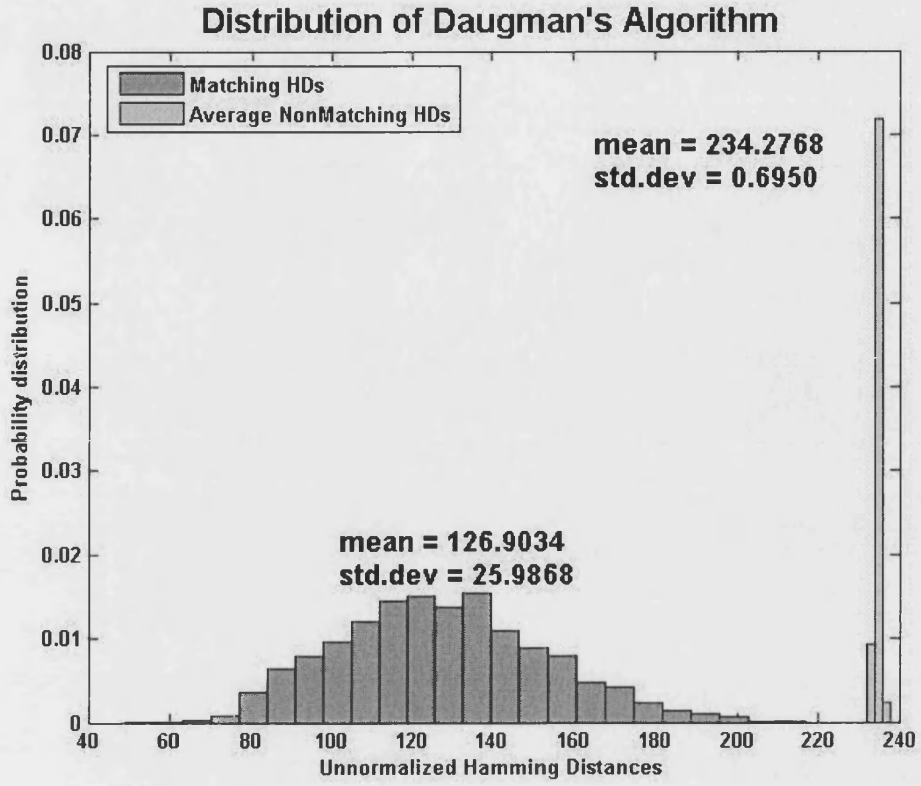

Figure 6-14 Distribution of Daugman's Algorithm Without Filter

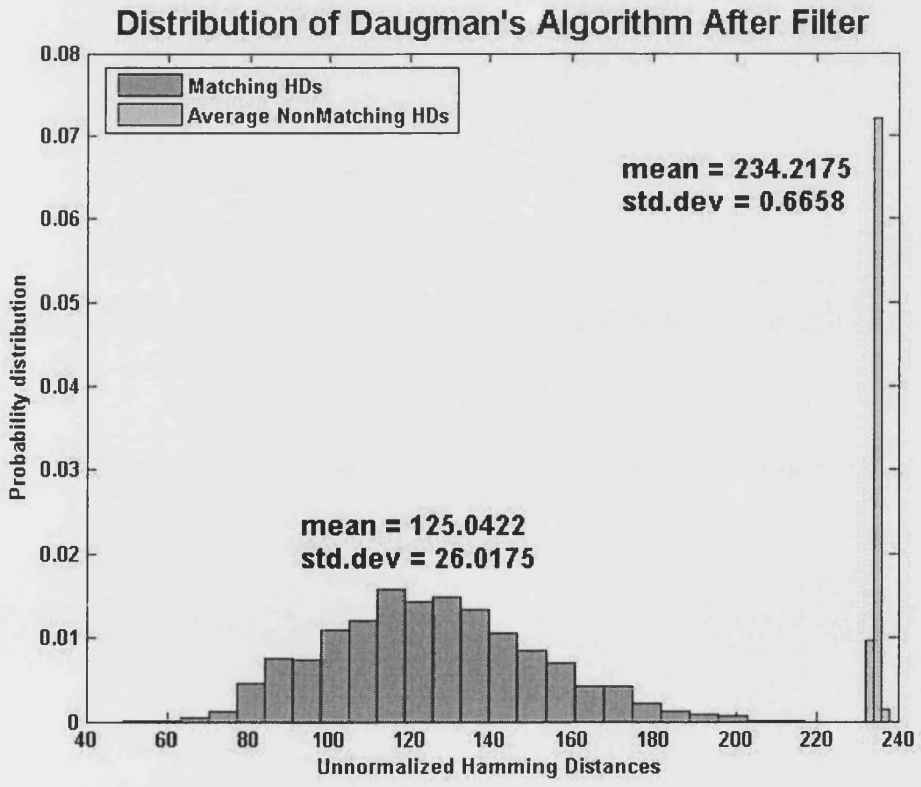

Figure 6-15 Distribution of Daugman's Algorithm After Filter

Stage / Criterion	Without Filter	With Filter
EER (10^{-3})	7.7	3.7
Decidability Index	5.8412	5.9324

Table 6-7 Results Comparison on Daugman's Algorithm

6.3.5 Results on Tan's Iris Transform

As a leading researcher in iris recognition and the provider of CASIA iris image database, Tan's algorithm is also chosen as another transform to test the performance of our eyelash removal algorithm. The testing environment and all the evaluating criterions will still be the same as before. The following results show that the proposed eyelash removal algorithm could enormously improve the performance of Tan's iris coding method.

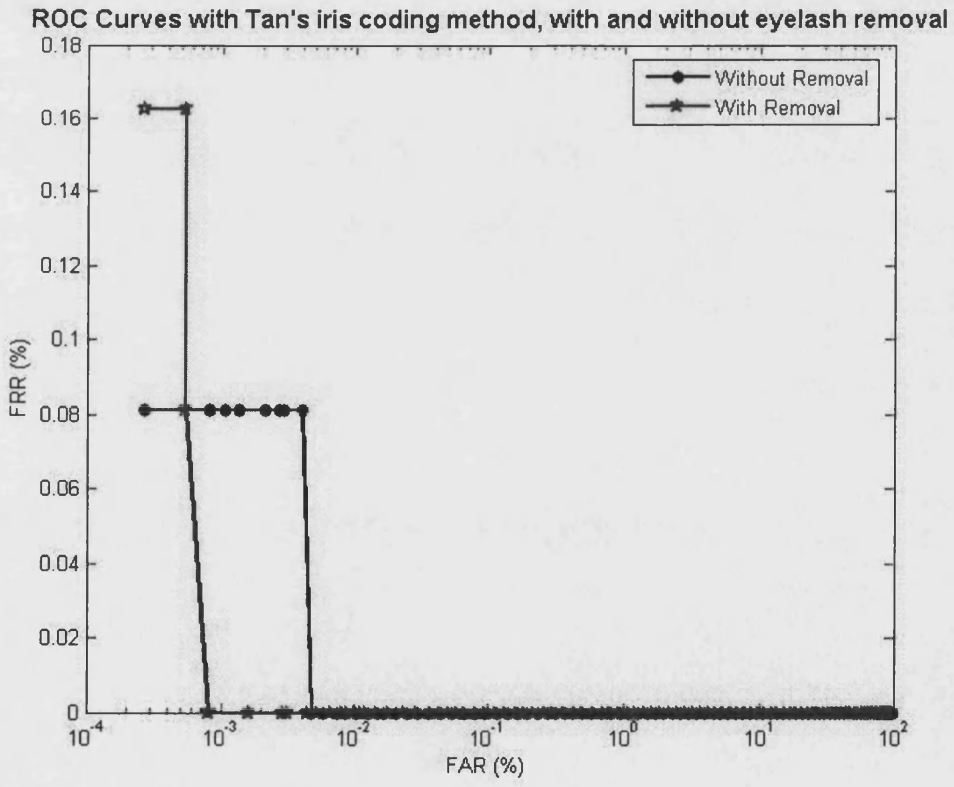

Figure 6-16 ROC Curve With Tan's Iris Coding Method, With and Without Eyelash Removal

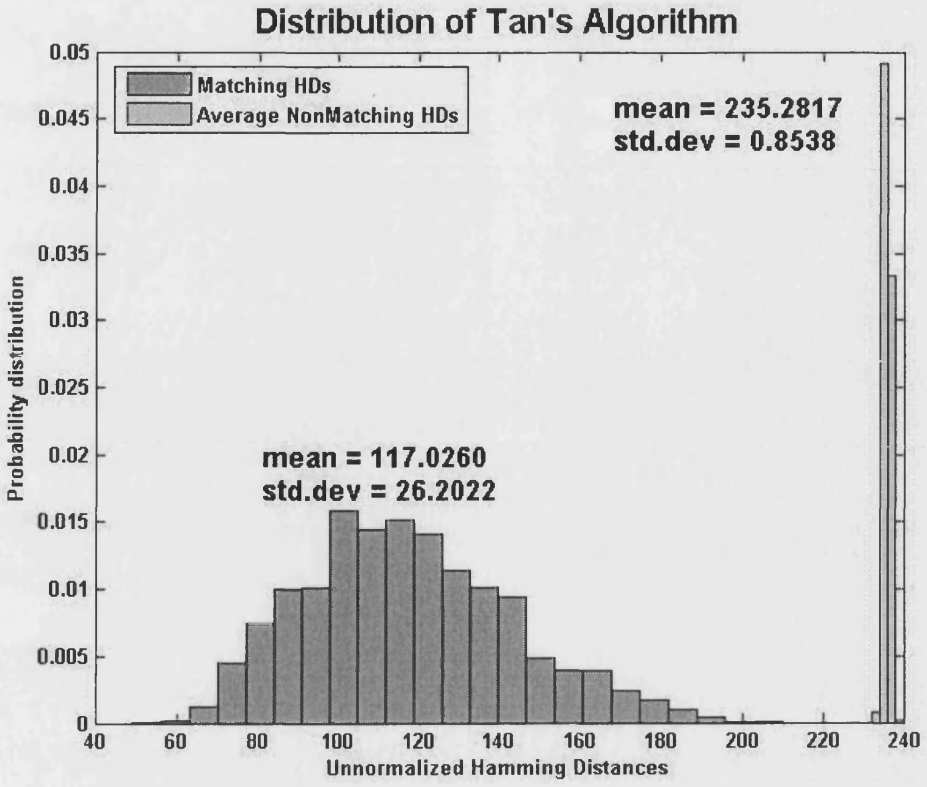

Figure 6-17 Distribution of Tan's Algorithm Before Filter

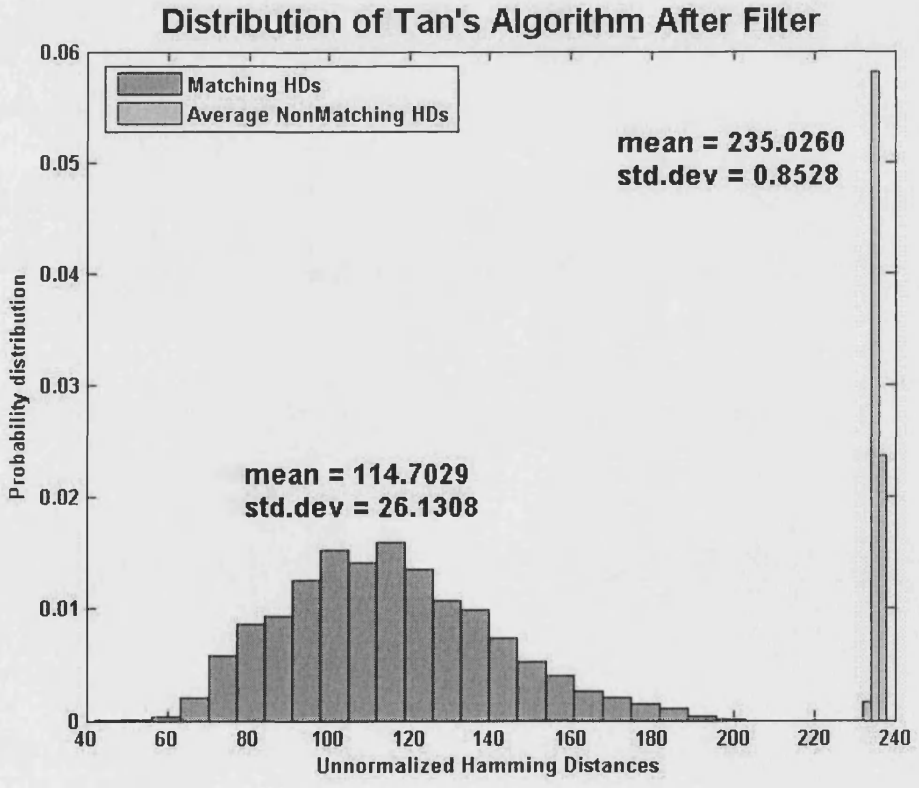

Figure 6-18 Distribution of Tan's Algorithm After Filter

Stage / Criterion	Without Filter (ms)	With Filter (ms)
EER (10^{-3})	2.4	0.397
Decidability Index	6.3792	6.5085

Table 6-8 Results Comparison on Tan's Method

6.4 Summary

This chapter has proposed an effective eyelash removal algorithm based on local area analysis. Three leading iris image coding methods (Tan, Daugman, Monro) have been chosen to test the performance of the proposed algorithm in the metrics of CRR, EER, ROC curve, match and non-match distribution, Decidability Index. Through extensive experiments, it shows that the proposed eyelash removal algorithm could greatly enhance the system performance in all the evaluating metrics for all the three leading iris image coding methods.

Unlike other previous eyelash removal methods, which generally tried to detect and mask the eyelashes or the eyelash areas, the proposed method recreates iris pixels occluded by eyelashes using information from their non-occluded neighbors. This method is derived from the following idea. The iris image texture is an inter-correlated area, in which the unique discriminative information is redundant. Statistically, the grayscale intensity of one pixel is highly related to neighbor pixel intensities. Thus if one pixel is occluded by eyelashes, we could reconstruct it with the information from its neighbor pixels. In this way, the achieved iris code will remain unabridged.

The main contributions in this chapter include the following points:

- Proposed the eyelash area verifying method based on the gradient variance of edge points in a windowed area. This method works well in detecting eyelash area in our experiments
- Using 1D non-linear filter to along a direction perpendicular to the eyelash to reconstruct the eyelash occluded pixel.

- Proposed an adaptive metric $Recover$ to decide if the filtered pixel is eyelash pixel or not. For each pixel, if $Recover$ is positive, the pixel is replaced by the filtered value, otherwise the filter is not applied.

The eyelash detection and filling methods are quite preliminary. Thus alternative methods should be investigated in future research. Some 'ridge' detector methods, such as Markov Random Field, could be used to detect eyelash existing in the iris area [94]. 'hole filling' is an extensively researched area for surface reconstruction and thus could be used for future eyelash filling. [95]

Image Inpainting is the area directly related to image reconstruction and thus would have many techniques exploitable for eyelash removal and iris texture reconstruction. Actually the method proposed in this chapter is also an image inpainting technique. How to utilize these methods to improve the recognition performance will be undertaken in future research. [98, 99]

7 Conclusion and Future Work

7.1 Conclusion

This thesis has been focusing on the image processing and coding problems for live iris recognition. The research aim is to enhance the recognition performance as well as reducing the processing time. Through the research in this thesis, four new algorithms have been proposed in iris localization, eyelid detection, iris image coding and eyelash removal. Extensive experiments and comparisons have been made for these proposed methods and encouraging performances have been achieved. This section will review the main contributions in each chapter.

Chapter two reviewed the state of the arts of the automated iris recognition technologies in most aspects, including biological foundation for iris recognition, iris image capture machine, iris liveness detection, image quality assessment, iris image segmentation, iris image normalization, iris image registration, feature extraction, matching and practical applications. In each aspect, the leading theories and methods have been introduced.

Based on extensive literature and standards review, the Bath Iris Recognition Research Environment is built as the foundation for the research project to be carried out. Chapter three illustrated the four parts in Bath Iris Recognition Research Environment: Iris Image Capturing System, Image Pre-processing system, Feature Extraction & Matching Scheme, Bath Iris Image Database. The building of this research environment is based upon extensive literature review and comparison. Although it did not propose something new, it is necessary for the future research.

A fast and robust iris localization algorithm based on Random Sample Consensus (RANSAC) is proposed in Chapter four. Experiments have been done on the image databases from NIST, Plymouth, Retica, Sarnoff, Bath and CASIA. The results showed that the proposed algorithm could not only maintain a high localization rate, but also perform the procedure much faster than the

leading algorithms proposed by Daugman or Wildes. Within the proposed iris localization algorithm, the contributions could be summarized as follows:

- A new pupil area finding method based on the standard deviation analysis for each projection line is proposed. According to the experiments, this method could greatly enhance the pupil finding accuracy.
- In edge point detection, a threshold adaptive canny edge detector is designed to make the number of edge points in a certain amount using a self-adaptive threshold variable.
- The RANSAC method is applied to the iris boundary fitting and the encouraging performance is achieved.
- Many additional checking criterions were proposed based on the 8 bit gray scale image.

Chapter four also reported a fast and robust eyelid removal algorithm, which could be carried out in a very high speed while still keeping satisfying correct removal rate. The main contributions in this method are the effective edge point selection method, which could effectively eliminate uninterested edge points while still keeping enough eyelid boundary edge points.

Chapter five proposed a local frequency amplitude variation based iris coding algorithm, following the research direction of local image variation analysis. Extensive experiments showed that the proposed algorithm could greatly reduce the processing time while still maintain a very high distinguishing capability.

An effective eyelash removal algorithm based on local area analysis has been proposed in chapter six. Unlike other previous eyelash removal methods, which generally tried to detect and mask the eyelashes or the eyelash areas, the proposed method recreates iris pixels occluded by eyelashes using information from their non-occluded neighbors. This method is derived from the following idea. The iris image texture is an inter-correlated area, in which the unique discriminative information is redundant. Statistically, the grayscale intensity of one pixel is highly related to neighbor pixel intensities. Thus if one pixel is occluded by eyelashes, we could reconstruct it with the information from its

neighbor pixels. In this way, the achieved iris code will remain unabridged. The main contributions in this chapter include the following points:

- Proposed the eyelash area verifying method based on the gradient variance of edge points in a windowed area. This method works well in detecting eyelash area in our experiments
- Using 1D non-linear filter to along a direction perpendicular to the eyelash to reconstruct the eyelash occluded pixel.
- Proposed an adaptive metric $Recover$ to decide if the filtered pixel is eyelash pixel or not. For each pixel, if $Recover$ is positive, the pixel is replaced by the filtered value, otherwise the filter is not applied.

Through the research in this thesis, two possible answers to the questions proposed at the beginning of this thesis could be given: (1) The local image variation is the essential unique information for one iris class to be differentiated from another. Apart from utilizing the local phase or intensity variations, this thesis used the local frequency variation, which also proved to be very effective. Statistically, the local iris image pixels are related to each other, which could be used to reconstruct occluded iris pixels. (2) The adoption of Fast Fourier Transform (FFT) makes the feature extraction procedure very time efficiency. Thus the fast representation of local feature information is a very effective way to speed up the coding process. Also the adoption of fast iris image pre-processing techniques would contribute to the system speed.

7.2 Future Work

Although much progress has been made in iris recognition research in Bath, a lot more still needs to be done. Future work will focus on the following area:

- ***Highly reliable and real time iris image quality assessment algorithm:*** Although in urgent need, this area is still under research. It is unlikely to make a universal iris image quality assessment algorithm for any system. The more practical way for camera maker is to provide their own assessing software to ease their given customers.
- ***Non-circular iris localization methods:*** Generally circles are used to fit the pupil and the limbus. But the pupil is not always circular, especially

when it is over dilated. Thus a non-circular iris localization method could describe the pupil boundary more precisely and thus improve the quality of the iris feature vector.

- ***Alternative non-linear filter for eyelash removal:*** The currently used 1D median filter works well but not perfect. Some eyelash positions are still visible after filtering. Thus an alternative filter is in need to improve the performance of the proposed eyelash removal algorithm.
- ***Combination of local phase, intensity and frequency feature in iris image coding:*** Since the local image variation is the essentially discriminative information for one iris class to be differentiated from another, it is hoped that the combination of these local variation information could lead a better performance.

Publication List

1. D. M. Monro, S. Rakshit and D. Zhang, "DCT-based Iris Recognition," IEEE Transactions on Pattern Analysis and Machine Intelligence, Vol. 29, No. 4, pp. 586-595, Apr 2007.

2. D. Zhang, D. M. Monro, S. Rakshit "Eyelash Removal Method for Human Iris Recognition," IEEE Proceedings of International Conference on Image Processing, Atlanta, Oct 2006

3. D.M. Monro, D. Zhang, "An Effective Human Iris Code with Low Complexity," IEEE Proceedings of International Conference on Image Processing, vol.3, pp. 277- 280, Sep 2005

4. D. M. Monro, D. Zhang, "Low Complexity Code for Human Iris Recognition," ID World, Barcelona, Nov 2004

5. D. M. Monro, D. Zhang, "Low Complexity transform for scalable human iris recognition," Workshop on Biometrics, British Machine Vision Association, London, Jun 2004

Reference

[1] A.K. Jain, R.M. Bolle and S. Pankanti, Eds., Biometrics: Personal Identification in a Networked Society, Norwell, MA: Kluwer, 1999.

[2] D. Zhang, Automated Biometrics: Technologies and Systems, Norwell, MA: Kluwer, 2000.

[3] J. L. Wayman, "Fundamentals of Biometric Authentication Technologies", *International Journal of Image and Graphics*, Vol. 1, No. 1, pp. 93-113, 2001.

[4] A. K. Jain, A. Ross and S. Prabhakar, "An Introduction to Biometric Recognition", *IEEE Transactions on Circuits and Systems for Video Technology, Special Issue on Image- and Video-Based Biometrics*, 2003.

[5] S. Prabhakar, S. Pankanti, and A. K. Jain, "Biometric Recognition: Security & Privacy Concerns", *IEEE Security & Privacy Magazine*, Vol. 1, No. 2, pp. 33-42, 2003.

[6] J. Campbell, "Speaker Recognition: A Tutorial", *Proceedings of IEEE*, Vol.85, No.9, pp.1437-1462, 1997.

[7] A. K. Jain, S. Prabhakar, L. Hong and S. Pankanti, "Filterbank-Based Fingerprint Matching", *IEEE Trans. Image Processing*, Vol. 9, No.5, pp.846-859, May 2000.

[8] D. Maltoni, D. Maio, A. K. Jain, and S. Prabhakar, Handbook of Fingerprint Recognition, Springer Verlag, 2003.

[9] D. Zhang and W. Shu, "Two Novel Characteristic in Palmprint Verification: Datum Point Invariance and Line Feature Matching", *Pattern Recognition*, Vol.32, No.4, pp.691-702, 1999.

[10] J. Yoo, M. Nixon and C. Harris, "Model-Driven Statistical Analysis of Human Gait Motion", *IEEE International Conference on Image Processing*, pp.285-288, 2002.

[11] T. Mansfield, G. Kelly, D. Chandler et al., Biometric Product Testing Final Report, issue 1.0, National Physical Laboratory of UK, 2001.

[12] A. Mansfield and J. Wayman, Best Practice Standards for Testing and Reporting on Biometric Device Performance, National Physical Laboratory of UK, 2002.

[13] I. Mann, The Development of the Human Eye, Grune and Stratton, New

York,1950.

[14] H. Davision, The Eye, Academic, London, 1962.

[15] F.H. Adler, Physiology of the Eye: Clinical Application, Fourth ed. London: The C.V. Mosby Company, 1965.

[16] P. C. Kronfeld, "The Gross Anatomy and the Embryology of the Eye," *The Eye*, Vol.1, pp.1-66, H. Davison Ed. Academic, London, 1968.

[17] H.P. Wasserman, Ethnic Pigmentation. New York: Elsivier, 1974.

[18] F.W. Newell, Ophthalmology Principles and Practice, 7th ed., St. Louis, MO: Mosby, 1991.

[19] L. Flom and A. Safir, "Iris Recognition System", United States Patent, No.4641349, 1987.

[20] R.G. Johnson, "Can Iris Patterns be Used to Identify People?", Chemical and Laser Sciences Division LA-12331-PR, Los Alamos National Laboratory, 1991.

[21] J.E. Siedlarz, "Iris: More Detailed than a Fingerprint", *IEEE Spectrum*, Vol.31, pp.27, 1994.

[22] McHugh, et al., "Handheld Iris Imaging Apparatus and Method" , United States Patent, No. 6289113, 1998.

[23] Rozmus, et al., "Method and Apparatus for Illuminating and Imaging Eyes through Eyeglasses", United States Patent, No. 6069967, 1997.

[24] McKendall, "Method of Verifying the Presence of an Eye in a Close-up Image", United States Patent, No. 6028949, 1997.

[25] J. Daugman, "Biometric Personal Identification System Based on Iris Analysis", United States Patent, No.5291560, 1994.

[26] Wildes et al., "Automated, non-invasive iris recognition system and method", United States Patent, No. 5751836, 1996.

[27] W. Lee, A.Yang, and J. Chae, "Apparatus and Method for Adjusting Focus Position in Iris Recognition System", United States Patent, US20020131622A1, 2002.

[28] J. Daugman, "High Confidence Visual Recognition of Persons by a Test of Statistical Independence", *IEEE Trans. Pattern Analysis and Machine Intelligence*, Vol.15, No.11, pp.1148-1161, 1993.

[29] J. Daugman, "Statistical Richness of Visual Phase Information: Update on Recognizing Persons by Iris Patterns", *International Journal of Computer*

Vision, Vol.45, No.1, pp.25-38, 2001.

[30] J. Daugman, "Demodulation by Complex-valued Wavelets for Stochastic Pattern Recognition", *International Journal of Wavelets, Multi-resolution and Information Processing*, Vol.1, No.1, pp.1-17, 2003.

[31] J. Daugman, "The Importance of Being Random: Statistical Principles of Iris Recognition", *Pattern Recognition,* Vol. 36, No. 2, pp.279-291, 2003.

[32] R. Wildes, J.C. Asmuth, etc., "A Machine-vision System for Iris Recognition", *Machine Vision and Applications*, Vol.9, pp.1-8, 1996.

[33] R.P. Wildes, "Iris Recognition: An Emerging Biometric Technology", *Proceedings of the IEEE*, Vol.85, pp.1348-1363, 1997.

[34] W.W. Boles, and B. Boashah, "A Human Identification Technique Using Images of the Iris and Wavelet Transform", *IEEE Trans. on Signal Processing*, Vol.46, pp.1185-1188, 1998.

[35] R. Sanchez-Reillo and C. Sanchez-Avila, "Iris Recognition With Low Template Size", *International Conference on Audio and Video-Based Biometric Person Authentication*, pp.324-329, 2001.

[36] C. Sanchez-Avila, R. Sanchez-Reillo et al., "Iris-based Biometric Recognition using Dyadic Wavelet Transform", *IEEE Aerospace and Electronic Systems Magazine*, pp.3-6, 2002.

[37] C. Tisse, L. Martin, L. Torres and M. Robert, "Person Identification Technique using Human Iris Recognition", *Proc. of Vision Interface*, pp.294-299, 2002.

[38] Y. Zhu, T. Tan, Y. Wang, "Biometric Personal Identification Based on Iris Patterns", *Inter. Conf. on Pattern Recognition (ICPR'2000)*, Vol.II, pp.805-808, 2000.

[39] L. Ma, Y. Wang, T. Tan, "Iris Recognition Based on Multichannel Gabor Filtering", *Proc. of the Fifth Asian Conference on Computer Vision*, Vol. I, pp.279-283, 2002.

[40] L. Ma, Y. Wang, T. Tan, "Iris Recognition Using Circular Symmetric Filters", *the Sixteenth International Conference on Pattern Recognition*, Vol. II, pp. 414-417, 2002.

[41] S. Lim et al., "Efficient Iris Recognition through Improvement of Feature Vector and Classifier", *ETRI Journal*, Vol.23, No.2, pp.61-70, 2001.

[42] J. Daugman et al., "Demodulation, Predictive Coding, and Spatial vision",

Journal of Optical Society of America A, Vol.12, No.4, April 1995.

[43] J. Daugman, "Quadrature-phase Simple-cell Pairs Are Appropriately Described in Complex Analytic Form", *Journal of Optical Society of America A*, Vol.10, No.2, 1993.

[44] J. Daugman, "Uncertainty Relation for Resolution in Space, Spatial Frequency, and Orientation Optimized by Two-Dimensional Visual Cortical Filters", *Journal of Optical Society of America A*, Vol.2, pp.1160-1169, 1985.

[45] J. Daugman, "Complete Discrete 2D Gabor Transforms by Neural Networks for Image Analysis and Compression", *IEEE Trans. Acoustics, Speech, and Signal Processing*, Vol.36, No.7, pp.1169-1179, 1988.

[46] J. Daugman, "Two-Dimensional Spectral Analysis of Cortical Receptive Field Profiles", *Vision Research*, Vol. 20, pp.847-856, 1979.

[47] J. Daugman, "Biometric Decision Landscapes", Technical Report No. TR482, University of Cambridge Computer Laboratory, 1999.

[48] P. Burt, E. Adelson, "The Laplacian Pyramid as a Compact Image Code", *IEEE Trans. Communication*, Vol. COM-31, No.4, pp.532-540, 1983.

[49] L. Brown, "A Survey of Image Registration Techniques", *ACM Computing Surveys*, 24(4), pp.325-376, 1992.

[50] A. Jain, R. Duin, J. Mao, "Statistical Pattern Recognition: A Review", *IEEE Trans. Pattern Analysis and Machine Intelligence*, Vol.22, No.1, pp.4-37, 2000.

[51] C. Liu and H. Wechsler, "A Gabor Feature Classifier for Face Recognition", *the Eighth IEEE International Conference on Computer Vision*, Vol. II, pp.270-275, 2001.

[52] C. Liu and H. Wechsler, "Gabor Feature Based Classification Using the Enhanced Fisher Linear Discriminant Model for Face Recognition", *IEEE Trans. Image Processing*, Vol.11, No.4, pp.467-476, 2002.

[53] S. Mallat, "A theory for Multiresolution Signal Decomposition: the Wavelet Representation", *IEEE Trans. On Pattern Anal. and Machine Intell.*, Vol.11, No.7, pp.674-693, 1989.

[54] I. Daubechies, Ten Lectures on Wavelets, CBMS-NSF conference series in applied mathematics, SIAM, 1992.

[55] S. Mallat, A Wavelet Tour of Signal Processing, Academic Press, 1999.

[56] B. Jawerth and W. Sweldens, "An Overview of Wavelet based Multiresolution Analyses", SIAM Review, Vol.36, No.3, pp.377-412, 1994.

[57] S. Mallat, "Zero-Crossings of a Wavelet Transform", *IEEE Trans. on Info. Theory*, Vol.37, No.4, pp.1019-1033, 1992.

[58] S. Mallat and S. Zhong, "Characterization of Signals from Multiscale Edges", *IEEE Trans. on Pattern Analysis and Machine Intelligence*, Vol.14, No.7, pp.710-732, 1992.

[59] Q. Tieng and W. Boles, "Recognition of 2D Object Contours Using the Wavelet Transform Zero-Crossing Representation", *IEEE Trans. on Pattern Analysis and Machine Intelligence*, Vol.19, No.8, pp.910-916, 1997.

[60] P. Phillips, A. Martin, C. Wilson, M. Przybocki, "An Introduction to Evaluating Biometric Systems", *IEEE Transactions on Computers*, Vol.33, No.2, pp.130-132, 2000.

[61] P. Philips and H. Moon and S. Rizvi and P. Rauss, "The FERET Evaluation Methodology for Face-Recognition Algorithms", *IEEE Transactions on Pattern Analysis and Machine Intelligence*,Vol.22, No.10, pp.1090-1104, 2000.

[62] J. Beveridge and K. She and B. Draper and G. Givens, "Parametric and Nonparametric Methods for the Statistical Evaluation of Human ID Algorithms", *Third Workshop On the Empirical Evaluation of Computer Vision Systems*, 2001.

[63] J. Beveridge, K. She, B. Draper and G. Givens, "A Nonparametric Statistical Comparison of Principal Component and Linear Discriminant Subspaces for Face Recognition", *IEEE Conference on Computer Vision and Pattern Recognition*, pp.535-542, 2001.

[64] R. Bolle, S. Pankanti, N. Ratha, "Evaluation Techniques for Biometric-Based Authentication Systems (FRR) ", *IBM Computer Science Research Report RC 21759*, 2000.

[65] R. Bolle, N. Ratha and S. Pankanti, "Evaluating Authentication Systems Using Bootstrap Confidence Intervals", *IEEE workshopon Automatic Identification Advanced Technologies*, 1999.

[66] J. Wayman, "Confidence Interval and Test Size Estimation for Biometric Data", National Biometric Test Center (collected works), pp.91-101, 2000.

[67] B. Efron and R. Tibshirani, "Bootstrap Methods for Standard Errors, Confidence Intervals, and Other Measures of Statistical Accuracy", *Statistical Science*, Vol.1, pp.54-75, 1986.

[68] J. Wayman, A. K. Jain, D. Maltoni, and D. Maio, *Biometric Systems: Technology, Design and Performance Evaluation*, Springer Verlag, 2003.

[69] Kenneth R. Castleman, Digital Image Processing, Prentice-Hall International, Inc., 1996.

[70] Vladimir N. Vapnik, The Nature of Statistical Learning Theory, Springer, 1995.

[71] K. Fukunaga, Introduction to Statistical Pattern Recognition, Academic Press, 2nd Edition, 1991.

[72] E.R. Davies, Machine Vision-Theory Algorithms Practicalities, 2nd Edition, Academic Press, London, 1997.

[73] D. Newsome, I. Loewenfeld, "Iris Mechanics II. Influence of Pupil Size on Details of Iris Structures", *American Journal of Ophthalmology,* 1971, Vol.71, No.2, pp.553-573

[74] Gregersen, "Structural Variations of the Crypts and 'Bridge Trabeculae' of the Human Iris" *ACTA Ophth*, 1959, pp.37-119

[75] H. Wyatt, "A 'minimum-wear-and –tear' Meshwork for the Iris, *Vision Research*, 2000, pp.2167-2176

[76] Murata, "Ultrastructural Changes of the Myoepithelium of the Dilator pupillae during myosis and mydriasis in the in the rat iris", *Archives of Histology and Cytology*, 1998, pp.29-36

[77] L. Ma, "The study of personal identification methods based on iris recognition", *PhD thesis*, 2003.

[78] J. Daugman, "anti-spoofing liveness detection", *Personal webpage slides*, 2006.

[79] J. Daugman, "The importance of being random: Statistical principles of iris recognition", *Pattern Recognition,* vol. 36, no. 2, pp 279-291.

[80] G. Zhang and M. Salganicoff, "Method of Measuring the Focus of Close-up Images of Eyes", United States Patent, No.5953440, 1999.

[81] N. D. Kalka, J. Zuo, V. Dorairaj, N. A. Schmid, and B. Cukic, "Image Quality Assessment for Iris Biometrics", Proceedings of 2006 SPIE Conf. on Biometrics Technology for Human Identification III, 17-18 April,

Orlando, Vol 6202, pp. 61020D-1-62020D-11.

[82] Y. Chen, S. Dass and A. Jain, "Localized Iris Image Quality Using 2-D Wavelets", *Proc. of International Conference on Biometrics (ICB)*, pp. 373-381, Hong Kong, January, 2006.

[83] G. Kee, "Improved Techniques for an Iris Recognition System with High Performance", *Australian Joint Conference on Artificial Intelligence*, 2001, pp.17-188

[84] Dae Sik Jeong, Hyun-Ae Park, Kang Ryoung Park, Jaihie Kim: "Iris Recognition in Mobile Phone Based on Adaptive Gabor Filter". *ICB* 2006: 457-463

[85] D. M. Monro and D. Zhang, "An effective human iris code with low complexity," *Proc. IEEE International Conference on Image Processing (ICIP)*, Genoa, 2005.

[86] J. Thornton, M. Savvides and Vijaya Kumar, "Robust Iris Recognition Using Advanced Correlation Techniques," *Proc of Intl. Conf. on Image Analysis and Recognition (ICLAR 2005),* September 2005.

[87] M. Fischler, R. Bolles, "Random Sample Consensus: A Paradigm for Model Fitting with Application to Image Analysis and Automated Cartography", *Communications of the ACM*, 1981, Vol. 24, No. 6, pp.381-395

[88] A. Lacey, N. Pinitkarn, "An Evaluation of the Performance of RANSAC Algorithms for Stereo Camera Calibration", *BMVC* ,2000

[89] T. Chen, K. Chung, "An Efficient Randomized Algorithm for Detecting Circles", *Computer Vision and Image Understanding*, 2001, pp.172-191

[90] Jiali Cui, Li Ma, Yunhong Wang, Tieniu Tan, Zhenan Sun, "A Fast and Robust Iris Localization Method based on Texture Segmentation", *Biometric Technology for Human Identification,* 2004,5404:401-408

[91] D. Zhang, "Detecting eyelash and reflection for accurate iris segmentation", *International Journal of Pattern Recognition and Artificial Intelligence,* vol. 1, No.6 , pp. 1025-1034, 2003.

[92] http://webvision.med.utah.edu/.

[93] http://www.deeperwants.com/cul1/homeworlds/journal/archives/000048.html

[94] J. Woods, "Markov Image Modelling", IEEE Transactions on Automatic

Control, vol 23, issue 5, pp. 846-850, 1978.

[95] Wang, J.; Oliveira, M.M, "A hole-filling strategy for reconstruction of smooth surfaces in range images". Computer Graphics and Image Processing, 2003. SIBGRAPI 2003. XVI Brazilian Symposium on. 12-15 Oct. 2003 Page(s):11 – 18.

[96] Zhenan Sun, Tieniu Tan, Yunhong Wang, Robust Encoding of Local Ordinal Measures: A General Framework of Iris Recognition, ECCV workshop on Biometric Authentication 2004

[97] http://www.cbsr.ia.ac.cn/Iris.htm

[98] Bertalmio, M, Sapiro, G., Caselles, V., Ballester, C. Image Inpainting. *SIGGRAPH 2000*, pages 417-424.

[99] Chan, T., Shen, J. Mathematical Models for Local Deterministic Inpaintings. UCLA CAM TR 00-11, March 2000.